

N O T I C E

THIS DOCUMENT HAS BEEN REPRODUCED FROM
MICROFICHE. ALTHOUGH IT IS RECOGNIZED THAT
CERTAIN PORTIONS ARE ILLEGIBLE, IT IS BEING RELEASED
IN THE INTEREST OF MAKING AVAILABLE AS MUCH
INFORMATION AS POSSIBLE



UNIVERSITY OF ILLINOIS
URBANA

AERONOMY REPORT NO. 90

THE URBANA COHERENT-SCATTER RADAR: SYNTHESIS AND FIRST RESULTS

(NASA-CR-153186)	THE URBANA	N80-23531
COHERENT-SCATTER RADAR:	SYNTHESIS AND FIRST	
RESULTS (Illinois Univ.)	98 p HC A05/MF A01	
	CSCL 17I	Unclas
		G3/32 20109

by
K. P. Gibbs
S. A. Bowhill

December 1, 1979

Library of Congress ISSN 0568-0581



Supported by
National Aeronautics and Space Administration
National Science Foundation

Aeronomy Laboratory
Department of Electrical Engineering
University of Illinois
Urbana, Illinois

AERONOMY REPORT
NO. 90

THE URBANA COHERENT-SCATTER RADAR:
SYNTHESIS AND FIRST RESULTS

by

K. P. Gibbs
S. A. Bowhill

December 1, 1979

Supported by
National Aeronautics
and Space Administration
Grant NSG 7506
National Science Foundation
Grant ATM 78-15224

Aeronomy Laboratory
Department of Electrical Engineering
University of Illinois
Urbana, Illinois

ABSTRACT

The Urbana coherent-scatter radar system has been synthesized and several hundred hours of echo power and line-of-sight velocity data obtained. The coherent-scatter radar utilizes a diode array previously constructed and components from the Urbana meteor radar. An improved receiving system permits a time resolution of one minute in the data.

Echo power from the F_2 region shows a high degree of variability from day to day. Examples of changes in power level at shorter time scales are also observed. Velocity data show the existence of gravity waves and occasionally exhibit vertical standing-wave characteristics.

TABLE OF CONTENTS

ABSTRACT	iii
TABLE OF CONTENTS	v
LIST OF FIGURES	vii
1. INTRODUCTION	1
1.1 <i>Early Developments in Scatter Propagation</i>	1
1.2 <i>Turbulent Scatter Theory</i>	2
1.3 <i>First Indication of Ionospheric Backscatter</i>	4
1.4 <i>Development of Thomson-Scatter Radars</i>	5
1.5 <i>Mesospheric Radar Studies</i>	6
1.6 <i>Mesospheric, Stratospheric, Tropospheric (MST) Radars</i>	7
1.7 <i>Objectives and Scope of This Study</i>	8
2. URBANA COHERENT-SCATTER RADAR SYSTEM	10
2.1 <i>Development of the Urbana Radar</i>	10
2.2 <i>Radar Hardware</i>	10
2.2.1 <i>Transmitter</i>	10
2.2.2 <i>Antenna and transmit/receive switch</i>	11
2.2.3 <i>Radar director</i>	14
2.2.4 <i>Receiving system</i>	14
2.3 <i>Data Processing Hardware</i>	19
2.4 <i>Software</i>	20
2.4.1 <i>Theory</i>	20
2.4.2 <i>Data collection</i>	21
2.4.3 <i>Post processing and data transfer</i>	24
2.4.4 <i>Plotter software</i>	24
3. MESOSPHERIC COHERENT-SCATTER OBSERVATIONS AT URBANA	26
3.1 <i>Observation Program and Introductory Remarks</i>	26
3.2 <i>Echo Power Data</i>	26
3.3 <i>Velocity Data</i>	29
3.4 <i>Observations of an Entire Day</i>	33
4. SUMMARY AND SUGGESTIONS FOR FUTURE RESEARCH	51
4.1 <i>Summary</i>	51
4.2 <i>Suggestions for Future Research</i>	51
4.2.1 <i>Improved range resolution</i>	51

	Page
4.2.2 <i>Measurement of horizontal velocity</i>	52
4.2.3 <i>Additional data processing</i>	52
APPENDIX I RECEIVING SYSTEM BLANKER	54
APPENDIX II RADAR DIRECTOR TIMING INFORMATION	58
APPENDIX III DATA COLLECTION PROGRAMS	60
APPENDIX IV POST-PROCESSING PROGRAMS	74
APPENDIX V PLOTTING PROGRAMS	78
REFERENCES	87

LIST OF FIGURES

Figure		Page
2.1	40.92-MHz transmitter. In the foreground of the figure are the control panel, the power meters and the circuit-breaker panel. The large metallic cylinder in the center of the picture is a pressurized, tuned cavity housing the driver tube. One of the four output cavities is seen in the background on the left. The equipment located immediately in front of the output cavity in the figure is the transmitter for the Urbana laser radar	12
2.2	Final switching stage of pulse modulator. The three large tubes seen here are ML-5682 triodes. ML-5682 tubes are also used in the driver and power amplifier cavities	13
2.3	(a) Overhead view of coherent-scatter antenna. The group of utility poles in the center of the figure form a reference line toward the south. The transmission line to the transmitter appears at the right of the figure. (b) Ground-level view of the coherent-scatter antenna	16
2.4	Feedline for the coherent-scatter system. Twin seven-inch coaxial lines run approximately 450 feet from the switch shed to the antenna. The meteor-radar antenna can be seen at the right of the figure	17
2.5	Bottom view of switching shed. The output to the coherent-scatter antenna is at the right center of the figure while the output to the meteor-radar antenna is at the upper left. The metallic bands in the center of the foreground delineate one of the four tubes used in the transmit/receive switch . .	18
2.6	Illustration of the coherent-integration process	23
3.1	Vertical profile of scattered power at Urbana beginning at 854 GST on April 21, 1978	27
3.2	Vertical profile of scattered power at Urbana beginning at 800 GST on April 11, 1978	28
3.3	Vertical profile of scattered power at Urbana beginning at 1114 GST on May 18, 1978	30

Figure	Page
3.4	Line-of-sight velocity at Urbana beginning at 854 CST on April 21, 1978 31
3.5	Line-of-sight velocity at Urbana beginning at 800 CST on April 11, 1978 32
3.6	Line-of-sight velocity at Urbana beginning at 1016 CST on April 13, 1978 34
3.7	Vertical profile of scattered power at Urbana beginning at 812 CST on May 24, 1978 35
3.8	Vertical profile of scattered power at Urbana beginning at 1012 CST on May 24, 1978 36
3.9	Vertical profile of scattered power at Urbana beginning at 1212 CST on May 24, 1978 37
3.10	Vertical profile of scattered power at Urbana beginning at 1421 CST on May 24, 1978 38
3.11	Vertical profile of scattered power at Urbana beginning at 1621 CST on May 24, 1978 39
3.12	Horizontal profile of scattered power at Urbana beginning at 812 CST on May 24, 1978 40
3.13	Horizontal profile of scattered power at Urbana beginning at 1012 CST on May 24, 1978 41
3.14	Horizontal profile of scattered power at Urbana beginning at 1212 CST on May 24, 1978 42
3.15	Horizontal profile of scattered power at Urbana beginning at 1421 CST on May 24, 1978 43
3.16	Horizontal profile of scattered power at Urbana beginning at 1621 CST on May 24, 1978 44
3.17	Line-of-sight velocity at Urbana beginning at 812 CST on May 24, 1978 45
3.18	Line-of-sight velocity at Urbana beginning at 1012 CST on May 24, 1978 46
3.19	Line-of-sight velocity at Urbana beginning at 1212 CST on May 24, 1978 47
3.20	Line-of-sight velocity at Urbana beginning at 1421 CST on May 24, 1978 48

Figure		Page
3.21	Line-of-sight velocity at Urbana beginning at 1621 CST on May 24, 1978	49
A1.1	Blanker/preamplifier unit. The blanker is contained in the box at the upper right and controlled by the circuit at the lower right. A commercial preamplifier appears in the upper left of the figure	55
A1.2	Drive circuitry for the receiving system blanker	56
A1.3	RF section of the radar receiving system blanker	57
A2.1	Timing diagram for the radar director	59

1. INTRODUCTION

1.1 *Early Developments in Scatter Propagation*

The use of radio waves as a means for investigating the ionosphere began in the early twentieth century with sounding experiments such as those of *Appleton and Barnett* [1925]. A British Broadcasting Corporation transmitter operating at a frequency near 1 MHz led to observations of a reflecting layer at a height of roughly 85 km. Continued study of the ionosphere was the direct result of attempts to understand and improve long-range communication.

The earliest over-the-horizon communication was the familiar multiple-hop short-wave or HF beam transmission. *Eokersley* [1932] used commercial facsimile communication links to investigate the propagation of wavelengths between 14 and 50 m. Evidence in that experiment suggested a scattering source of "ionic clouds" above 100 km for these frequencies.

World War II saw the development of higher-power, higher-frequency radio equipment for use in communication and radar. Reports of anomalous radio propagation during the war led to investigation of over-the-horizon propagation at microwave frequencies by the process of tropospheric ducting due to evaporation over the ocean. A by-product of that study was the discovery that the field strength beyond the radio horizon decreased more slowly, even in the absence of ducting, than predicted by the smooth sphere theory. *Booker and Gordon* [1950] advanced the theory that the propagation beyond the radio horizon is due to fluctuations in the permittivity of the troposphere caused by thermal instabilities. This mode of propagation is known as tropospheric-scatter propagation.

Bailey et al. [1952] predicted and subsequently discovered ionospheric-scatter propagation based on the theory of *Booker and Gordon* [1950]. A test path of 1245 km from Cedar Rapids, Iowa to Sterling, Virginia was used with transmission at 49.8 MHz. The results of *Bailey et al.* [1952] indicated that the returned signal was scattered from the *D* region of the ionosphere.

Both the tropospheric- and mesospheric-scatter modes of propagation were widely accepted by 1955 [*Norton and Weisner*, 1955]. Extensive observations had been made by *Bailey et al.* [1955] although national security interests limited the amount of information which could be published at the time. In addition, *Villaro and Weisskopf* [1955] presented a theoretical analysis of

ionospheric scatter. They found that turbulent mixing in the presence of a strong gradient of electron density was responsible for the ionospheric scatter propagation. The subsequent study of the mesospheric turbulent regions by VHF backscatter is of interest in this paper.

1.2 Turbulent Scatter Theory

Turbulent flow in a fluid occurs whenever certain conditions for stability are violated. In general, the motion of a fluid is governed by the continuity equation

$$\vec{\nabla} \cdot \vec{v} = 0 \quad (1.1)$$

and the equation of motion is given by the Navier-Stokes equation for the velocity field $v(x, t)$:

$$\left(\frac{\partial \vec{v}}{\partial t} + (\vec{v} \cdot \Delta) \vec{v} \right) + \nabla \alpha (\nabla \alpha \vec{v}) + \frac{\nabla p}{\rho} = 0 \quad (1.2)$$

where \vec{p} , ρ , and \vec{v} are the pressure, density and velocity in the fluid and ν is the kinematic viscosity related to μ , the coefficient of viscosity by $\nu = \mu/\rho$. The characteristic linear dimension with which a particular flow is associated is usually termed L , and a representative velocity is V . A dimensionless parameter, the Reynolds number Re , associated with the above equations, is given by

$$Re = \frac{VL}{\nu} \quad (1.3)$$

The magnitude of this quantity determines the nature of the fluid flow, the condition for turbulence being $Re \gg 1$. The Reynolds number is, however, not the only parameter concerning turbulent flow.

When a fluid is flowing in a turbulent manner eddies of different scale sizes are formed. The largest scale eddies are fed by the large-scale dynamics of the ionosphere, namely the overall global circulation and the superimposed planetary waves, tides and gravity waves. The energy pumped into the turbulent flow must be dissipated in some manner. The large-scale eddies disintegrate into smaller eddies over a short period of time and while doing so, dissipate energy through viscous damping. As shown in a dimensional argument by *Villars and Weisskopf* [1955], the amount of energy lost to viscous damping eventually reaches the amount of energy input into a given scale size of eddy. This scale is then the smallest eddy, and the energy has been entirely dissipated. Only under certain conditions is turbulence energetically possible. Energy which is extracted by the turbulence

is that which could not be maintained as potential energy in the fluid. This condition for energy balance is given in terms of the Richardson number Ri :

$$Ri = \omega_B^2 / (\partial V_0 / \partial z)^2 \quad (1.4)$$

where ω_B is the Brunt-Vaisala frequency for buoyancy oscillations, $(\partial V_0 / \partial z)$ is the vertical shear in the mean flow, V_0 is the horizontal velocity of the mean flow and z is perpendicular to the planes in which the fluid is stratified. When one considers that ω_B^2 , the numerator, is a measure of the static stability and that $(\partial V_0 / \partial z)^2$ is related to the perturbing effect of the wind shear then it is clear that a smaller Richardson number implies greater tendency toward instability. So, if the Richardson number is lower than some critical value turbulence is energetically possible. A critical value of $\frac{1}{4}$ is often used. The above two criteria can then be used to evaluate the nature of expected turbulence in the atmosphere.

Rastogi and Bowhill [1975] used typical values for the Richardson and Reynolds numbers to examine the occurrence of turbulence. Their results show that one would not expect the atmosphere to be turbulent as a whole below the turbopause. Instead, the Reynolds criterion is virtually always satisfied but the Richardson criterion can be satisfied only over regions small with respect to scale height. Hence, the turbulence is expected to be intermittent; namely, it does not occur at all times and heights.

Finally, the scattering induced by the turbulence must be considered. The following analysis was considered by *Villars and Weisskopf* [1955] and others, and was discussed most recently by *Rastogi and Bowhill* [1976a]. When diffusion does not occur, the continuity equation for electron density is given by:

$$\frac{\partial N}{\partial t} = q - L - \nabla \cdot (N\vec{v}) \quad (1.5)$$

where q is a production term, L a loss term, and $\nabla \cdot (N\vec{v})$ a transport term. Production and loss mechanisms are such that $q - L \approx 0$. Because of the collisions of electrons with neutrals the velocity in (1.5) is taken to be that of the neutrals which are assumed to form an incompressible fluid. Under these conditions the velocity can be factored and the transport term then is $\vec{v} \cdot \nabla N$. In addition, ∇N is generally vertical causing $\partial N / \partial t \approx 0$ since the vertical velocities are generally very small. It should be evident that any small deviation \vec{u} in the velocity field will produce a $\vec{u} \cdot \nabla N$ transport term

and hence a fluctuation in electron density. In this manner the turbulence couples to the electron density.

An expression for the scattering cross section can be found using Booker scattering theory. Let ℓ be a characteristic length scale associated with wave number $k = \ell^{-1}$, characteristic velocity u_ℓ and characteristic time t_ℓ . Then the fluctuations in electron density at scale ℓ are given by

$$\langle \delta N_\ell^2 \rangle \propto N'^2 u_\ell^2 t_\ell^2 \quad (1.6)$$

where N' , the gradient of electron density at scales larger than ℓ is assumed known. Following the analysis of *Rastogi and Bowhill* [1976a] the length ℓ is assumed small and the turbulence is assumed to be isotropic and homogeneous at this scale. Using (1.6) above, several results from the theory of statistical turbulence, and a result due to Booker the radar cross section

$$\sigma \propto r_e^2 N'^2 k_B^{-2} E(k_B) T^2(k_B) \quad (1.7)$$

is obtained where r_e is the standard electron radius and $E(k)$ is the energy spectrum of the turbulence. The above result is then used to relate the measured signals to the turbulence by which they are produced.

Turbulence is not the only cause of perturbations in the electron density which give rise to backscatter. As discussed earlier, for small scales the turbulence is damped by the viscosity of the fluid. However, scattering from thermal fluctuations can occur producing what is now commonly called Thomson or incoherent scattering. A review of Thomson scatter and its use as an experimental tool has been written by *Evans* [1969]. The study of mesospheric turbulence induced coherent backscatter is an outgrowth of Thomson-scatter studies of the *F* and *F* regions of the ionosphere. The development of Thomson-scatter radars will therefore be discussed in the following sections.

1.3 First Indication of Ionospheric Backscatter

The continued development of radar technology throughout the 1950's prompted *Gordon* [1958] to suggest that the study of the ionosphere by radio waves scattered incoherently from free electrons was possible with state of the art equipment. *Bowles* [1958] verified the existence of this incoherent scatter using a 4-MW pulse power 40.92-MHz transmitter in conjunction with a large aperture antenna at Long Branch, Illinois. Although the data collected at that time were very noisy the existence of a scattering region at 85 km

is quite visible in photographs taken from A-scope displays of the receiver output. This echo was interpreted as due to turbulence-induced scatter rather than incoherent scatter by virtue of its similarity to ionospheric-scatter propagation results in both scattering cross section per unit volume and fading rate [Bowles, 1964; Blair *et al.*, 1961].

Additional observations by Bowles [1961] showed that the broadening of the received spectrum for altitudes above 100 km was not as great as predicted by Gordon [1958] for completely incoherent scattering. Theoretical work such as that of Dougherty and Farley [1960] indicated that the influence of the ions on the scattering is important when the radar wavelength is larger than the Debye shielding length. The spatial variation of the electron density at scales greater than the Debye length is constrained to be that of the ions by virtue of local charge neutrality. The observed Doppler shift is therefore associated with the motion of the ions. The partial coherence in the returned signal caused by the ion-electron interaction led to the name Thomson-scatter. Several of the radars discussed below were designed without complete understanding of the Thomson-scatter spectrum effect.

1.4 Development of Thomson-Scatter Radars

By the early 1960's several radar facilities designed for ionospheric study had been constructed. The radar proposed by Gordon [1958] was constructed at Arecibo, Puerto Rico on the basis of fully incoherent scattering. The expected wide spectrum of returned signal implied low energy per unit bandwidth and therefore a large aperture antenna. A spherical reflector surface of wire mesh 305 m in diameter with a radius of curvature of 245 m is set in a limestone sink-hole. A line source is suspended above the reflector and can be moved to point the beam 20° off the zenith in any direction. A 430-MHz 2-MW pulse transmitter is used for the Thomson-scatter studies. Further details of the system can be found in Gordon and Lalonde [1961].

The Millstone Hill Observatory at Westford, Massachusetts originally employed a 440-MHz tracking radar using a 2.5-MW pulse transmitter and a steerable 25-m diameter paraboloid antenna. Ionospheric-scatter measurements were made by Pineo *et al.* [1960] using the original system. Later a vertically pointed 70-m paraboloid antenna was used with the 440-MHz transmitter

for additional measurements while a 1295-MHz transmitter was added to drive the original antenna [Evans and Loewenthal, 1964].

The scatter radar built at Jicamarca, Peru was based in part on a suggestion by Bowles [1961] that ion gyroresonance sidebands could be observed by a radar pointed perpendicular to the magnetic field in the ionosphere. Hence, the location in Peru near the geomagnetic equator was chosen for a 49.92-MHz 4-MW pulse transmitter with a 290-m-by-290-m crossed-dipole array. The transmitter and antenna are designed so that the two orthogonal sets of dipoles can be operated independently and simultaneously to produce various polarizations. The modules of the crossed arrays can be fed using different coaxial cable lengths to produce beam steering. The facility at Jicamarca is described in detail by Rastogi and Bowhill [1975].

Additional radar facilities include the French bistatic radar built in 1962 at St. Santin and later modified to a quadristatic configuration [Bauer et al., 1974]. The transmitter operates in a continuous wave mode with 150 kw of power at 935 MHz. The Stanford Research Institute radar operating at 1300 MHz was originally located at Menlo Park, California [Leadabrand, 1967] and later relocated to Chatanika, Alaska for auroral-zone Thomson-scatter studies [Leadabrand et al., 1972]. The British also operated a radar facility at Malvern, England on 400 MHz [William and Taylor, 1974] although this facility is no longer in use.

The various radars mentioned above were used during the early 1960's primarily in the study of the E and F regions of the ionosphere [Greenhow et al., 1963; Evans, 1967; Evans, 1969]. The Thomson-scatter method was used to obtain electron-density profiles, electron and ion kinetic temperatures, and to identify the major ionic constituents by comparison with theoretical curves. Partial-reflection techniques were used extensively in the D region [e.g. Gregory, 1961].

1.5 Mesospheric Radar Studies

The Thomson-scatter radar facilities discussed above were used for D-region studies beginning in the mid 1960's. LaLonde [1966] reported D-region 430-MHz echoes at Arecibo. VHF echoes were observed at Jicamarca by Flock and Balsley [1967] who found the predominant feature to be an echoing region near 75 km. Between 90 and 110 km the equatorial electrojet dominated the returns. Ioannidis and Farley [1974] and Armisted et al. [1972] reported echoes in the region below 80 km. A coherent-scatter model was

required in the D region at UHF since the electron density predicted by Thomson-scatter theory to produce the observed echo power would have been too large.

The first measurements of spectrum or autocorrelation measurements in the mesosphere were reported by *Woodman and Guillan* [1974] at Jicamarca. A velocity measurement along the line of sight of the radar beam was obtained from the autocorrelation function. It was concluded that short-period fluctuations in measured wind velocities were due to gravity-wave fluctuations and that neutral atmosphere turbulence produced by wind shears was responsible for the observed echo power. In this investigation the signal-to-noise ratio of the data was improved by the process of coherent integration. The correlation time of the backscattered signals was longer than the interpulse period of the radar so that successive samples for a given altitude could be summed together with the signal tending to add and the noise tending to cancel.

An extension of the above work was performed by *Rastogi and Woodman* [1974] at Jicamarca. In that investigation it was shown that the echoes throughout the 15 to 85 km region were due not to Thomson scattering, i.e. the thermal motion of the electrons, but rather were turbulence induced. It was shown that the mean echo power for the received signals was 4 dB above that expected from Thomson-scattering theory. The authors then suggest that the intermittent nature of the echoes indicates the turbulent nature of this region. Indeed, the echo power often varied by ≈ 20 dB over a one or two minute period indicating a nonthermal mechanism was responsible. The same conclusion was reached in a recent paper by *Rastogi and Bowhill* [1976b]. The large fluctuations in the echo power are directly related to fluctuations in the rate of energy dissipation per unit mass due to turbulence. The studies described in this paragraph confirmed the turbulence induced origin of scattering in the mesosphere and resulted in the construction of several radars for the study of dynamics in the mesosphere, stratosphere, and troposphere. (abbreviated M, S, and T). These MST radars utilize the coherent nature of the returns and the Doppler shift produced by the motion of the turbulent scattering region along the line of sight of the radar beam.

1.6 Mesospheric, Stratospheric, Tropospheric (MST) Radars

Several of the radar facilities initially used for Thomson scatter have been employed to collect coherent-scatter data from altitudes below the F

region. *Woodman and Guillen* [1974] measured winds and turbulence in the stratosphere and mesosphere at Jicamarca. The Doppler shift of the returned signal indicated the motion of the scattering layer along the line of sight of the radar beam. Data collected at that time were limited to one height at a time. With the installation of a new computer, simultaneous multiheight mesospheric observations were made [*Harper and Woodman*, 1977]. Recently, waves in the lower stratosphere were observed by *Ruster et al.* [1978] at Jicamarca.

The 430 MHz radar at Arecibo was employed by *Aso et al.* [1977] for the measurement of middle atmospheric dynamics. As discussed by *Woodman and Guillen* [1974] the echo intensity for coherent scatter depends on the energy spectrum of the turbulence. Only the spatial Fourier component of the refractive-index fluctuations corresponding to the probing wavelength contributes to the scattering. *Rastogi and Bowhill* [1976b] predicted that the wave number k_{\parallel} of the Arecibo transmitter exceeds, for mesospheric heights, the critical wave number k_c , above which the turbulent energy spectrum decreases exponentially. *Aso et al.* [1977] verified the prediction of *Rastogi and Bowhill* [1976b] but showed the existence in the stratosphere of turbulence at the probing wave number. Additional UHF measurements at the tropopause have been made by *Balsley and Farley* [1976] using the 1290 MHz Chatanika, Alaska radar.

During the recent past several new MST facilities have been designed and constructed. Considerations for the design and use of MST radars are discussed by *Balsley* [1978a,b]. The SOUSY radar near Lindau, Federal Republic of Germany [*Czechowsky et al.*, 1976] and the Sunset radar in Colorado [*Green et al.*, 1975a,b; *Wamock et al.*, 1978] have obtained velocity measurements throughout the troposphere and stratosphere. A portable radar at Poker Flat, Alaska was also used in tropospheric measurements [*Ecklund et al.*, 1977]. A permanent MST radar installation is underway at Poker Flat based on a prototype radar which is located at Platteville, Colorado [*Ecklund et al.*, 1979]. First results from limited operation at Poker Flat have been reported [*Balsley et al.*, 1980]. The SOUSY, Sunset, Platteville, and Poker Flat radars are all VHF radars as is the Urbana radar which is discussed below.

1.7 Objectives and Scope of This Study

The three principal objectives of this study are: (1) to describe the

development of the Urbana coherent-scatter radar system, (2) to obtain echo power and radial velocity measurements with a time resolution which allows the observation of wave phenomena in the mesosphere, and (3) to begin assembling a data base from which scientific information can be obtained. An outline of this study is given below.

Chapter 2 describes the development of the Urbana radar. The various hardware subsystems are discussed and the operations performed at each stage of data processing are described.

Observations characteristic of the first data collected from the Urbana radar are shown in Chapter 3. Specific features of the data are illustrated and discussed in detail.

Conclusions and suggestions for future work appear in Chapter 4.

2. URBANA COHERENT-SCATTER RADAR SYSTEM

2.1 *Development of the Urbana Radar*

In 1956 the National Bureau of Standards operated the Long Branch Radio Propagation Transmitting Station WWI near Havana, Illinois. Among other experiments conducted at this station a 40.92-MHz pulsed radar with a flat four-acre dipole array was utilized by *Bowles* [1958] to verify the existence of incoherent scatter from the mesosphere. The Havana radar was subsequently used by the Smithsonian Astrophysical Observatory and was made available to the University of Illinois in 1971. A multistatic meteor radar was constructed at the Urbana field station using the 40.92-MHz transmitter [*Edwards*, 1974; *Hess and Geller*, 1976].

Because of interest in coherent scatter from the ionosphere, elements from the dipole array at Havana were used in a vertically pointing dipole array constructed at Urbana. The work on the antenna and associated feed system was completed in 1976 [*Altman and Bowhill*, 1976]. Collection of coherent-scatter data then became a problem of modification of the meteor-radar system.

P. K. Rastogi made the first observations of coherent scatter using the Urbana radar during July, 1976. While these verified the potential operation of the radar for coherent scatter, the data output was limited to oscilloscope A-traces and chart recorder outputs from a boxcar integrator. In November, 1977 the first attempt to use a computer for coherent integration and complex autocorrelation of real-time data was made. However, because of poor performance in various sections of the meteor-radar system being used in the scatter system, notably the receiver, no significant data were collected.

After testing and repair of various components a lower noise figure receiving system was obtained and preliminary correlation data were collected in March, 1978. Further improvements in the hardware brought the system to its present condition. Much of the hardware for the coherent-scatter radar is shared with the meteor radar. Detailed descriptions of these subsystems are therefore not included in the following, but important operating parameters are repeated.

2.2 *Radar Hardware*

2.2.1 *Transmitter*. The transmitter utilized at Urbana for both the meteor radar and coherent-scatter radar was built in 1958 by Continental

Electronics Manufacturing Company of Dallas, Texas. Designed as a prototype for the Distant Early Warning (DEW) line of radars, the transmitter has a 4-MW peak pulse output power rating with nominal average output power of 20 kW. The radar operates at 40.92 MHz with pulse widths ranging from 3 μ s to 100 μ s. Presently the system is operated with a 20- μ s pulse at a pulse repetition frequency of 400 Hz.

The final amplifier stage consists of four water-cooled triode tubes (Machlett ML-5682) in grounded-grid configuration. The tubes are mounted in pressurized cylindrical cavities to minimize arcing. The cavities are resonated at the input and output of the tubes. Water cooling is provided to maintain operating temperature near 100°F. A cavity pair is shown in Figure 2.1.

The transmitter final stage is actually two pairs of tubes with each pair driving one side of a balanced coaxial line. The driver amplifier, delivering 0.6 MW peak pulse power, is a single ML-5682 triode configured in the same manner as the output tubes. Power from the driver is split first to obtain the 180° phase shift between pairs of final tubes, then again to properly phase the drive to each tube in the pair.

The intermediate power amplifier is a 4CX5000 tube which operates at reduced plate voltage with respect to the ML-5682 tubes. Plate dissipation of 5 KW necessitates a pressurized chamber with water-cooled walls. The 4CX5000 is in turn driven by a Continental Electronics 814B VHF transmitter. Using a pair of 4CX1000 A's connected in parallel the 814B provides drive pulses with a peak power of 3 kW. Various lower power stages drive the 814B from the gated RF pulse provided by the radar director.

The pulse modulator produces amplified, shaped pulses which are transformer coupled into a final switching stage. Three parallel ML-5682 tubes switch current in the pulse modulation transformer, producing the required high voltage pulse on the secondary. Partial control of the transmitter output power is obtained by controlling the step-up ratio of the transformer. The final switching stage is shown in Figure 2.2. A more detailed description of the transmitter can be found in *Hess and Geller*, [1976].

2.2.2 *Antenna and transmit/receive switch.* In conjunction with a powerful transmitter coherent scatter radar requires the use of a high-gain narrow-beam antenna. The characteristics of the Urbana dipole array are

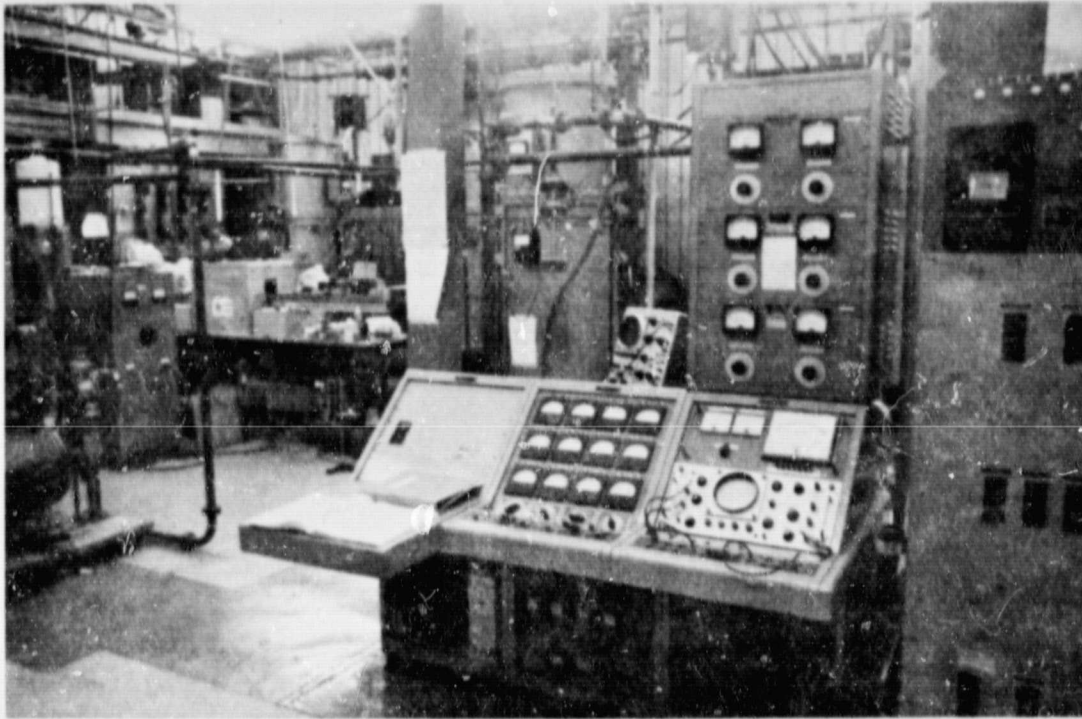


Figure 2.1 40.92-MHz transmitter. In the foreground of the figure are the control panel, the power meters and the circuit-breaker panel. The large metallic cylinder in the center of the picture is a pressurized, tuned cavity housing the driver tube. One of the four output cavities is seen in the background on the left. The equipment located immediately in front of the output cavity in the figure is the transmitter for the Urbana laser radar.

ORIGINAL PAGE IS
OF POOR QUALITY

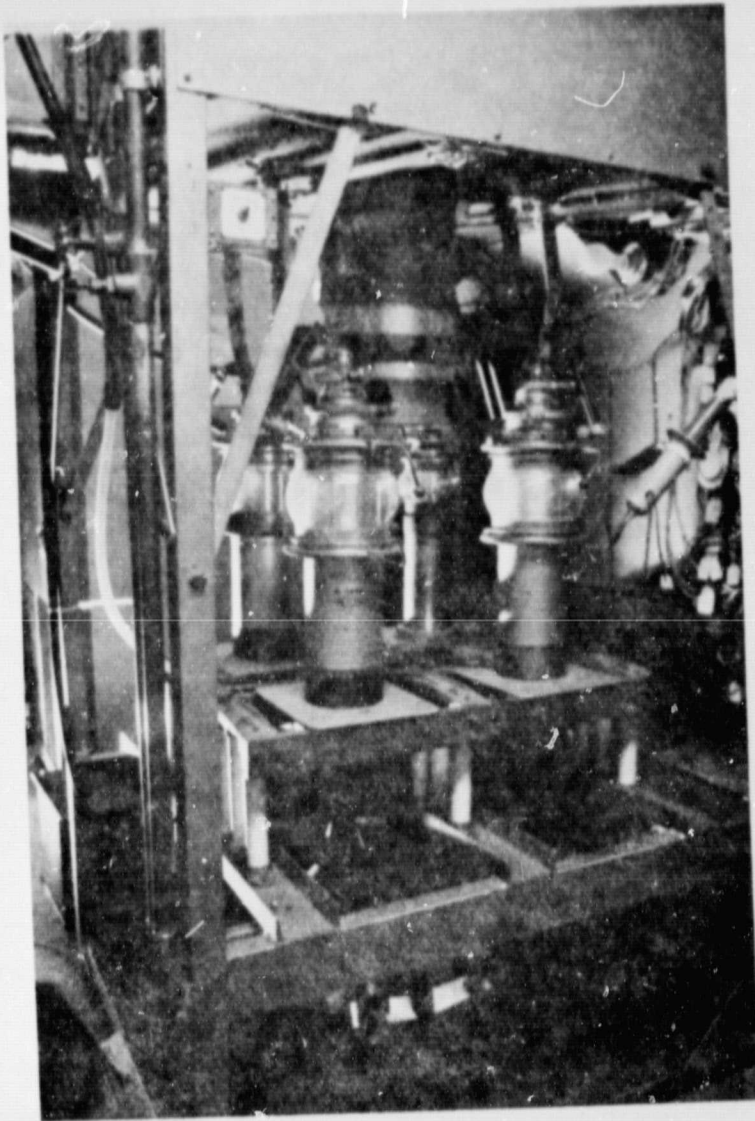


Figure 2.2 Final switching stage of pulse modulator. The three large tubes seen here are ML-5682 triodes. ML-5682 tubes are also used in the driver and power amplifier cavities.

given in Table 2.1 [Allman and Bowhill, 1976]. The array is organized into groups of twenty-eight pairs of half-wave dipole elements called cells. Six cells are connected in parallel to form a group. The 1008-element array consists of six groups. The feed system for the antenna employs open-air transmission line transformers for matching. The feed line from transmitter to antenna is 450 ft. of balanced coaxial line built from aluminum construction tube. The inner conductor of three inch diameter and outer conductor of seven-inch diameter are separated at seven-foot intervals by teflon spacers. The antenna is shown in Figure 2.3 while the feed line is pictured in Figure 2.4.

The antenna is connected to the transmitter via a transmit/receive (T/R) switch to allow monostatic operation. Four gas-filled tubes are employed forming a transmit/receive switch for each side of the balanced coaxial line. The transmitter voltage causes breakdown in the tubes and the resulting low impedance is transformed so as to isolate the receiver during the transmit pulse and the transmitter while receiving. Recent tests measured the recovery time of the switch at 400 μ s when operating with 1-MW peak pulse power. Details of the T/R switch, antenna, and feed system design and construction are given by Allman and Bowhill [1976]. The transmit/receive switch shed is shown in Figure 2.5.

2.2.3 *Radar director.* The radar director at Urbana consists of two separate units; one for radio frequency (RF) synthesis and one for timing and pulse generation. The RF section contains crystal oscillators at the transmitter frequency of 40.92 MHz and the receiver local oscillator frequency of 35.42 MHz. Mixing these two frequencies and phase shifting by $\pm 45^\circ$ yields quadrature reference signals at the intermediate frequency of 5.5 MHz.

The timing section of the radar director is driven by an external master clock of 100 kHz derived from a 5-MHz reference. Every pulse interval is a multiple of the base 10- μ s period. The transmitter, analog-to-digital converter (ADC), blanker, and the oscilloscope displays are all driven by various pulses from the radar director. A detailed description of the associated circuitry is given by Hess and Geller [1976]. Timing information for the radar director is given in Appendix II.

2.2.4 *Receiving system.* The receiving system for the Urbana coherent-scatter radar shares a receiver and quadrature phase detector with the meteor-radar system. To protect the receiving system and lower the noise figure, a blanker/preamplifier unit which can be located near the T/R switch has been

Table 2.1

Antenna parameters for the Urbana coherent-scatter radar.

Aperture illumination efficiency (η_i)	0.69, -1.5 dB
Antenna efficiency (η_a)	0.17, -7.6 dB
Radiation efficiency ($\eta_r = \eta_a/\eta_i$)	0.25, -6.0 dB
Physical aperture (A_o)	11000 m ²
Effective aperture ($\eta_a A_o$)	1870 m ²
Directivity ($g_o = 4\pi A_o \eta_i/\lambda^2$)	1800, 33 dB
Power gain ($g_p = \eta_r g_o$)	450, 27 dB

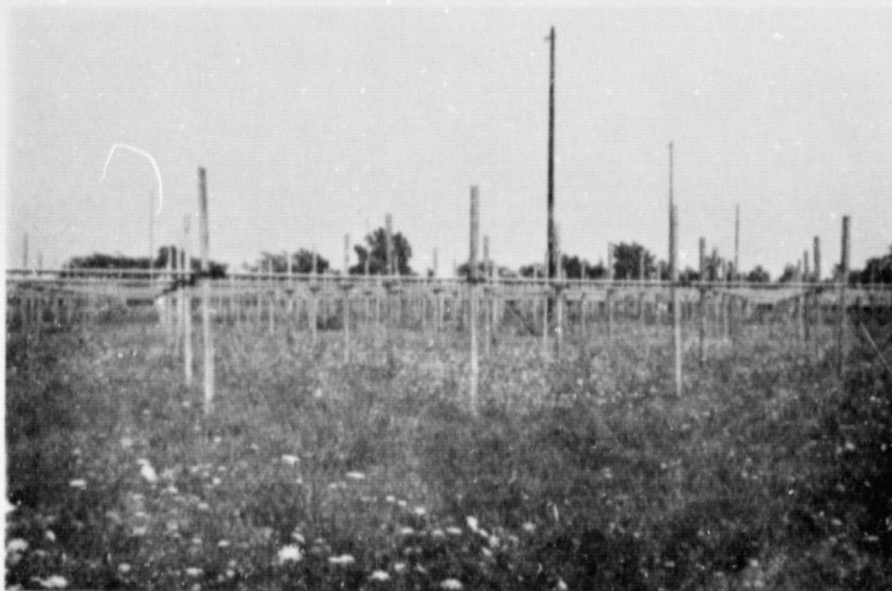


Figure 2.3 (a) Overhead view of coherent-scatter antenna. The group of utility poles in the center of the figure form a reference line toward the south. The transmission line to the transmitter appears at the right of the figure. (b) Ground-level view of the coherent-scatter antenna.

ORIGINAL PAGE IS
OF POOR QUALITY

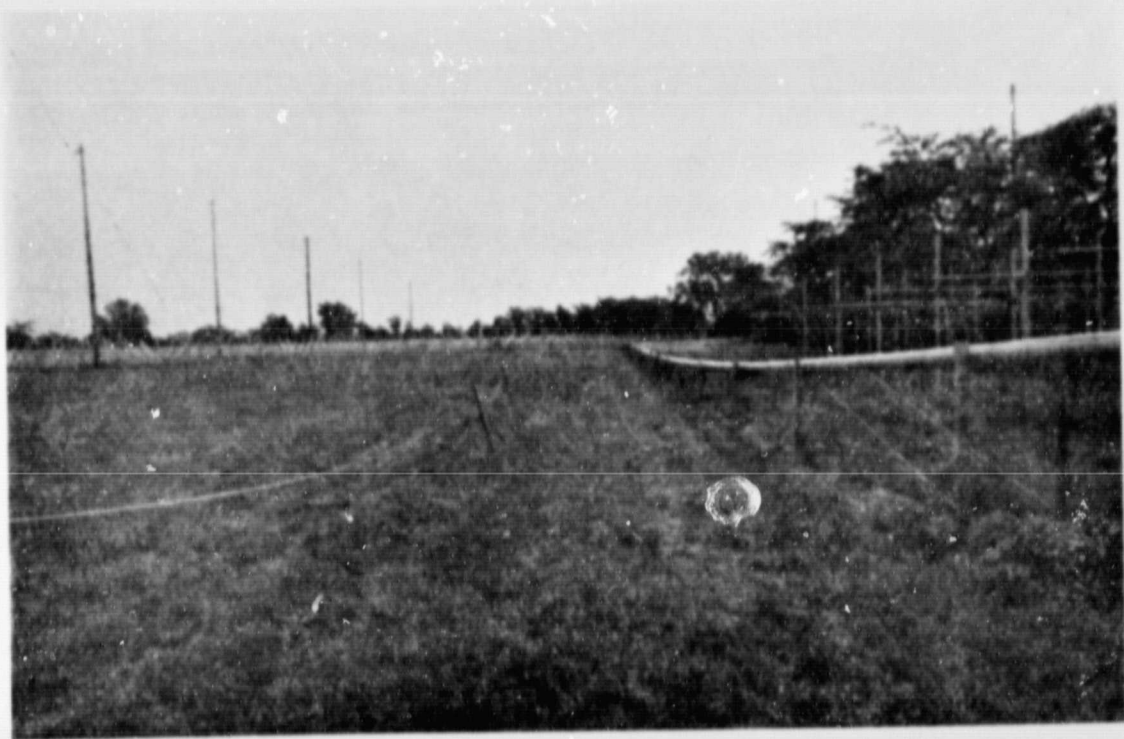


Figure 2.4 Feedline for the coherent-scatter system. Twin seven-inch coaxial lines run approximately 450 feet from the switch shed to the antenna. The meteor-radar antenna can be seen at the right of the figure.

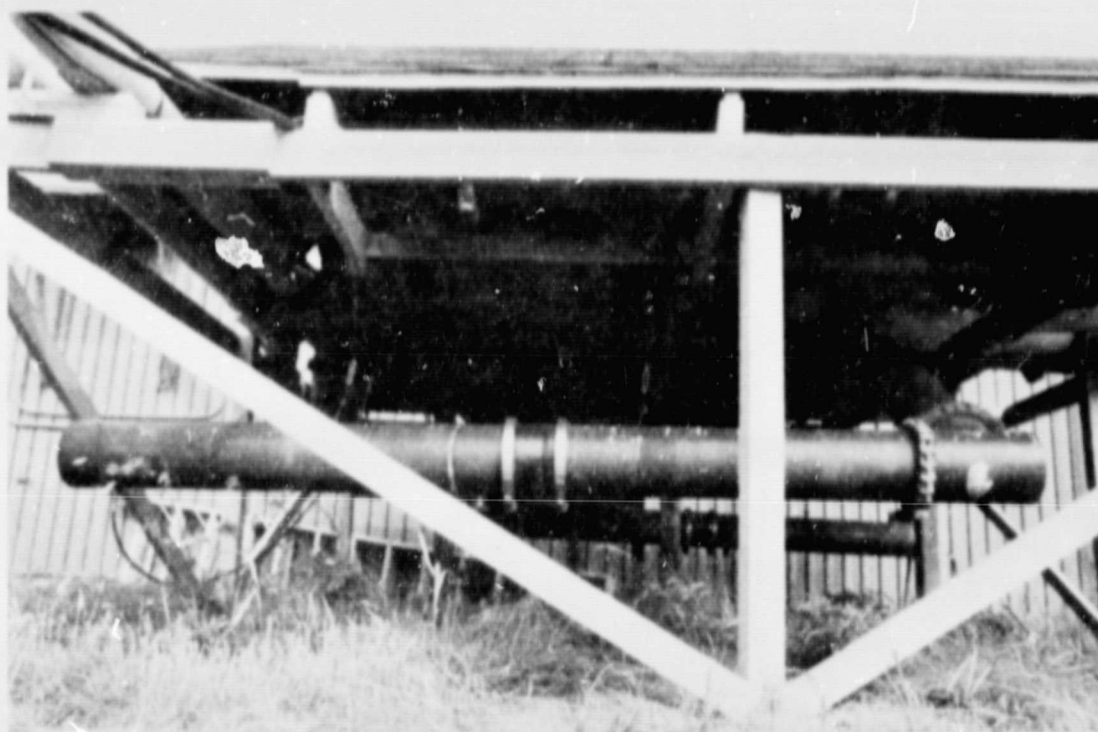


Figure 2.5 Bottom view of switching shed. The output to the coherent-scatter antenna is at the right center of the figure while the output to the mirror-radar antenna is at the upper left. The metallic bands in the center of the foreground delineate one of the four tubes used in the transmit/receive switch.

constructed. The blanker utilizes PIN diodes to provide low insertion loss and high power handling capability. A low noise preamplifier immediately follows the blanker and essentially determines the noise figure of the system. The blanker/preamplifier unit is located roughly 60 feet from the receiver in order to minimize the degradation in noise figure due to coaxial cable between the T/R switch and receiver. Information on the blanker is contained in Appendix I.

The receiver is single conversion with a bandwidth of 230 kHz centered around 40.92 MHz. A toggle-switch attenuator is located between the mixer and the IF section to provide control of signal levels at the 5.5 kHz IF frequency. The receiver output is amplified and applied to two four-quadrant multiplier chips which also receive the appropriate quadrature phase references at 5.5 MHz generated by the radar director. The quadrature-detected signals are filtered to reduce the bandwidth to 75 kHz. An additional outboard filter is added for coherent scatter to bring the bandwidth down to 40 kHz. A detailed description of the receiver and phase detector is given by *Hess and Geller, 1976*].

2.3 Data Processing Hardware

Analog-to-digital conversion for the Urbana radar is performed by a Hewlett Packard 5610 converter. The 5610 is a 10-bit A/D converter operating at 100 kHz with an accuracy of $\pm \frac{1}{2}$ LSB. A 16-channel multiplexor is also provided. Control of the converter is performed by an outboard sequencing circuit and several mode switches on a custom built interface.

The majority of the data processing for the Urbana radar system is accomplished by the Digital Equipment Corporation PDP-15 computer located at the field station. The PDP-15 contains 32K of core memory, an extended arithmetic element for hardware multiply and divide, a real-time clock and a high-speed data channel for input/output. In addition, four DECtape units provide medium speed bulk storage while four fixed-head disks are used for high-speed storage and system software. Data transfer to other computers can be accomplished using the high-speed paper tape reader/punch. A General Electric Terminet 1200 teletype producing hard copy at 120 characters per second and an Infoton cathode-ray terminal operating at 9600 baud provide the operator interface.

The plotting for the coherent-scatter experiment is performed on a Hewlett Packard 9830A desktop computer. The 9830A is a small, slow general-

purpose machine which utilizes a BASIC interpreter in ROM. Additional ROM chips for string variables, matrix operations, paper tape reader control and plotter control extend the capabilities of the computer. The 9830A at the Aeronomy Laboratory contains 16K of RAM and a single digital tape cassette unit which is an integral part of the computer. Digital cassettes are used for both program and data-file storage.

2.4 Software

2.4.1 *Theory.* The purpose of the system software is to produce echo power and velocity measurements at the desired sample heights. The power and velocity information can be obtained from either time domain or frequency domain information by finding respectively the autocorrelation function or the power spectrum. The frequency spectrum approach utilizes narrowband filters to obtain the energy at various frequencies. The output of the filters is then sampled and digitized. In the time domain approach used at Urbana the phase detector outputs are sampled and autocorrelated digitally.

The phase detector output consists of both noise and signal components. Furthermore the noise and signal are uncorrelated so that the autocorrelation of the sum of signal and noise is the sum of the autocorrelations of each component taken separately. The signal energy is concentrated about the Doppler frequency of the returned signal while the noise has a band-limited spectrum. Thus the signal is correlated for times much longer than the correlation time of the noise and as *Woodman and Guillen* [1974] showed the signal is correlated for times longer than the interpulse period while the noise is not. The process of coherent integration where the samples taken on successive pulses are added can thereby improve the signal-to-noise ratio of the resulting sum. The coherent integration period is chosen as a compromise between improvement in signal-to-noise ratio and time resolution in the autocorrelation process which follows.

The power in the returned signal can be calculated from the zeroth lag of the signal autocorrelation. If $R(\tau)$ is the autocorrelation of a process $x(t)$ then considering the definition

$$R(\tau) = E\{x(t + \tau) x^*(t)\} \quad (2.1)$$

one has with $\tau = 0$

$$R(0) = E\{x(t) x^*(t)\} = E\{|x(t)|^2\} \quad (2.2)$$

which is an expression for the power. However, as pointed out above the

noise will contribute primarily at the zeroth lag of the total autocorrelation. If the noise power is assumed constant over the sampled altitudes and slowly varying then changes in power calculated from the zeroth lag of the total autocorrelation function will be due to changes in signal power. Relative fluctuations in power over altitude and time are therefore measured.

The motion of the scattering regions can be measured using the Doppler shift of the returned signal. If V_p is the radial velocity of the scattering region and f_d is the Doppler frequency then

$$f_d = \frac{2V_p}{\lambda} \quad (2.3)$$

where $\lambda = 7.33$ meters is the radar wavelength. Hence

$$V_p = \frac{\lambda f_d}{2} = \frac{\lambda \omega_d}{4\pi} = \frac{\lambda}{4\pi} \cdot \frac{d\phi}{dt} \quad (2.4)$$

where ω_d is the radian Doppler frequency, and ϕ is the phase of the autocorrelation function. To estimate $\frac{d\phi}{dt}$ one recalls that $\phi(0) = 0$, i.e. the autocorrelation is real at the zeroth lag by definition. So one has the following:

$$\frac{d\phi}{dt} = \left. \frac{\phi(t_2) - \phi(t_1)}{t_2 - t_1} = \frac{\phi(t_2)}{t_2} \right|_{t_1 = 0} \quad (2.5)$$

A weighted average of the values calculated at lags one to three is used to obtain the velocity measurement.

2.4.2 Data collection. The first state of data processing for the Urbana radar consists of data collection and reduction to autocorrelation functions in real time. There are four distinct processes which occur in real time: input, coherent integration, correlation and averaging. These four tasks are interlaced by the software in such a way that the latter three are interrupted whenever the analog to digital converter is sampling. The characteristics of the data collection process are discussed below.

The altitude region of interest for the coherent-scatter experiment is from 60 to 90 km, or a 30 km interval. The altitude interval determines the number of samples in the following manner: the distance to a scatterer is determined by measuring the time taken by the radar pulse to travel to the scatterer and return. One has

$$R = \frac{ct}{2} \quad (2.6)$$

where R is the range, c the speed of light and t the time for the wave to travel up and back. A time difference of $\Delta t = t_2 - t_1$, between sample pulses results in a range resolution ΔR given by

$$\Delta R = \frac{c(t_2 - t_1)}{2} \quad (2.7)$$

The 10- μ sec conversion time of the analog-to-digital converter therefore corresponds to a range resolution of 1.5 km and 20 samples are required to cover the 30 km region of interest.

The cosine and sine channels of the phase detector are sampled on alternate radar pulses requiring a pair of pulses to obtain a complex sample at each of the 20 heights. With the pulse repetition frequency of the radar at 400 Hz a pulse pair requires 5 msec. Twenty-five such pairs of pulses fill an input buffer after 1/8 second. The input is double-buffered so that data collection can continue on an interrupt basis while processing occurs.

The coherent-integration process adds the corresponding complex values at each height reducing the twenty-five complex sample sets to a single set of twenty complex values. Note that the twenty-five additions can add no more than five bits to the ten-bit words from the analog-to-digital converter so that fifteen-bit words are produced. Single-precision addition which saves processor time is therefore possible on the 18-bit PDP-15. The process of coherent integration is illustrated in Figure 2.6.

The data from the most recent 1/8-second coherent integration interval is correlated with data from the previous intervals. Consider a stack of data sets, each set containing twenty coherently integrated complex samples. After each 1/8-second period the latest set of samples is pushed onto the top of the stack into the present time slot while the oldest data are lost at the bottom of the stack. Thus the complete complex autocorrelation for all lags and for each of the twenty heights must be completed during the 1/8-second coherent integration time. The speed of the PDP-15 allows a multibit-multibit complex autocorrelation to be performed out to lag 12, or to 1.5 seconds. The output of the complex autocorrelation function is a real value at lag zero, and real and imaginary values for lags 1 to 12. Twenty-five numbers are thus produced for each of the twenty heights every 1/8 second. The data are now double-length words as a result of multiplication during autocorrelation.

The autocorrelation functions are then converted to floating point and

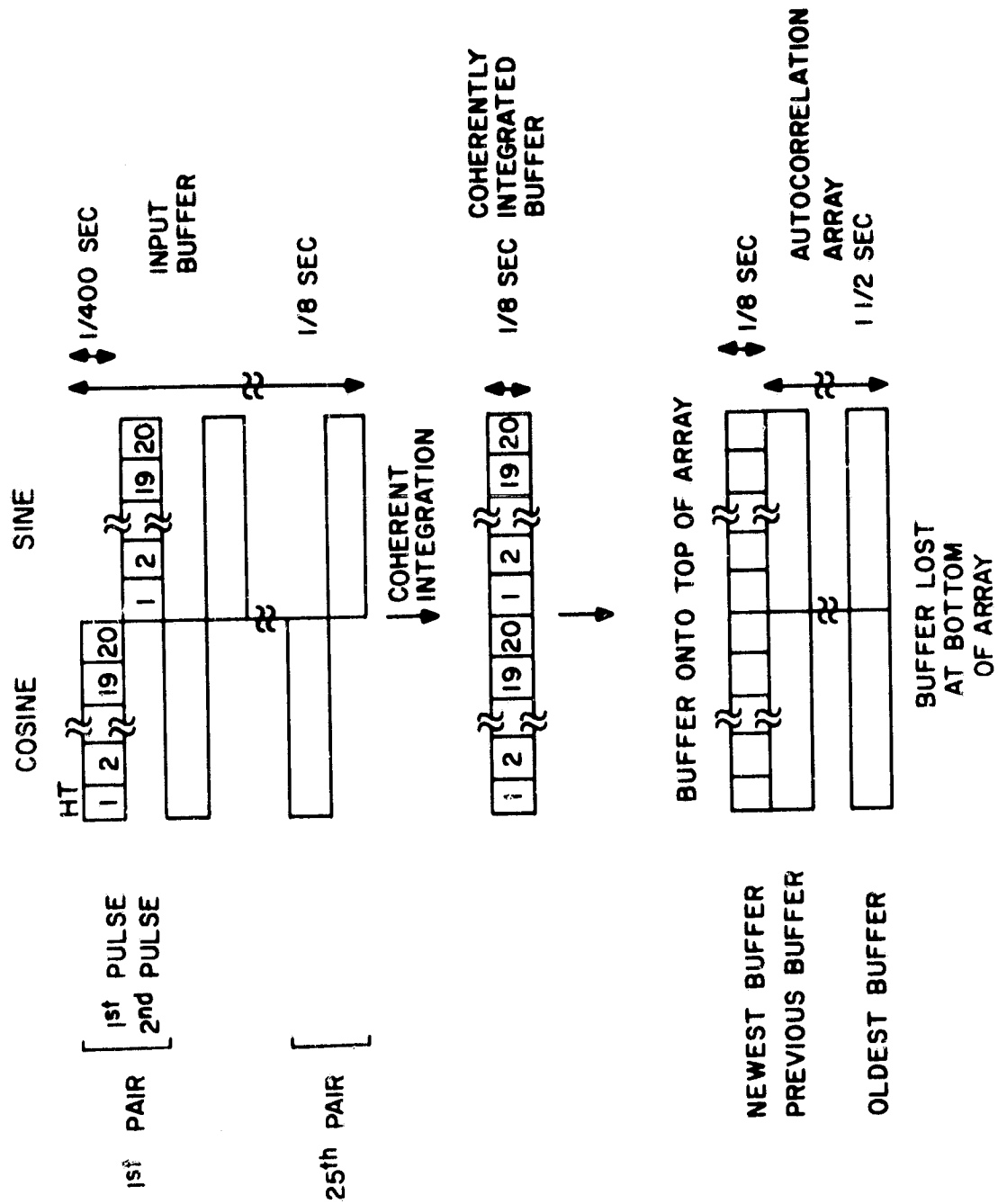


Figure 2.6 Illustration of the coherent-integration process.

PRECEDING PAGE BEING NOT FILMED

are averaged for one minute by adding. Four of the one-minute arrays formed by averaging are stacked to produce an output buffer which becomes a single record on disk. Three records form a file, and ten files fill the disk. There are three disks available so that after six hours the data collection terminates and the averaged autocorrelation functions are either processed or stored on DECTape for later processing. Data-collection programs are listed in Appendix III.

2.4.3 *Post processing and data transfer.* Upon completion of data collection the correlation functions stored on DECTape or disk are processed to obtain useful scientific information. At the present time values for the returned echo power and the velocity of the scattering region are calculated at each sample height for every minute. The output of these programs is to paper tape so that data may be transferred to the HP-9830 for plotting.

The power and velocity are calculated from the autocorrelation function as described previously. The logarithm of the power is punched onto paper tape to increase the dynamic range of the data which can be transferred. The velocity program tests the autocorrelation function for noise characteristics by comparing the amplitude of the autocorrelation at lags 1 through 3 to the real part of the autocorrelation at lag 0. If at a given lag the ratio is too small then that lag is not used in the velocity calculation. If all three lags fail the test a value of zero is punched onto the velocity tape as a signal to the plotter software that no velocity was calculated at that point. The post-processing programs are listed in Appendix IV.

2.4.4 *Plotter software.* The plotting of data from the coherent-scatter radar involves two stages: (1) transfer of data from paper tape to cassette tape, and (2) plotting of data from the cassette tapes. To store the data on cassette a paper tape containing two hours of power or velocity data are read into the HP-9830. Additional information which identifies the data are typed into the 9830. A cassette file is then formed from the data and identifying information. The use of cassette storage allows multiple use of the data file without the necessity of rereading the paper tape.

Three types of plots are made for each data set of two-hour duration. The velocity plot is one of velocity vs time at a given altitude. When the data exceeds an operator-controlled limit value or when the value zero occurs the data point is not plotted. Recall that zero was the signal value generated by the PDP-15 to indicate that no velocity value was calculated because

of the noise properties of the autocorrelation function. Two types of power plots are produced, the first being power vs altitude at a given time or power profiles. The power profiles show the variation in altitude of the scattered power but the temporal variation is best observed on the second plot, the power vs time at a given altitude. Both power plots employ a hiding routine to improve the readability by preventing crossings of the traces. Sharp increases in the power level which last for one minute are almost exclusively due to meteor echoes. These bursts of power tend to hide the scattered power values on the power profiles. A limit routine which clips one minute spikes to an operator controlled value helps minimize the meteor contamination of the power profile. Examples of these plots are shown below in Chapter 3. The plotting routines are given in Appendix V.

3. MESOSPHERIC COHERENT-SCATTER OBSERVATIONS AT URBANA

3.1 *Observation Program and Introductory Remarks*

The Urbana coherent-scatter radar was first operational on a day-to-day basis in April, 1978. Extensive data collection occurred in that month often on a sunrise to sunset basis. The collection of data continues at present so that a data base can be accumulated. As of January, 1979 242 hours of coherent-scatter data from the mesosphere has been collected on 34 days.

The figures shown in the sections which follow are not above average in their measurement quality. No smoothing is employed to obtain what appear to be continuous curves: rather the time resolution of the system, one minute as mentioned earlier, is sufficient to yield the plot quality obtained. The figures, however, are chosen to illustrate in a concise manner features of the observed data. Data from Urbana of a similar nature has been shown in *Miller et al.* [1978].

3.2 *Echo Power Data*

Power data from April 21, 1978 is shown in Figure 3.1. The presentation in this figure has been referred to earlier as power vs altitude at a fixed time, or power profiles. The areas of no returned signal power, generally below 66 km but not limited to this region, appear as essentially flat, evenly spaced lines. The bumps in the profile therefore exhibit power levels above the noise. In Figure 3.1 the power from the scattering regions is roughly 3 to 5 dB above the noise with the possible exception of the scattering region at 87 km at the end of the two-hour period. Activity such as is shown would be considered characteristic of a quiet day.

Note further the nature of the scattering regions during the two-hour period. A region centered at 69 km is steady for the entire period. A second layer near 73.5 km seems to drift slowly downward perhaps merging with the layer below by 1030 CST. Finally, a third distinct echoing layer appears at 79.5 km near 940 CST. The scattering regions in Figure 3.1 are well defined, change slowly or not at all in altitude, and can appear and disappear abruptly.

A more active day, April 11, 1978 is shown in Figure 3.2. The echo power is often 10 dB above the noise at altitudes above 69 km and scattered power is observed even at the lowest altitudes. The scattering regions appear more mobile particularly at the lower altitudes. Furthermore, it is not clear when the lowest layer near 63 km has disappeared. At 915 CST the

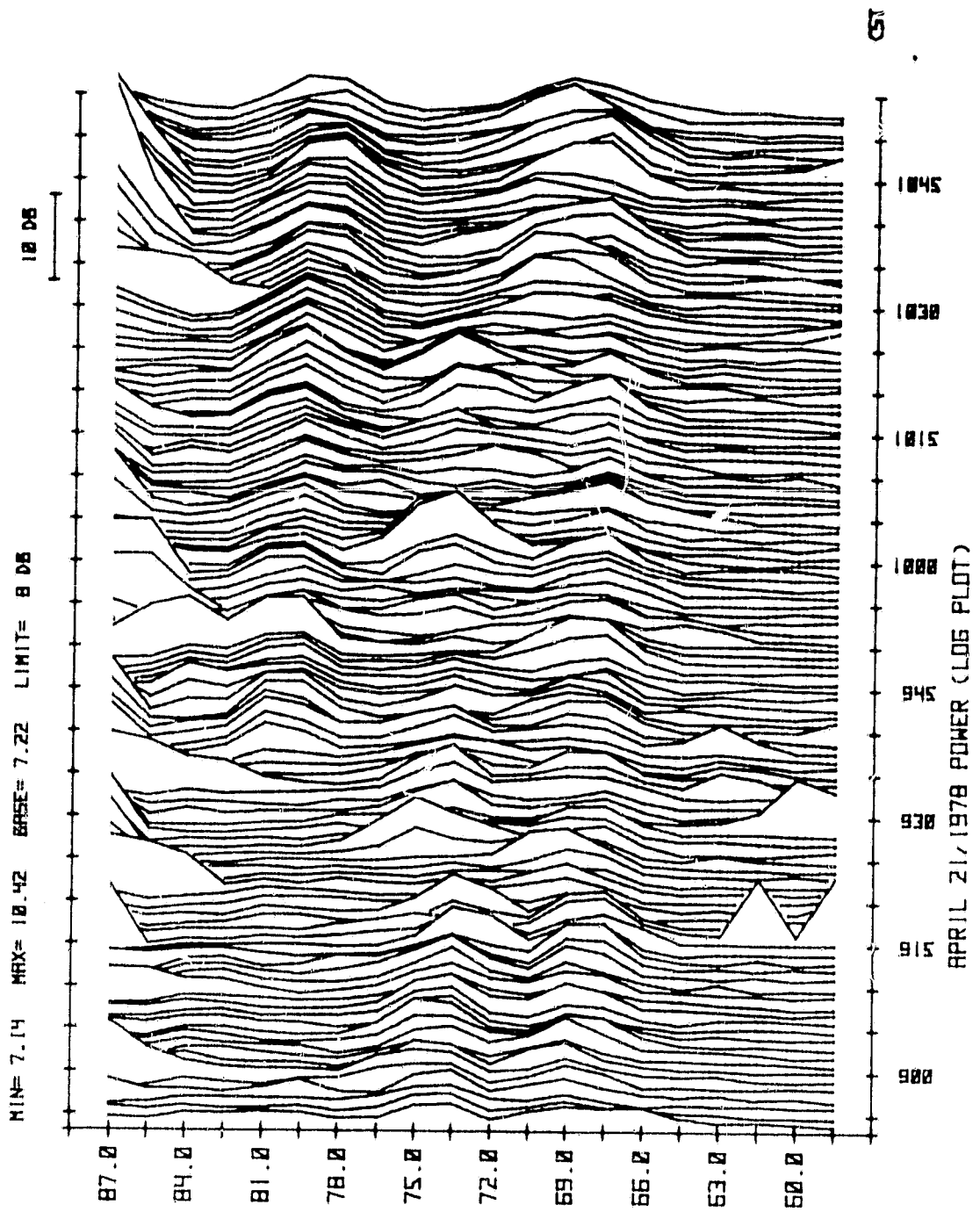


Figure 3.1 Vertical profile of scattered power at Urbana beginning at 854 CST on April 21, 1978.

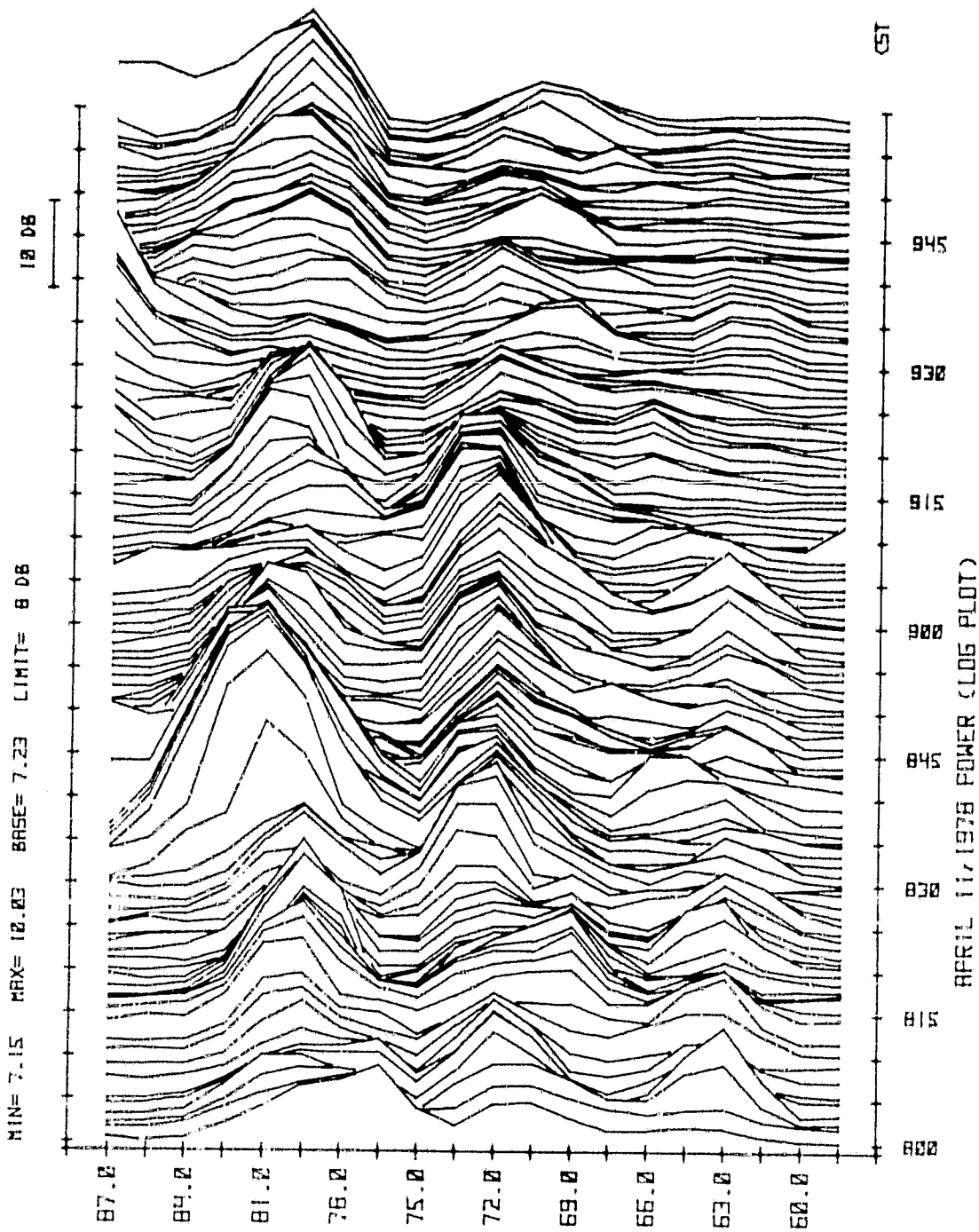


Figure 3.2 Vertical profile of scattered power at Urbana beginning at 800 CST on April 11, 1978.

APR 11 1978
POWER QUALITY

layer begins to merge with the layer above at 72 km but at 930 CST briefly reappears as a very weak scatterer only to be gone again by 945 CST. The high scattered power values obtained in Figure 3.2 are due to a solar flare which occurred shortly before the data set shown, at 740 CST.

An unusual example of variability is shown in Figure 3.3 from May 18, 1978. Note the slightly higher altitude of the plot exposing the region above 87 km alluded to in the previous examples. The highest region exhibits wide changes in scattered power. Furthermore, a lower power region directly below, at 82.5 km, seems to increase in power out of phase with the region above. The lower scattering layers, near 72 km, do not show the degree of change of the higher altitude layers.

3.3 *Velocity Data*

The wave nature of ionospheric dynamics is observed in Figures 3.4 and 3.5. The velocities shown here correspond to the power plots of Figures 3.1 and 3.2 respectively. Velocity data for April 21, 1978, Figure 3.4, indicates low amplitude oscillatory behavior particularly at 930 CST. Comparing the velocities with the power data in Figure 3.1 one observes that when the returned power is high the velocity curves are continuous. More precisely, if the autocorrelation function is very noisy due to low returned signal power then the velocity obtained from the autocorrelation function is not plotted. Generally the one-minute time resolution is adequate to produce smooth velocity curves. When higher frequency waves are present with high relative amplitude however, the rough velocity curve observed at 87 km is obtained. Note also that the mean value of the velocity for the two-hour period is negative, particularly at lower altitudes. The non-zero value of the mean indicates a horizontal component of velocity corresponding to the off-vertical pointing direction of the radar.

Higher amplitude velocities are observed in Figure 3.5. Again waves are readily observed, with an eight-minute period wave the predominant component. It should be noted that for the two examples given, the higher amplitude velocities correspond to the day with greater overall scattered power. Generally the more active days tend to produce higher velocities; however a few counter examples have been observed. Hour-to-hour variations in the scattered power do not appear to affect the nature of velocities obtained but rather the continuity of the plot as explained above.

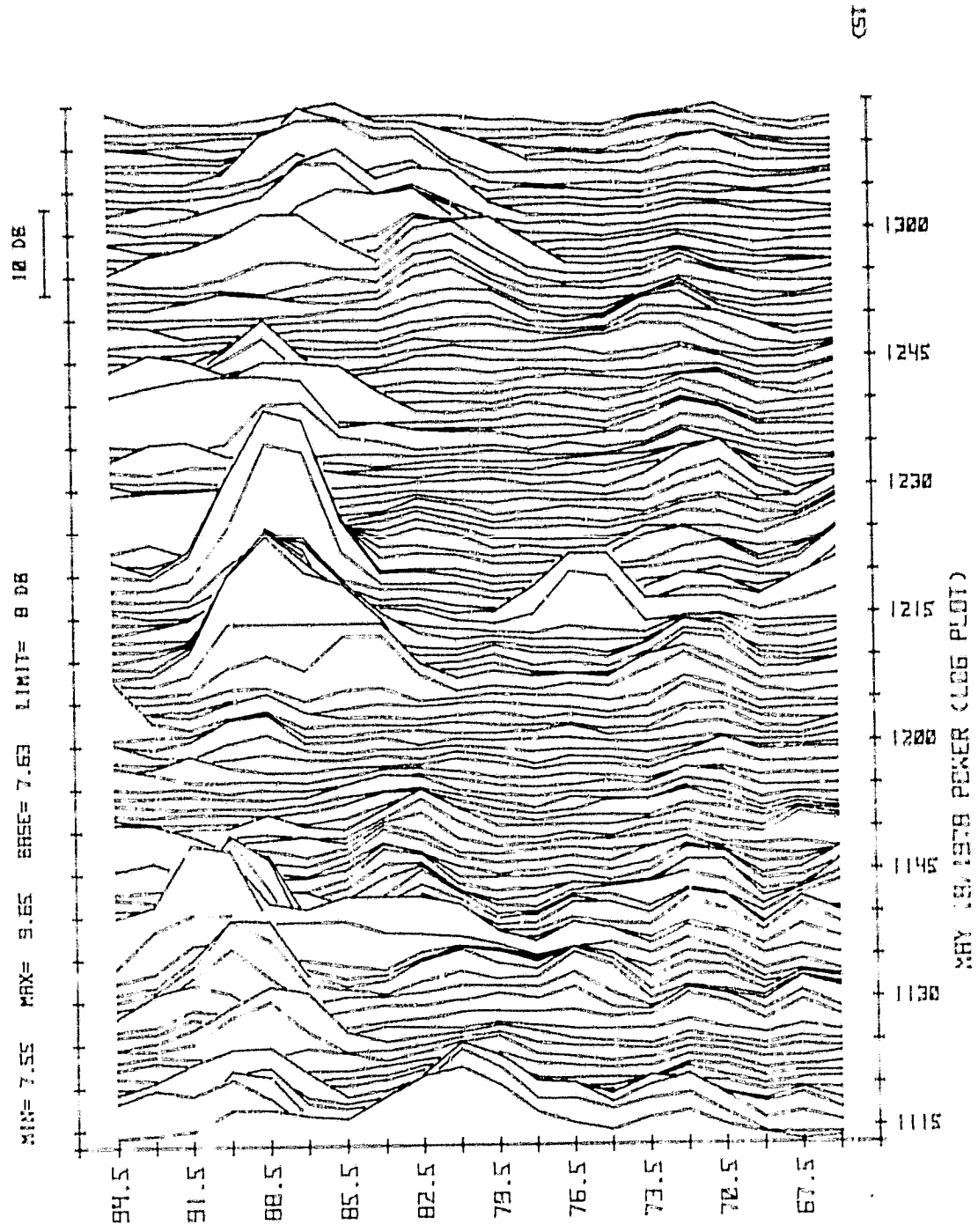


Figure 3.3 Vertical profile of scattered power at Urbana beginning at 1114 CST on May 18, 1978.

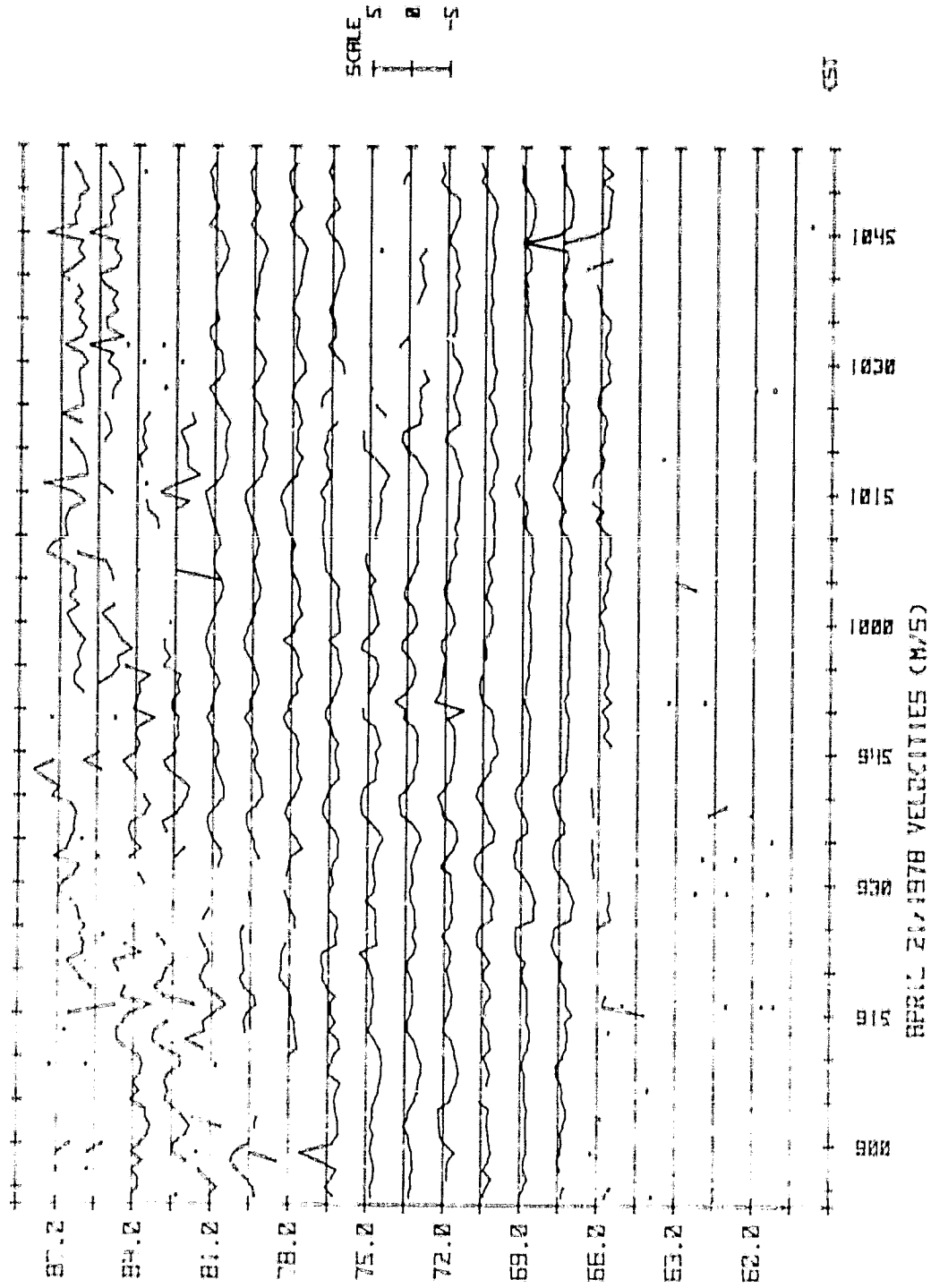


Figure 3.4 Line-of-sight velocity at Urbana beginning at 854 CST on April 21, 1978.

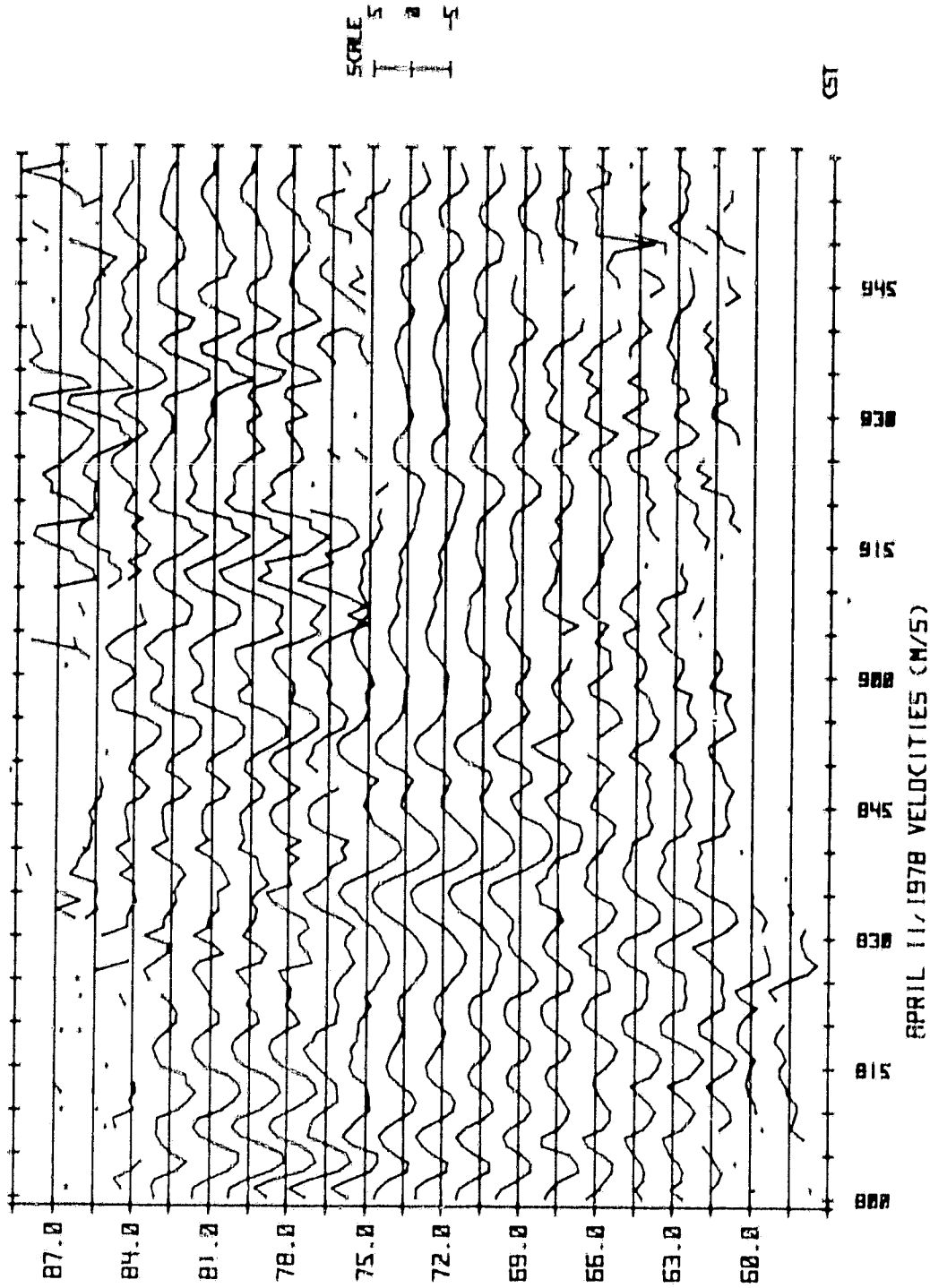


Figure 3.5 Line-of-sight velocity at Urbana beginning at 800 CST on April 11, 1978.

An additional feature of the velocity data is illustrated by a plot from April 13, 1978, Figure 3.6. Comparatively high velocities are observed throughout the two-hour period with examples of several frequencies of waves apparent. Of special interest in this figure is the evidence for vertical standing waves. Consider 1107 CST and examine the velocity as a function of altitude. The velocity changes sign at this time between 81 and 79.5 km and again at 69 km. The same behavior is readily observed at 1150 and 1210 CST. Similar evidence for vertical propagation of gravity waves occurs in other data sets.

3.4 *Observations of an Entire Day*

The data sets discussed above are two-hour segments which illustrate important aspects of the observations. Any physical processes which occur at longer periods however require the study of observations taken throughout the day. For this purpose the complete set of observations for May 24, 1978 are shown in Figure 3.7 to Figure 3.21. The plots are in three groups; 1. the power profiles, 2. the plots of power vs time at fixed altitude, and 3. the velocity plots. The data is continuous from 812 CST to 1820 CST save for a seven-minute transmitter failure at 843 CST and eight minutes at 1412 CST required to dump the data onto tape.

Comparison of Figures 3.7 and 3.12, the two power plots beginning at 812 CST, shows the manner in which the power plots complement each other. The power profiles in Figure 3.7 at 900 CST and 87 km are hidden so that one must use Figure 3.12 to determine how quickly the power level decreased. In addition, the software limiting routine apparent at 925 CST in Figure 3.7 is set to a low value so that the maximum readability of the power profiles is obtained. The same limiting routine is available on the power vs time at fixed altitude plots but is generally not employed so that the full value of one-minute peaks appear as in Figure 3.12. From the second plot one can judge if data have been clipped and if so the limit value is changed and a new plot obtained.

The data from May 24, 1978 show an active day. The velocities are high in amplitude and show many different frequencies, some with periods as long as twenty minutes. From 1315 to 1415 CST evidence of vertical propagation can be observed as wave crests occur at progressively later times for different altitudes. Finally, consider the scattering region between 84 and 94 km.

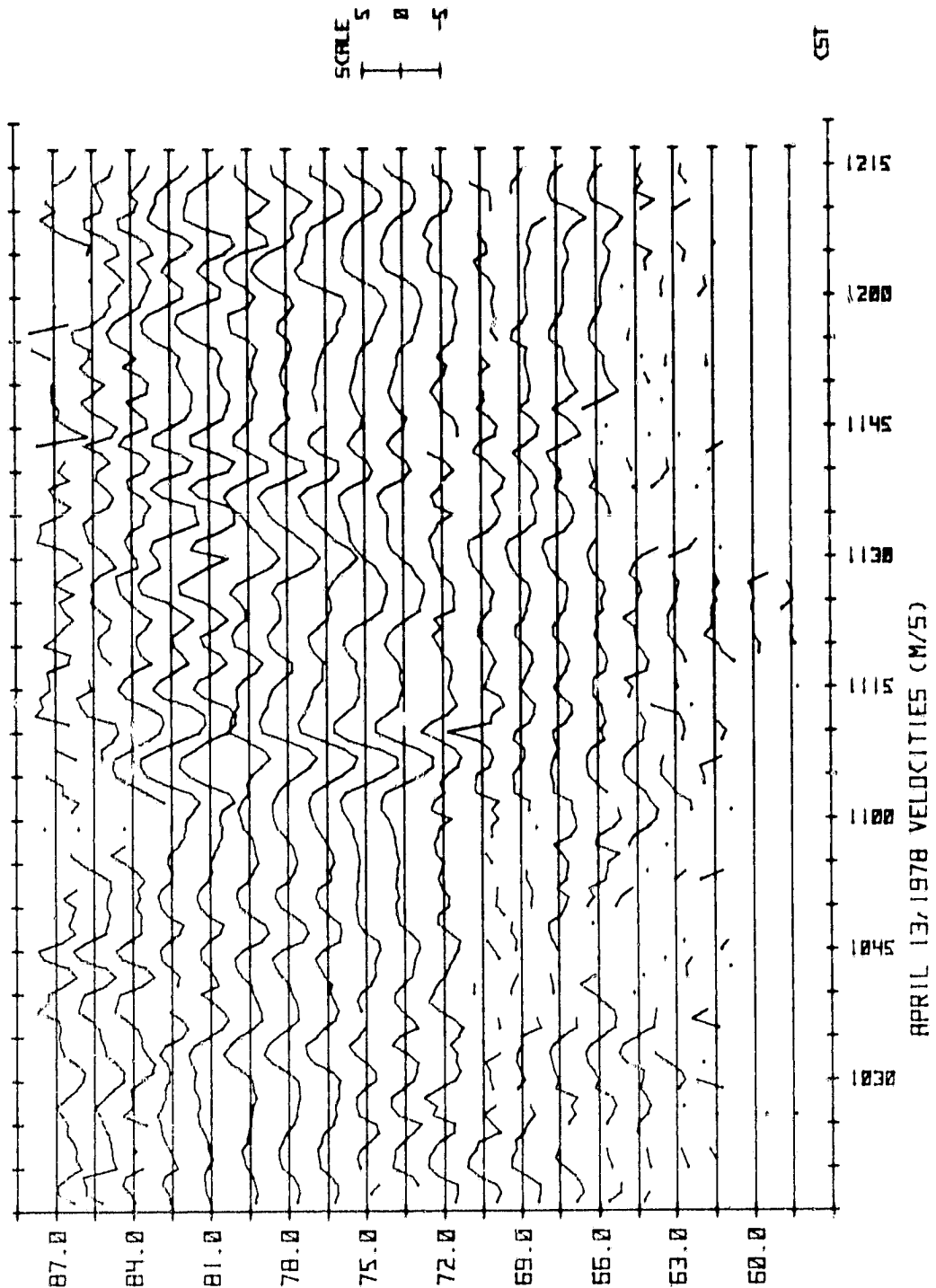


Figure 3.6 Line-of-sight velocity at Urbana beginning at 1016 CST on April 13, 1978.

ORIGINAL PAGE IS
OF POOR QUALITY

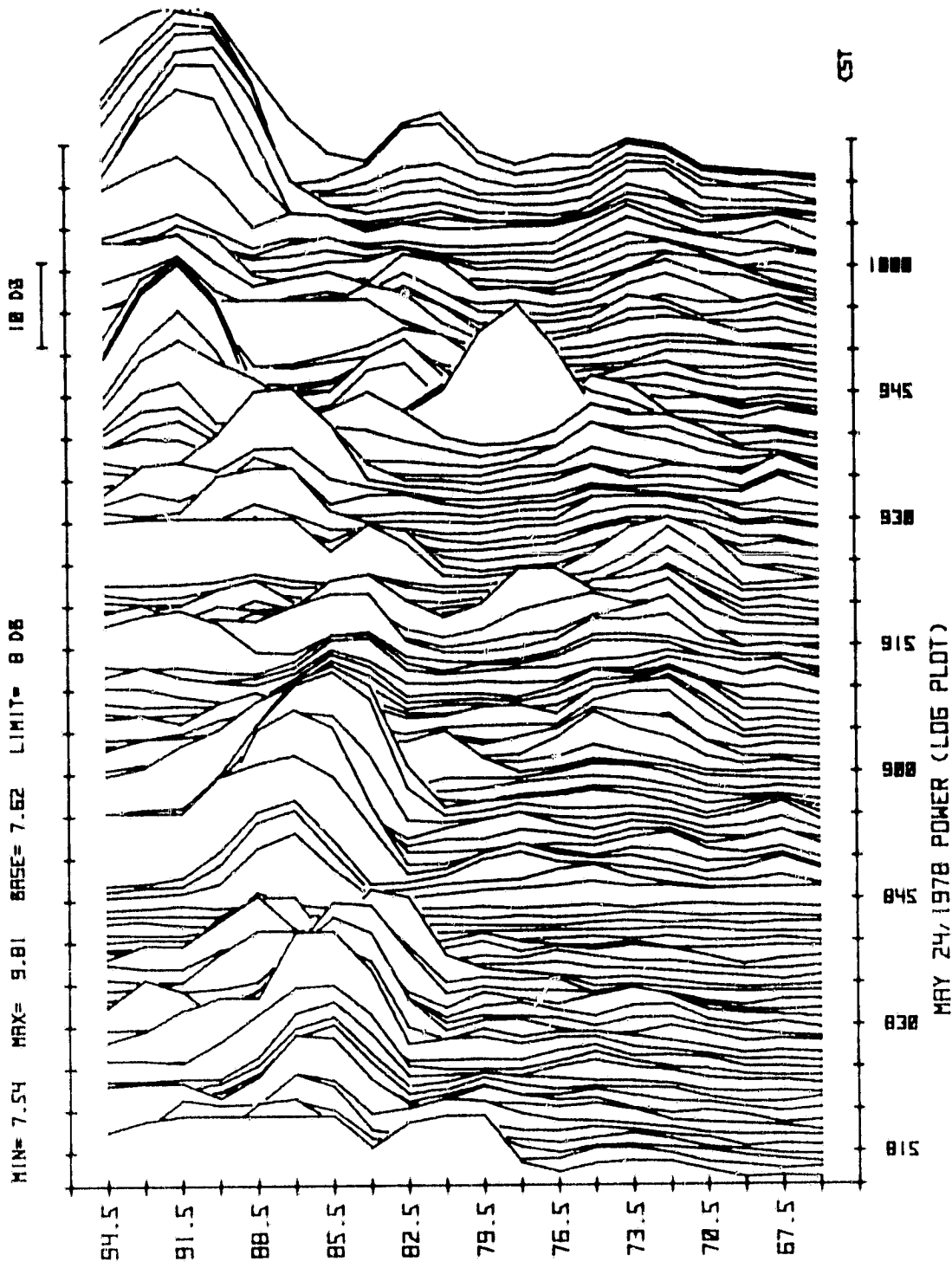


Figure 3.7 Vertical profile of scattered power at Urbana beginning at 812 CST on May 24, 1978.

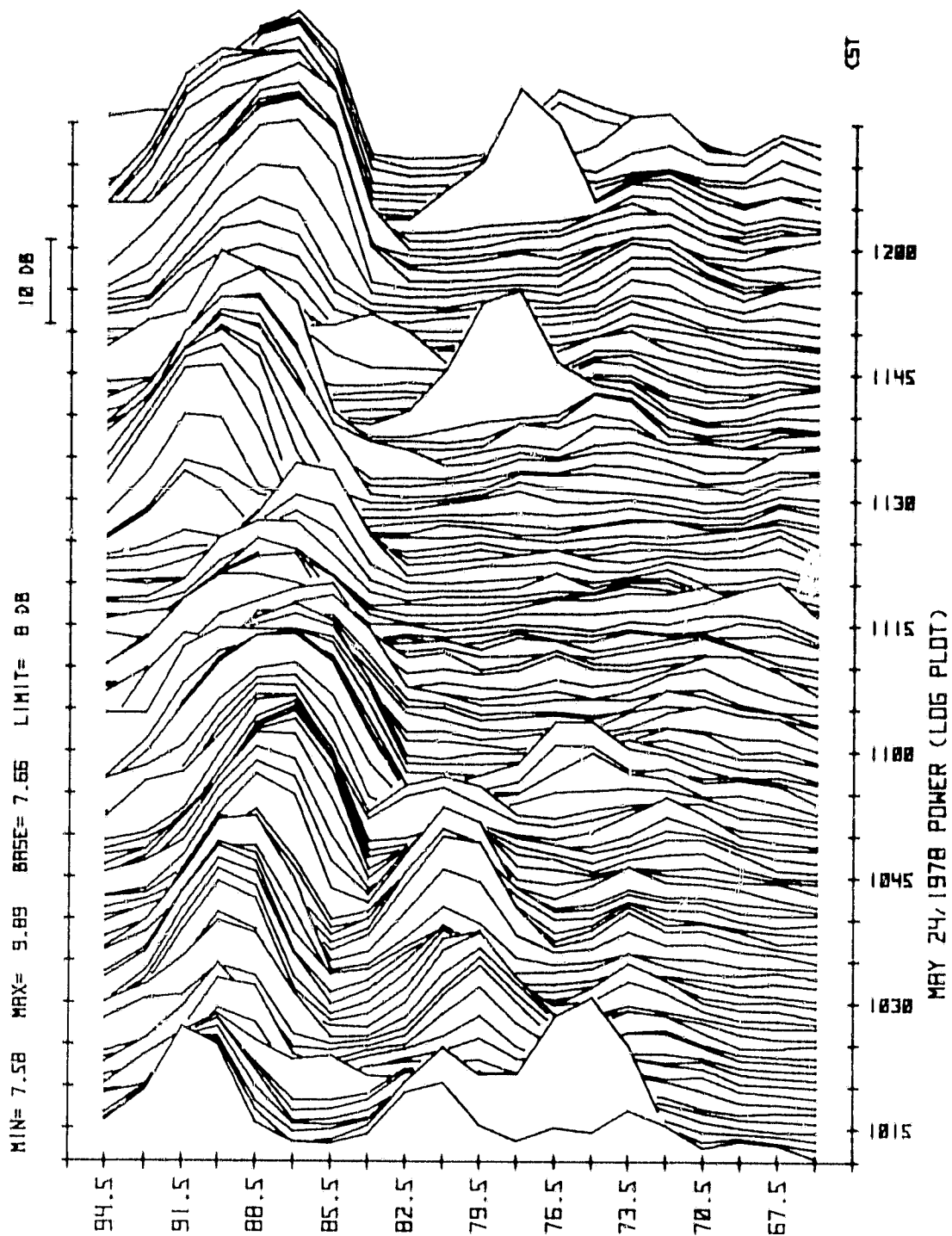


Figure 3.8 Vertical profile of scattered power at Urbana beginning at 1012 CST on May 24, 1978.

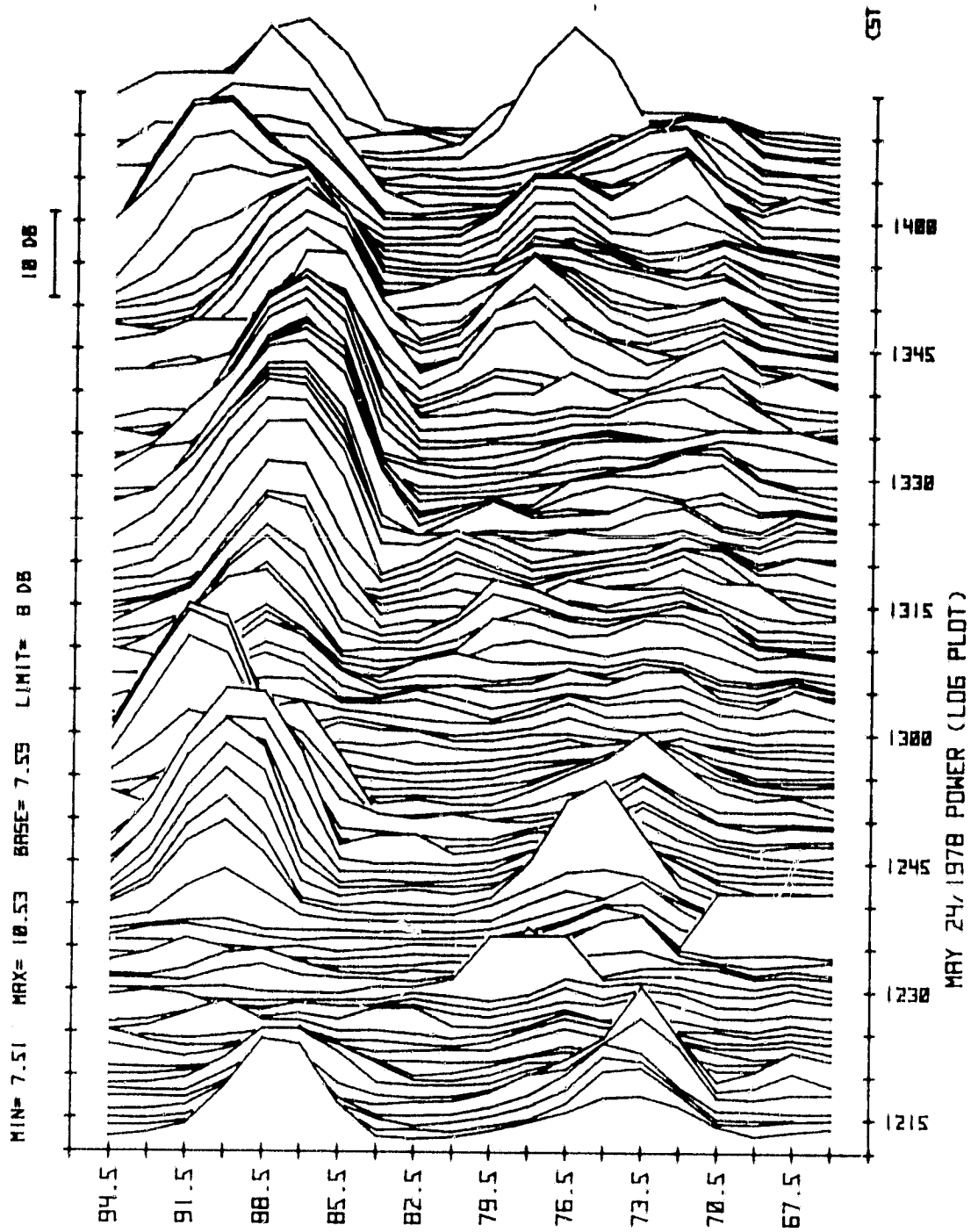


Figure 3.9 Vertical profile of scattered power at Urbana beginning at 1212 CST on May 24, 1978.

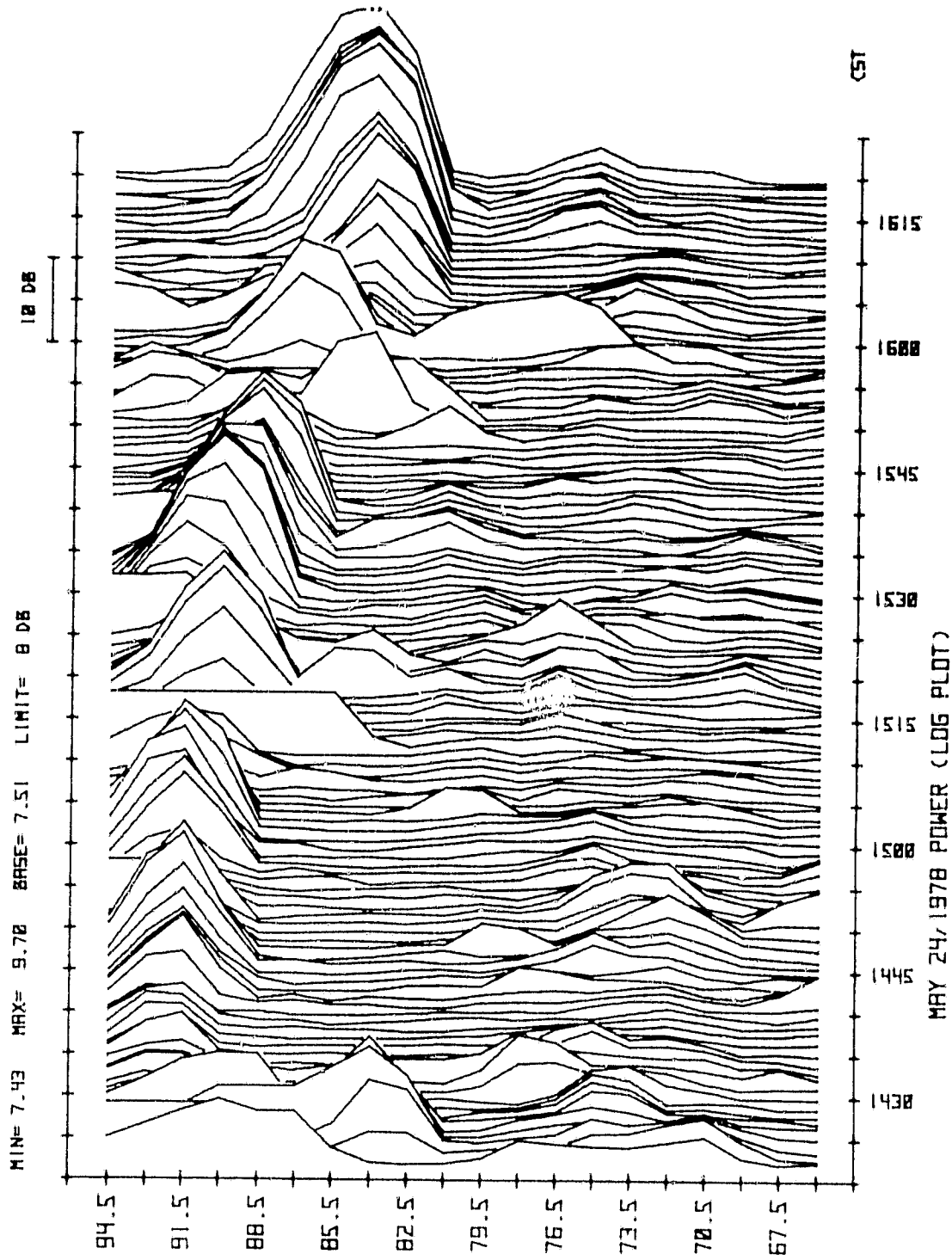


Figure 3.10 Vertical profile of scattered power at Urbana beginning at 1421 CST on May 24, 1978.

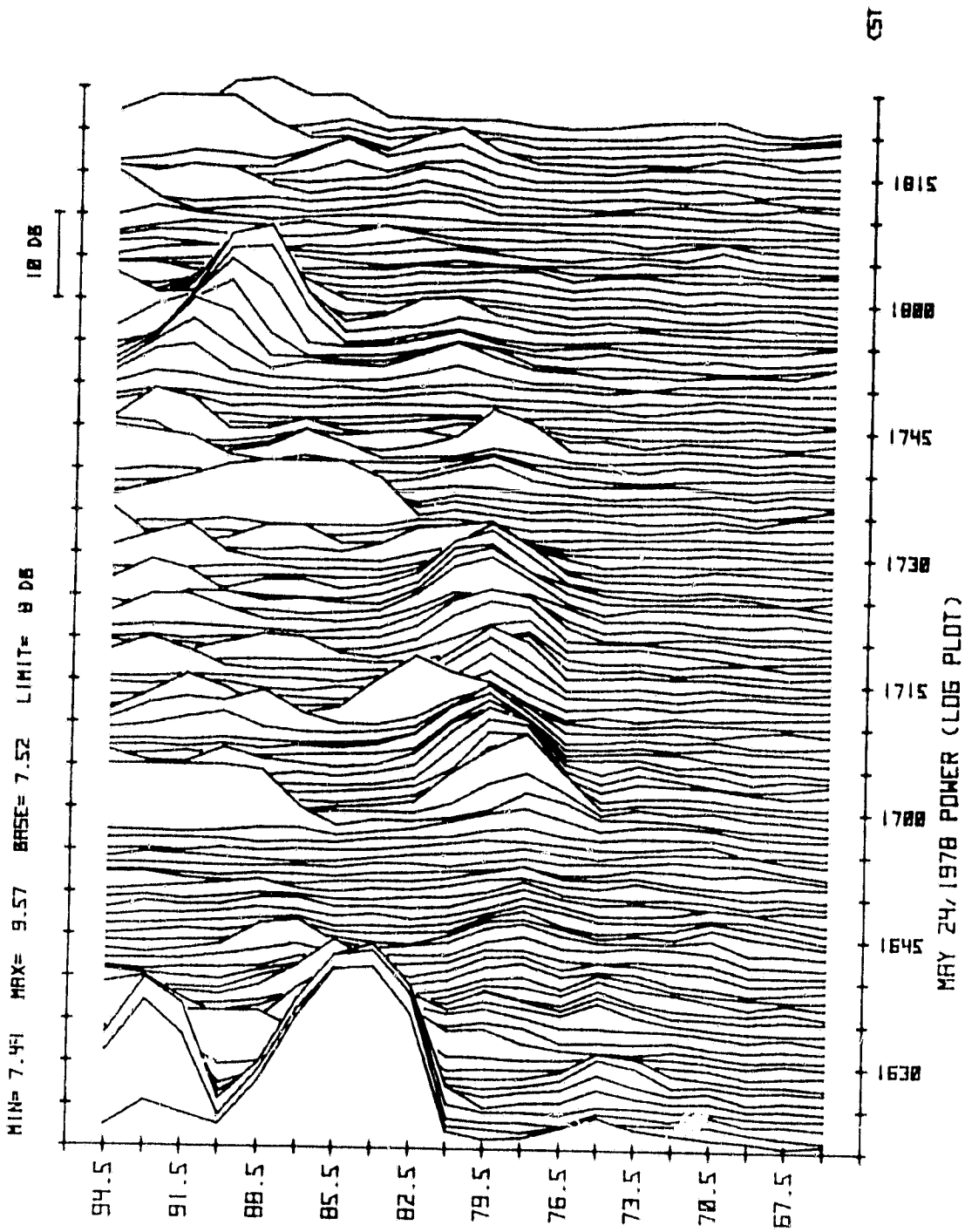


Figure 3.11 Vertical profile of scattered power at Urbana beginning at 1621 CST on May 24, 1978.

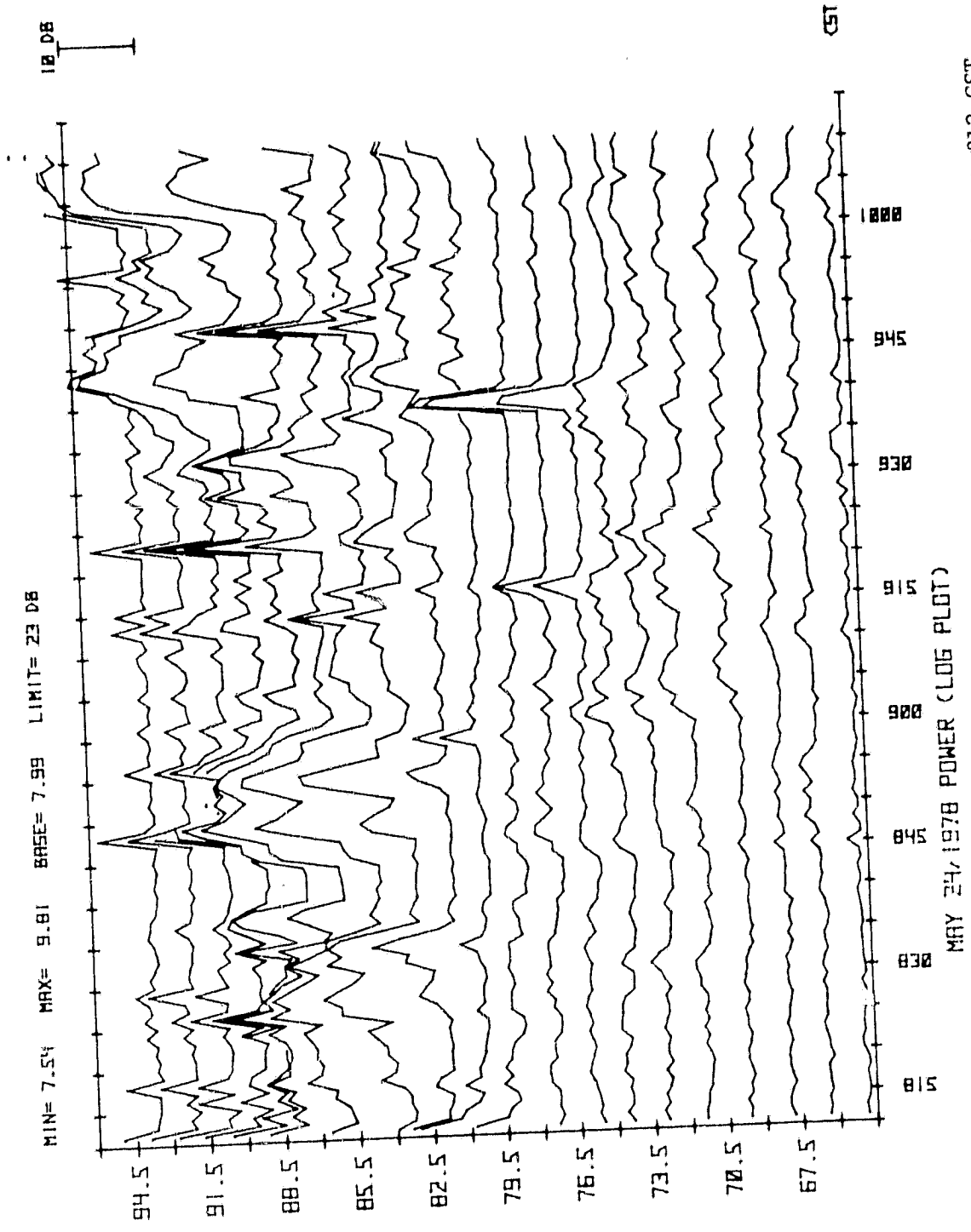


Figure 3.12 Horizontal profile of scattered power at Urbana beginning at 812 CST on May 24, 1978.

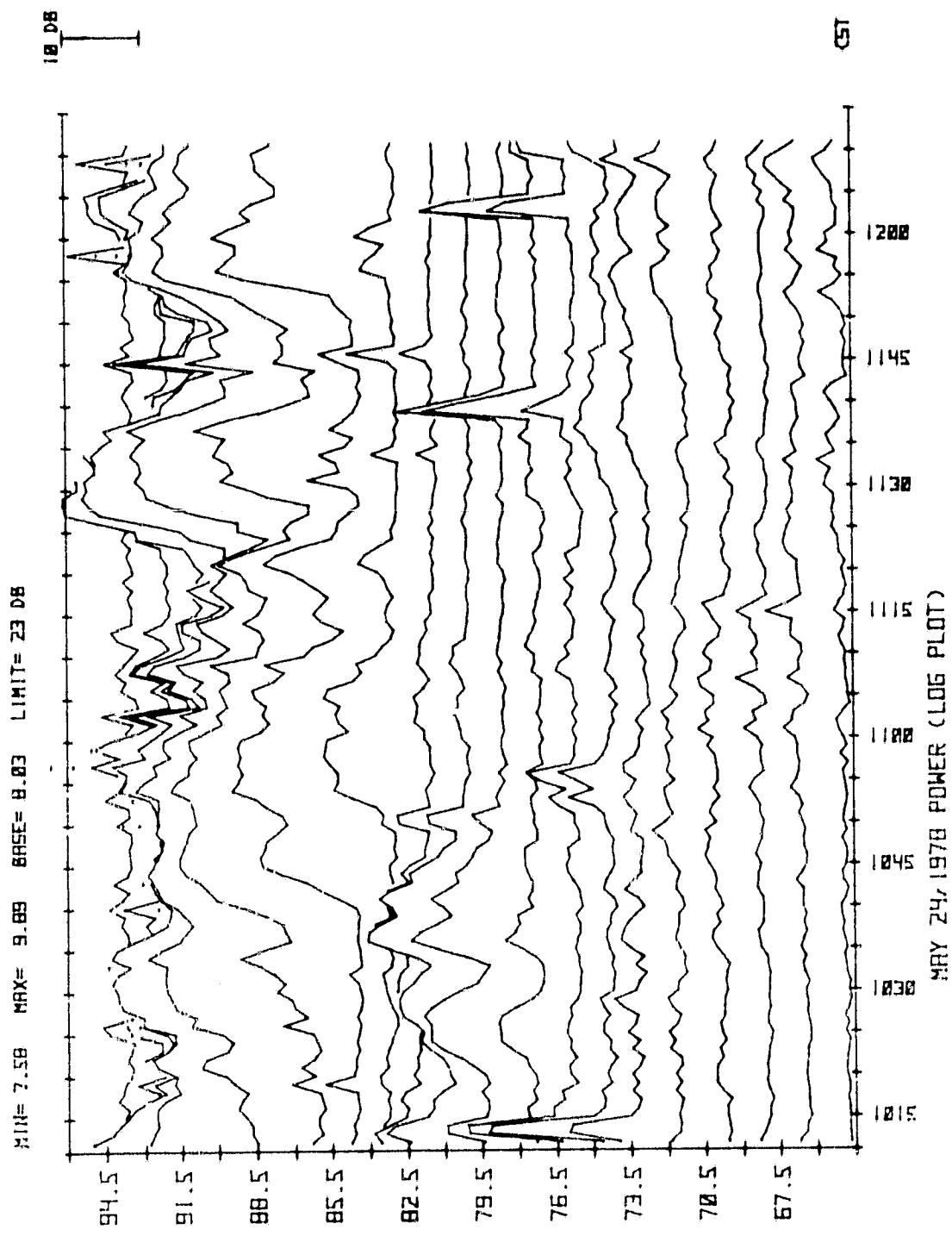


Figure 3.13 Horizontal profile of scattered power at Urbana beginning at 1012 CST on May 24, 1978.

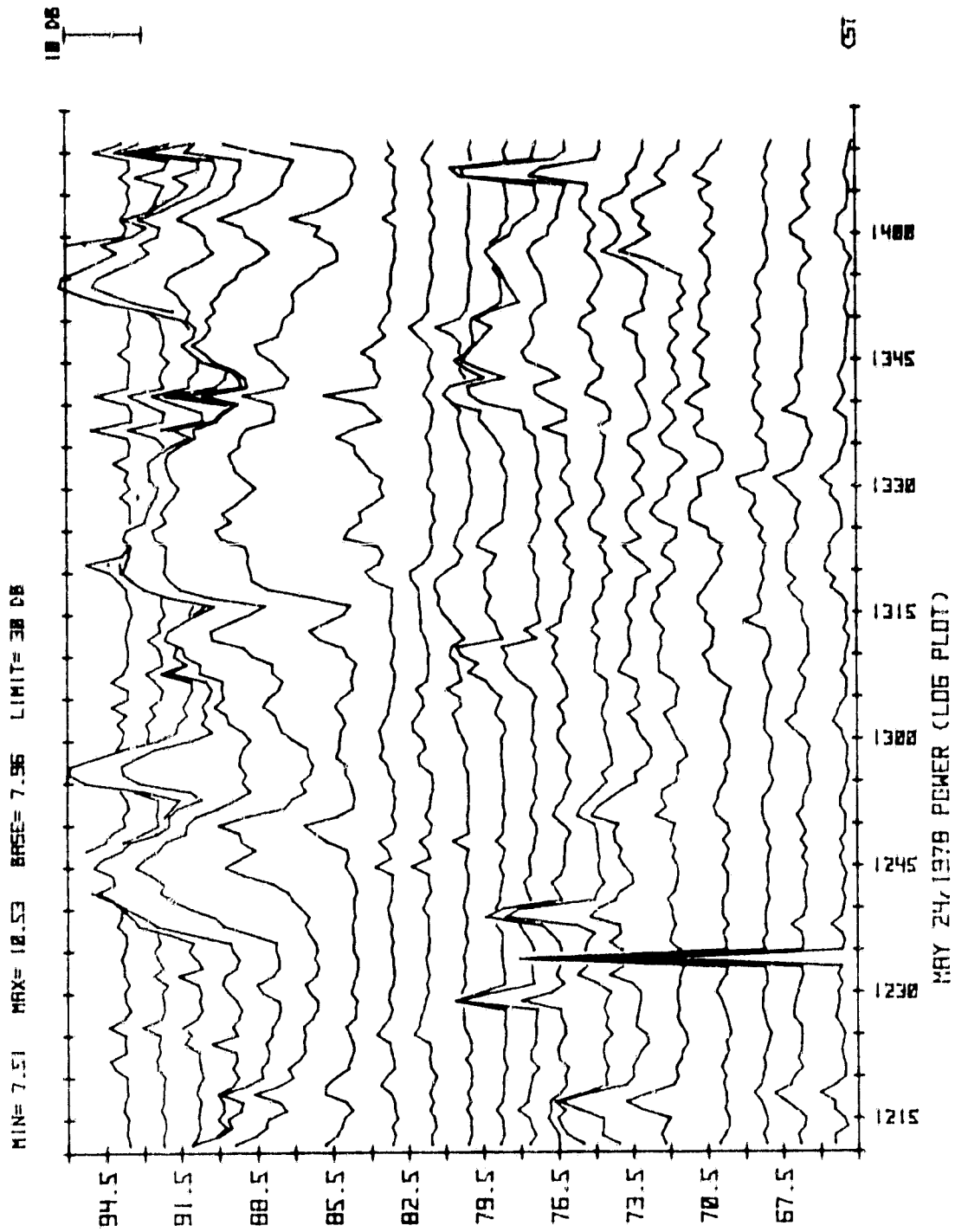


Figure 3.1.4 Horizontal profile of scattered power at Urbana beginning at 1212 CST on May 24, 1978.

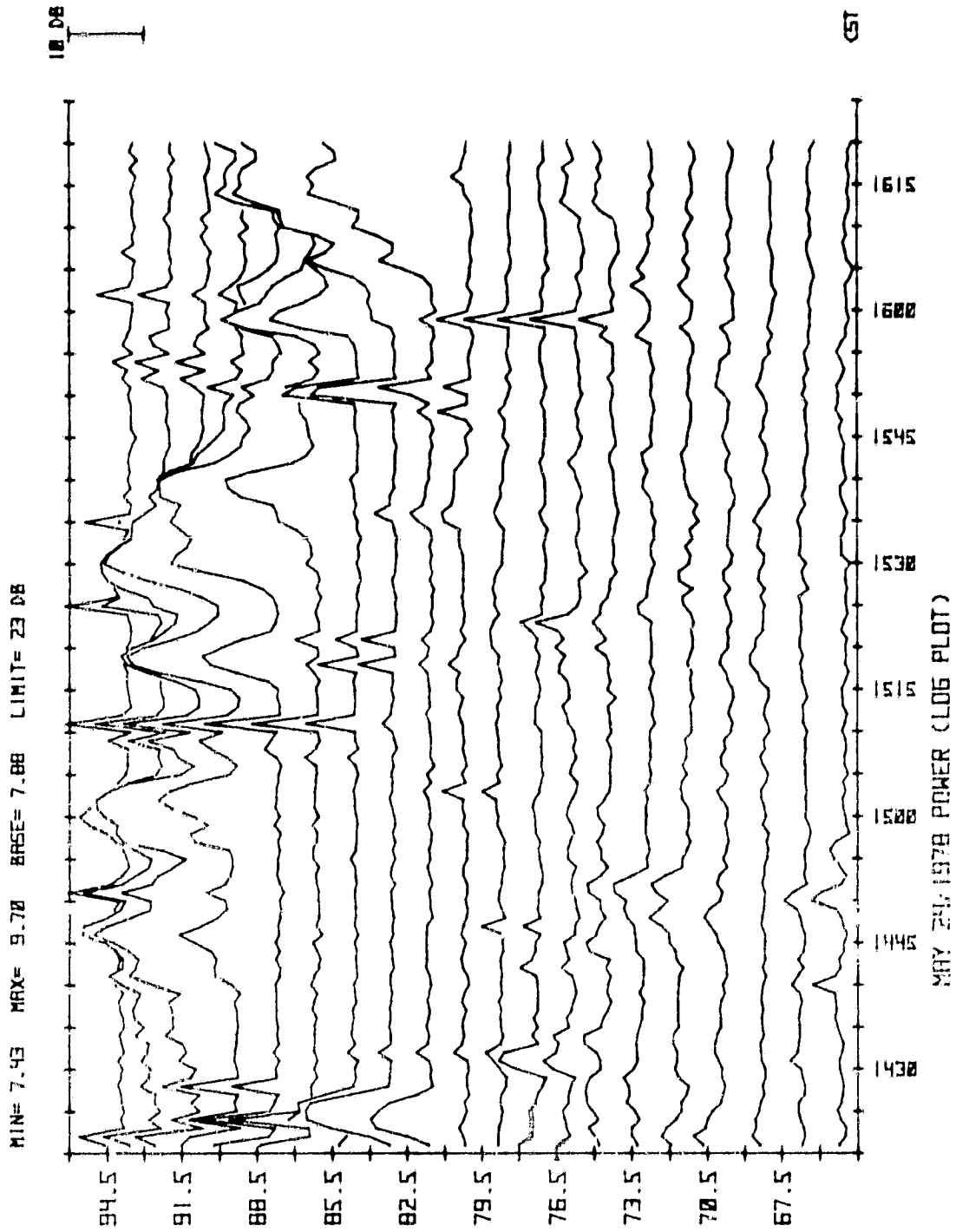


Figure 3.15 Horizontal profile of scattered power at Urbana beginning at 1421 CST on May 24, 1978.

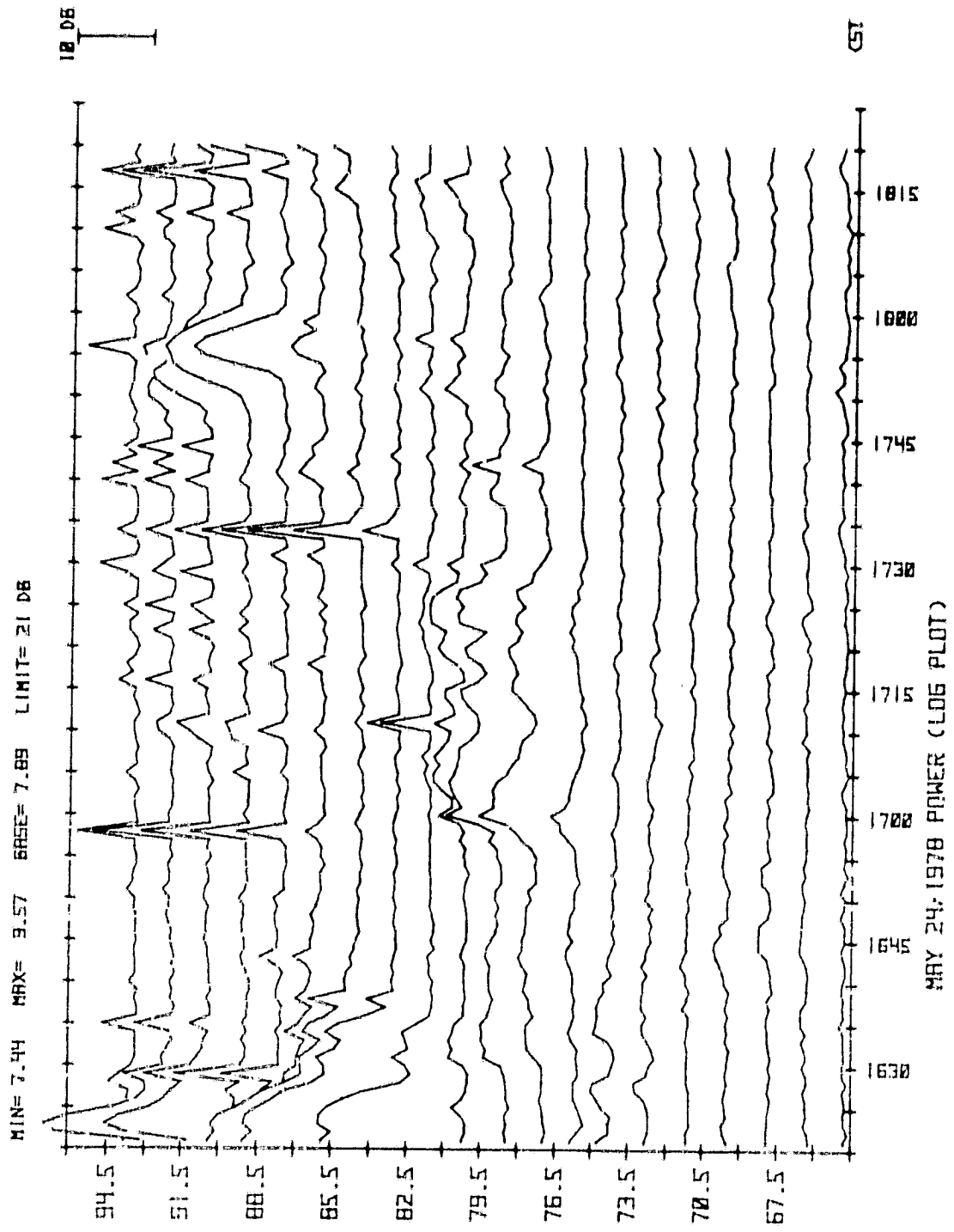


Figure 3.16 Horizontal profile of scattered power at Urbana beginning at 1621 CST on May 24, 1978.

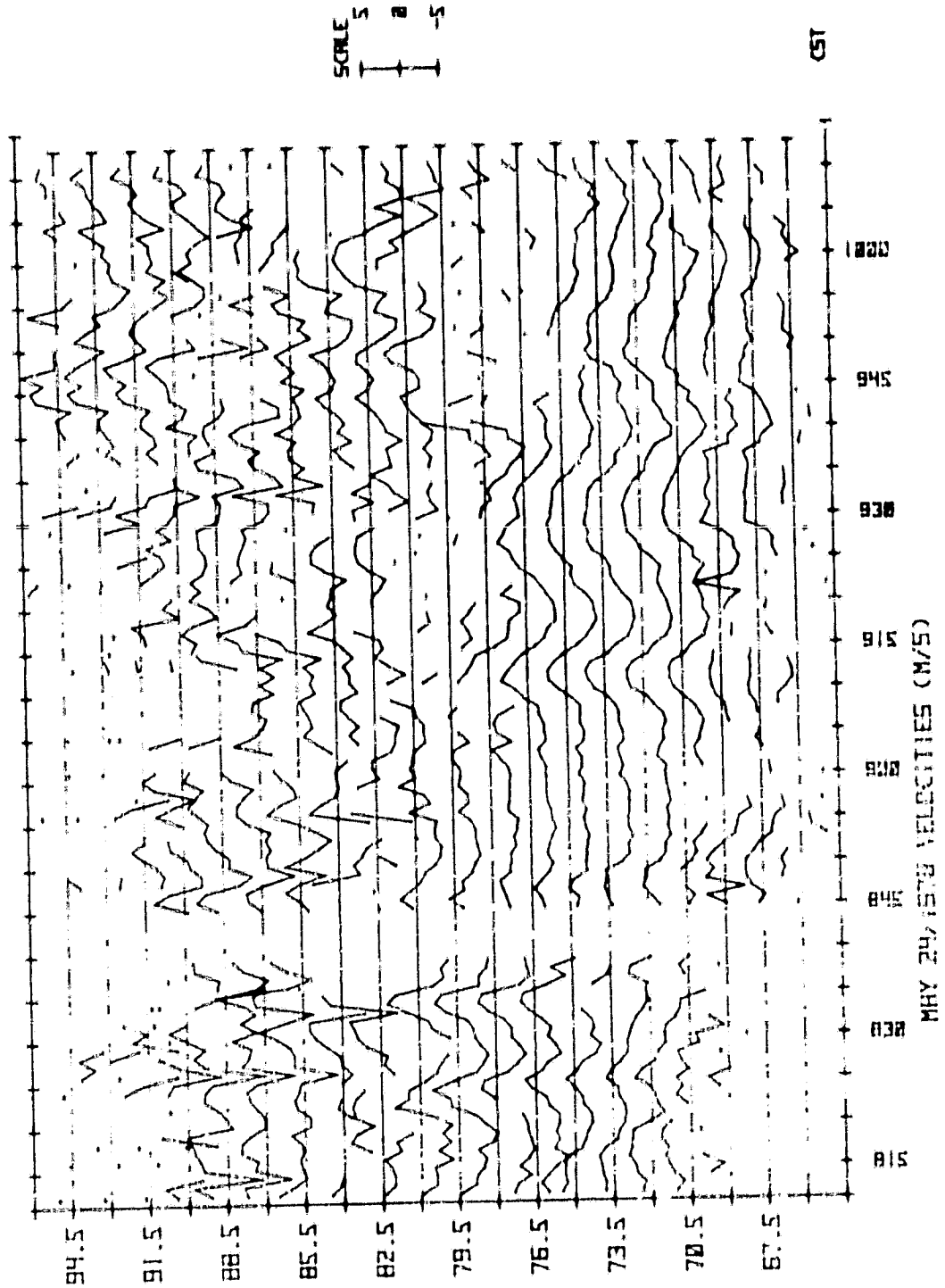


Figure 3.17 Line-of-sight velocity at Urbana beginning at 812 CST on May 24, 1978.

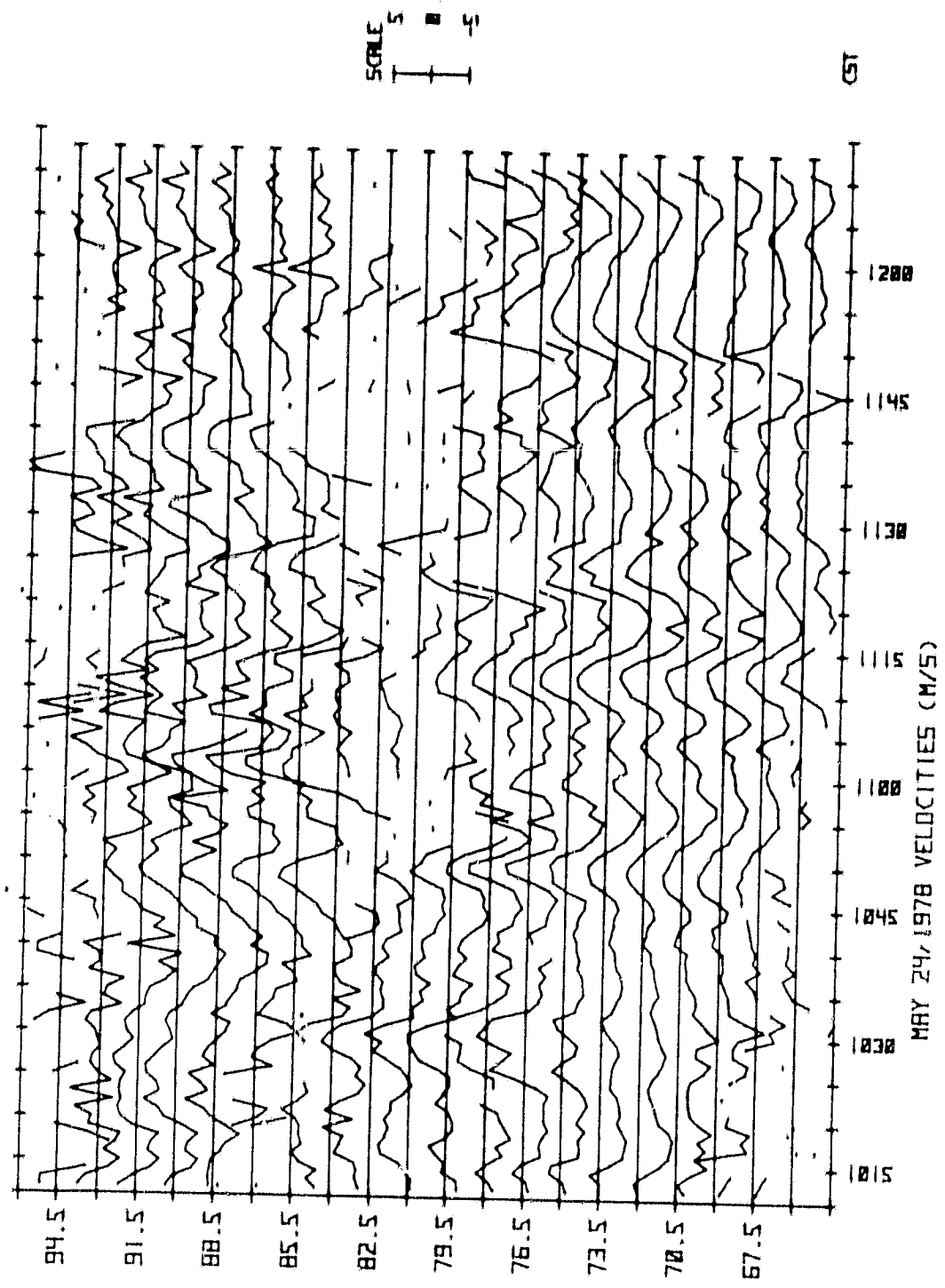


Figure 3.18 Line-of-sight velocity at Urbana beginning at 1012 CST on May 24, 1978.

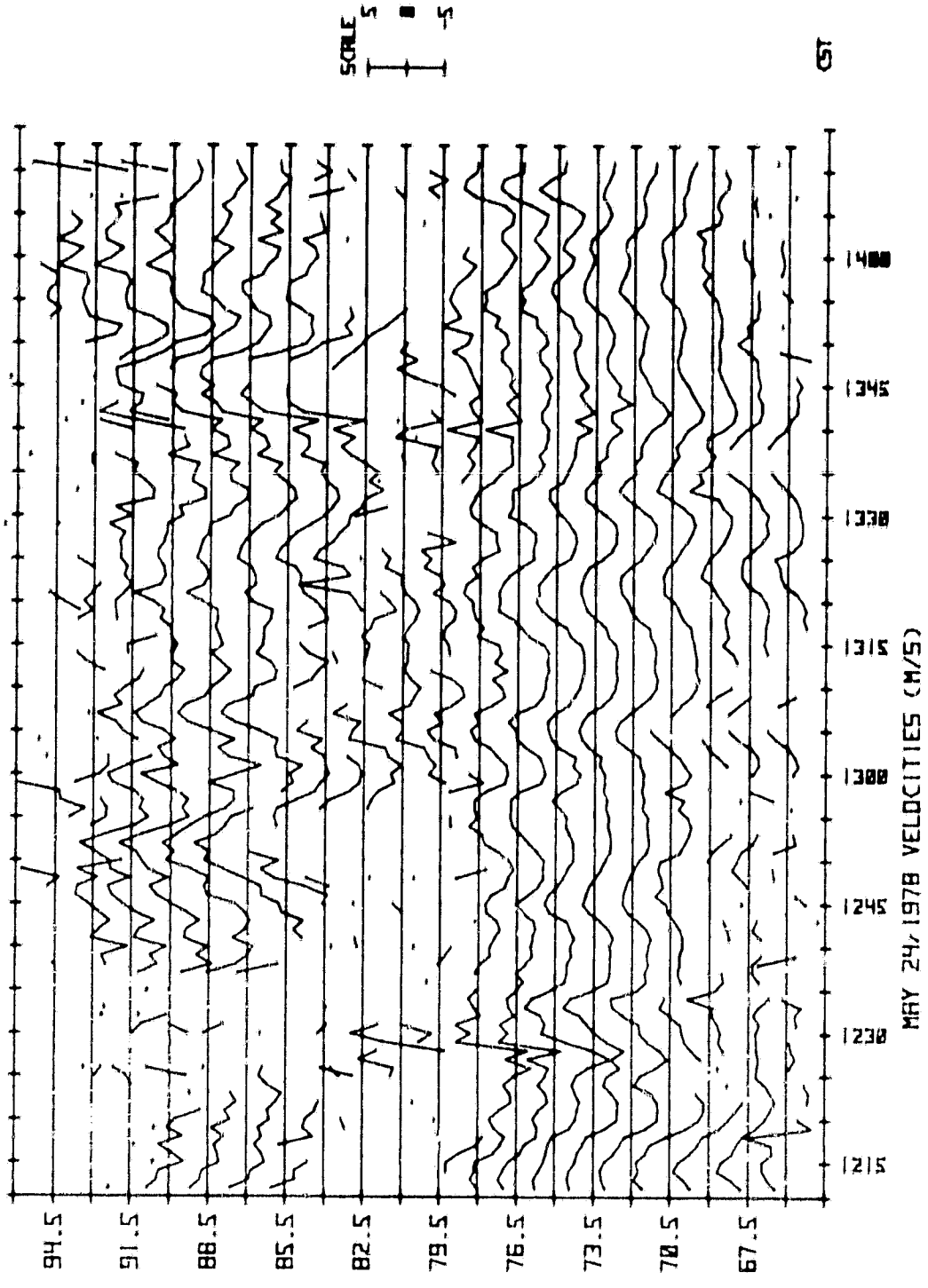


Figure 3.19 Line-of-sight velocity at Urbana beginning at 1212 CST on May 24, 1978.

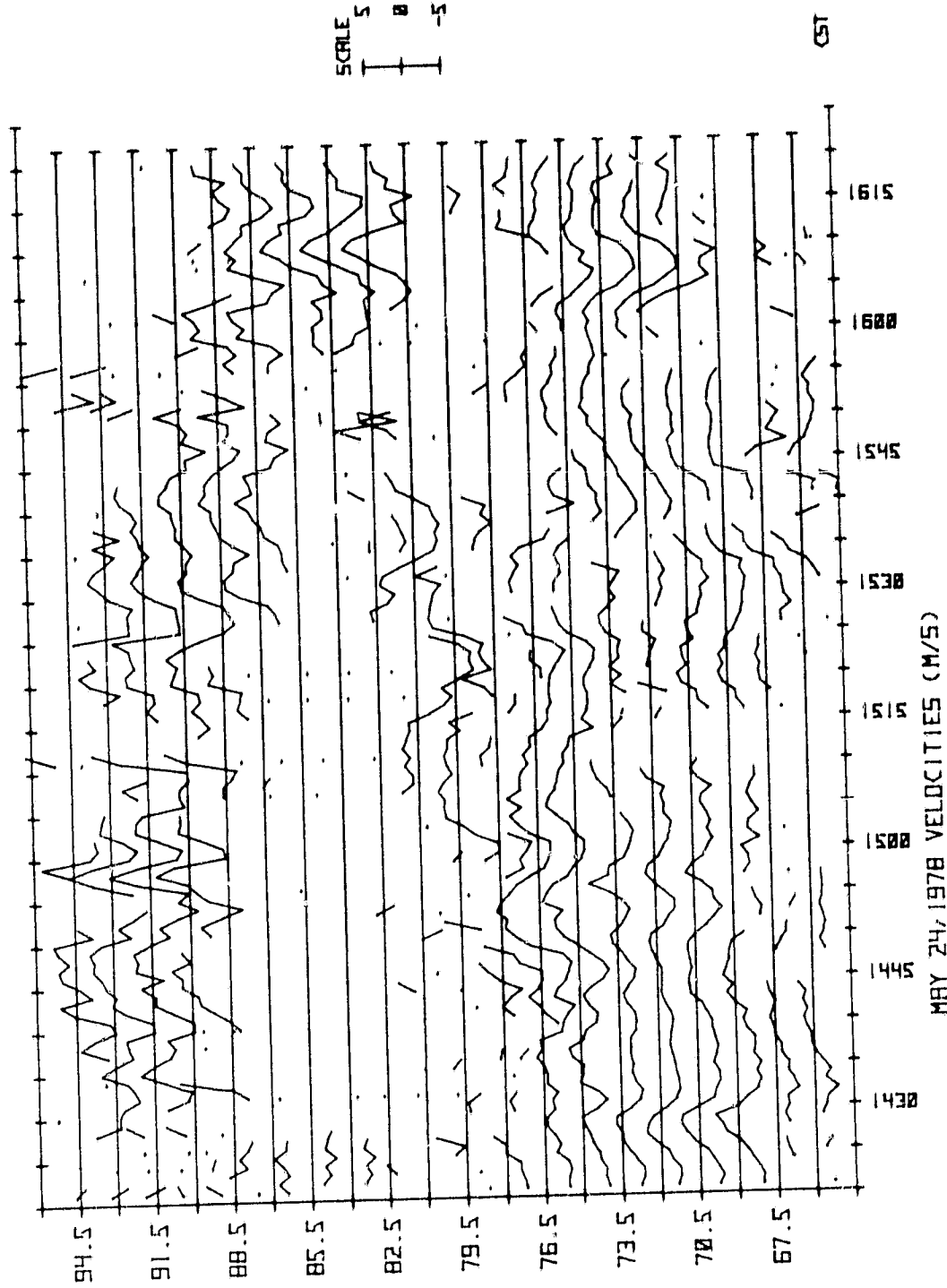


Figure 3.20 Line-of-sight velocity at Urbana beginning at 1421 CST on May 24, 1978.

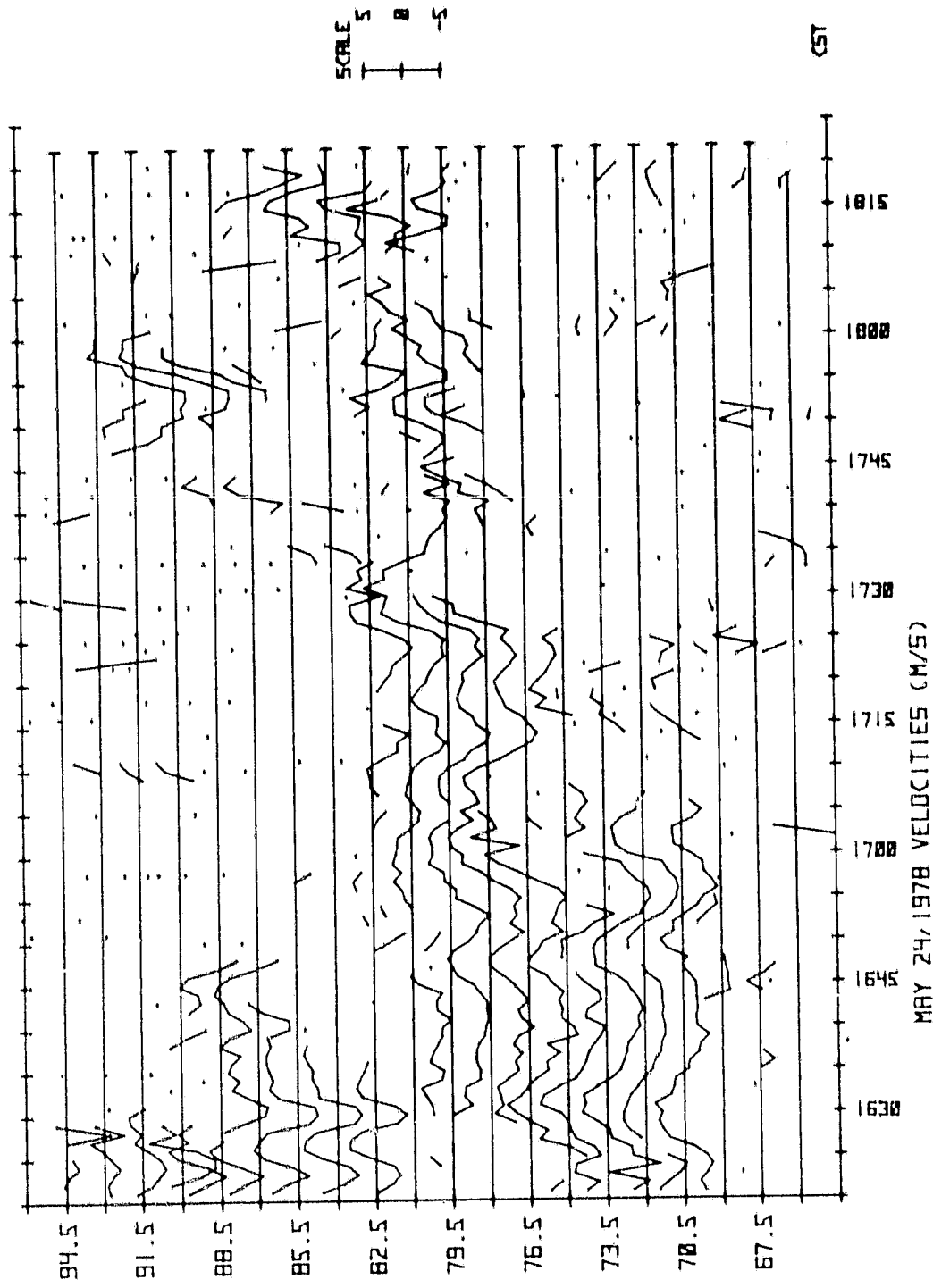


Figure 3.21 Line-of-sight velocity at Urbana beginning at 1621 CST on May 24, 1978.

In Figure 3.7 the region is not so well defined as later in the day yet still appears to be shifting in height. Throughout the day the layer moves slowly downward then in a shorter span of time moves back to the higher altitude and begins descending again. The slow descending process is most obvious from 1421 to 1621 CST. The layer appears to split before fading away at 1630 CST. Again at 1750 CST the layer is descending during it's brief reappearance. The long term motion of the scattering regions as shown in Figures 3.7 to 3.11 is seldom seen at the Urbana radar.

4. SUMMARY AND SUGGESTIONS FOR FUTURE RESEARCH

4.1 Summary

The principal conclusions of this study are summarized below.

(1) The Urbana coherent-scatter radar has been synthesized from the meteor radar by modification of the radar director and other meteor-radar components. A flat dipole array is used in conjunction with a 4-MW transmitter operating at 40.92 MHz and a receiving system connected to a minicomputer to obtain echo power and velocity measurements.

(2) The sensitivity of the Urbana radar allows data collection throughout the mesosphere on virtually all days. A time resolution of one minute is obtained which produces continuous plots of velocity without smoothing.

(3) The 242 hours of data collected from the mesosphere show the variability of scattering. Both active and quiet days are observed with echo power exhibiting a dynamic range of 20 dB. Gravity waves are observed with evidence for vertical standing waves.

4.2 Suggestions for Future Research

4.2.1 *Improved range resolution.* The turbulent layers which are responsible for coherent scatter have a vertical separation on the order of several kilometers, but a thickness on the order of tens to hundreds of meters as shown by *Rastogi and Bowhill* [1976b]. It is therefore desirable to obtain a range resolution of one kilometer or less so that the scattering regions can be studied separately. Detailed study of the vertical structure of the velocity field will also require improved height resolution.

The range resolution of a pulsed radar is limited by the pulse width and the associated receiver bandwidth. Decreasing the pulse width improves the range resolution: but if the pulse repetition frequency is not also adjusted then the average transmitted power will decrease thereby reducing system sensitivity. Coding the radar pulse allows the transmitter to be run at maximum average power with a long pulse while obtaining the range resolution corresponding to a fraction of the pulse width. The phase of the transmitter is varied during the pulse according to a code word. The minimum time between phase shifts determines the range resolution. The returned signal is decoded by correlation of the returned signal with the transmitted code.

Implementation of coding at Urbana will require several modifications to the system hardware. First, a radar director capable of producing the coded

low level RF for the transmitter must be constructed. The radar director would also control the decoding process. Second, the increased range resolution will require more altitude sampling bins to cover the entire mesosphere. The data rate will exceed the I/O capability of the PDP-15 and the present A/D. Furthermore, the CPU time required for decoding will not be available if more sample heights are used. A decoder-preprocessor external to the PDP-15 and under direct control of the radar director could decode the incoming signal and perform coherent integration. The PDP-15 would then have CPU time available for computing the autocorrelation functions for the greater number of altitudes.

4.2.2 *Measurement of horizontal velocity.* A monostatic radar can measure the velocity of the scattering medium along the line of sight of the antenna beam. If the beam is not strictly vertical then the horizontal component of velocity in the direction of beam tilt can be measured. Presently, the Urbana radar beam points about 1.5 degrees from the vertical in a generally southeasterly direction. Non-zero average values for velocity are therefore interpreted as horizontal velocity toward the southeast. By shifting the pointing direction to due south and again to due east two orthogonal horizontal velocity vectors could be obtained although these velocity values would be from different scattering volumes. In general, any two pointing directions not along the same line from the vertical can be used to obtain the orthogonal velocity components.

The Urbana array consists of three modules along a northeast/southwest line. As discussed earlier the modules are presently fed in phase which produces a pointing direction of roughly 1.5 degrees from the vertical in a southeasterly direction. The non-vertical direction of the beam is a direct result of the ground slope beneath the antenna. By feeding the modules with different phases the beam would be steered along the northeast/southwest line and two orthogonal pointing directions could be obtained.

4.2.3 *Additional data processing.* Data collected at the Urbana radar is routinely processed to obtain plots of echo power and line-of-sight velocity. The minute-by-minute variation of these parameters is readily observed but comparison at longer time intervals is more difficult. Obtaining one hour statistics from the data would facilitate long term comparisons and aid in the study of possible relationships between scattered power and observed velocity.

The utility of a one-hour average of velocity data has been discussed above. In addition to obtaining the average one would like to have parameters which indicate the relative amplitude of the velocity waves and the dominant wave period. The relative amplitude of the waves from hour-to-hour can be observed by calculation of the second moment about the mean, the variance of the line-of-sight velocity. It is important to subtract the mean here because the mean is assumed to be due to horizontal motion while the short-term velocity variation is the vertical component. The standard deviation, the square root of the variance, therefore provides a root-mean-square estimate of the wave amplitude. A parameter related to the dominant wave period may be calculated in either the frequency or time domain by calculating the Fourier transform or the autocorrelation function respectively.

One hour statistics for the scattered power serve primarily to relate the power data to the velocity information. A single power profile summarizing an hour of data would therefore be adequate but should not be obtained by averaging. Observations of scattered power at Urbana, as illustrated earlier, show short bursts of high returned power which are primarily due to meteor echoes. An average of the power data would thus be affected by the returns due to meteors. Calculation of a median value of power, however, would reduce the effect of short duration, high power returns and produce the desired characteristic power profile.

APPENDIX I RECEIVING SYSTEM BLANKER

The Urbana radar is a monostatic system and therefore requires a means of isolating the transmitter and receiver. The protection system consists of the high-power T/R switch and the low-power blanker illustrated below. During the transmit pulse the T/R switch limits the amplitude of RF on the receiver system input to roughly 60 volts across 50 ohms. The protection afforded by the blanker is therefore necessary to prevent damage to the receiving system which follows. The blanker/preamplifier unit is shown in Figure A1.1. Schematic diagrams for the drive circuitry and for the blanker itself are given in Figures A1.2 and A1.3 respectively.

ORIGINAL PAGE IS
OF POOR QUALITY

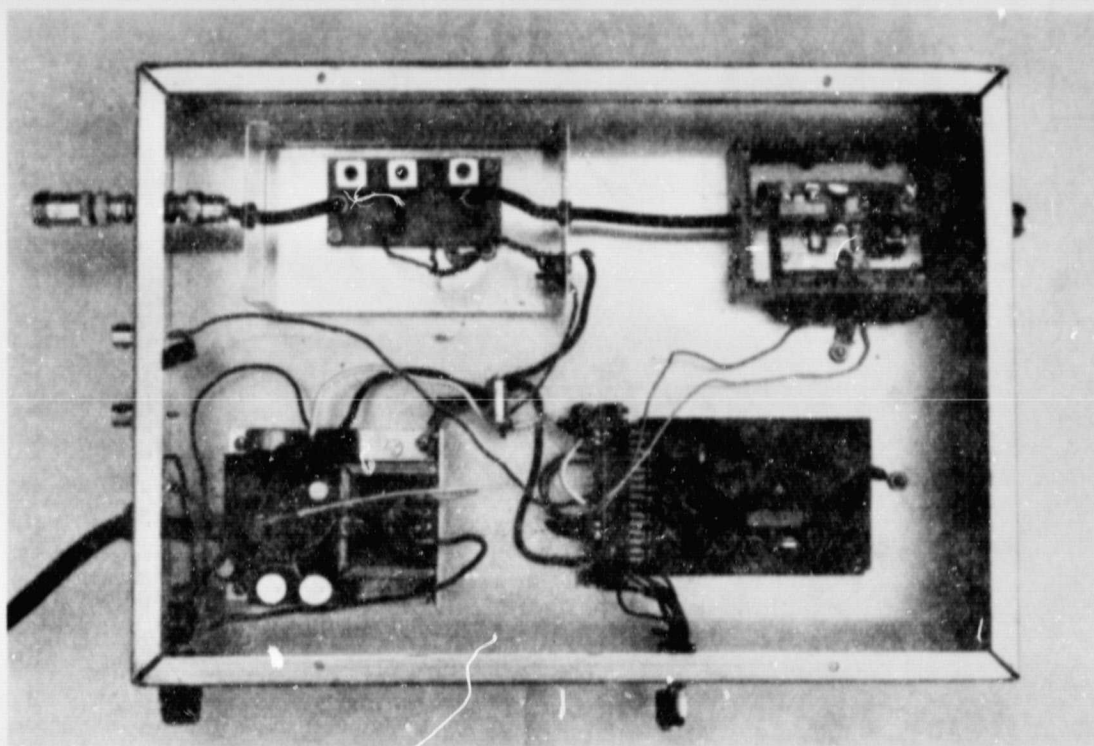


Figure A1.1 Blanker/preamplifier unit. The blanker is contained in the box at the upper right and controlled by the circuit at the lower right. A commercial preamplifier appears in the upper left of the figure.

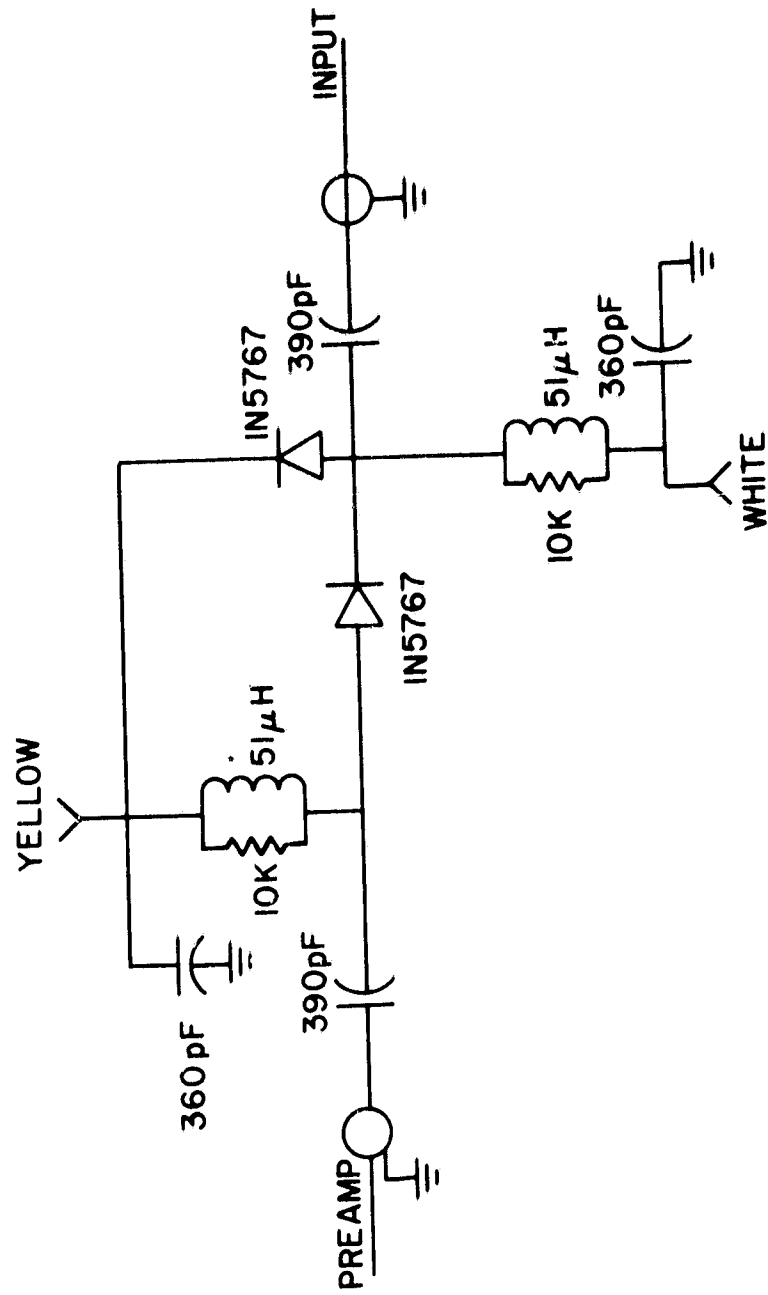


Figure A1.3 RF section of the radar receiving system blanker.

APPENDIX II. RADAR DIRECTOR TIMING INFORMATION

The circuitry employed in the radar director is shown in *Hess and Geller* [1976]. However the operation of the radar director was not described in that work. The definitions and timing diagram below explain the function of the various controls and the resultant pulse trains.

BASIC TIME PERIOD: The period of the main time base driving the radar director. A 1-MHz clock is divided down to 100 kHz to produce a 10 μ sec basic time period.

PRF WORD: A thumbwheel switch which determines the number of basic time periods between the leading edges of consecutive PRF pulses. The PRF word switch is set to 250 for the scatter radar producing a 400 Hz pulse repetition frequency.

RANGE WORD: A thumbwheel switch which determines the number of basic time periods between the leading edge of the PRF pulse and the following Range pulse. The range word should always be less than the PRF word. The range word is set 249 for the scatter radar which results in a Range pulse beginning 10 μ sec before the PRF pulse.

START/STOP: A thumbwheel switch which determines the number of sample pulses and when with respect to the PRF pulse they occur. The 4 switches on the left determine the start time, those on the right the stop time. The difference between the stop and start settings is the number of sample pulses. The first sample pulse occurs at Start +1 basic time periods after the leading edge of the PRF pulse. Start should be less than Stop. Settings generally are 40 and 60 for the coherent-scatter radar.

PULSE WIDTH: A set of toggle switches which determines the length of both the PRF and Range pulses. The pulse length is the number of basic time periods corresponding to toggle switches in the up position. The LSB is located at the left. A setting of seven or greater is used for the 20 μ sec transmitter pulse length.

PRF PULSE: A positive going pulse which drives the transmitter circuitry.

RANGE PULSE: A positive going pulse which drives the RF gater, blanker, and other equipment.

ECHO SAMPLE WINDOW (ESW): A negative going pulse train which drives the analog to digital converter. The width of the pulses is that of the driving time base pulse and the separation between pulses is the basic time period.

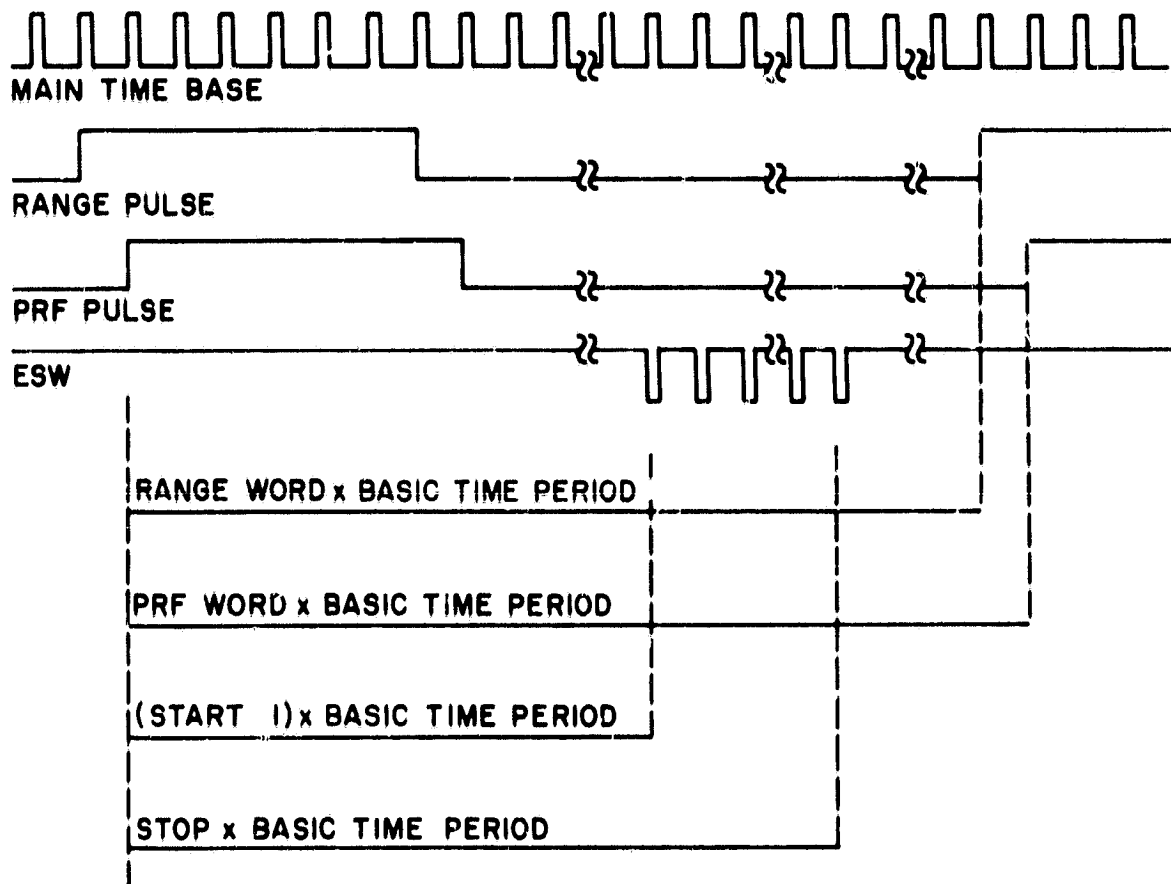


Figure A2.1 Timing diagram for the radar director.

APPENDIX III DATA COLLECTION PROGRAMS

The two programs below, FSCAT and DM are the real-time collection programs for the Urbana coherent-scatter radar. The program DM is required by program size constraints in the PDP-15. FSCAT is used to perform all the data collection and to produce correlation functions of 12 lags of 1/8 second for each of 20 sample altitudes at one-minute intervals. Twelve minutes of data form a file and ten files fill a disk. Data collection must be interrupted after six hours to empty the disks onto DECTape. Before running the program the file pointer must be edited to indicate the correct date. The edit command "L .SIX" is used to find the appropriate program lines. The date are then changed in the file name and the file extension shown in the line that follows may also have to be initialized with a new value. The modified program is compiled with the MACRO compiler and then transferred back onto DECTape. The .DAT slot assignment for loading and executing the programs is as follows: disks 1, 2, and 3 are assigned to slots 5, 6, and 7 respectively, and the DECTape unit containing the FSCAT and DM binary files is assigned to slot -4. Disks 1, 2, and 3 should be nulled before loading and execution begins.

DM program

```
CM      .GLOBL  CM
        .BLUCK 764z
        .END
```

FSCAT program

```

      .GLOBL  MAIN,CM,.DA,.PA
      .IODEV 5,6,7
SHAL=660000
CLON=700044
CLOF=700004
MAIN   DZM      SEQ#
      LAC      CM      /SET ADDRESS IN WRITE STMT
      DAC      BOUT+2
      DAC      WATE+2
      TAD      (7640  /POINT TO SEQ# ADDRESS
      DAC      SEQAD#
      IAC
      DAC      WDAD#   /AND SWITCH ADDRESS
      .ENTER 5,FILE
CLOCK  .TIMER  200,ADERR,7
      .TIMER  0,SYNC,6
      .IDLE
PAUS   0          /ENTRY
      .CLOSE  5
      LAC      SEQ
      JMS      .PA
      ISZ      EXT
GOO    .ENTER 5,FILE
      CLON
      .TIMER  0,SYNC,6
      .RLXIT  PAUS
SYNC   0          /RESTART ENTRY
      LAC      SEQ
      SNA!CLL
      IAC          /FAKE IT FOR FIRST RECORD
      LMQ
      CLA
      DIV
      3          /DIVIDE BY 3
      SZA      /TEST REMAINDER
      JMP      LEFT
L      .CLOSE  5
      ISZ      EXT
      LAC      SEQ   /TEST TO CHANGE DISKS

```

FSCAT program (cont.)

```

SAD      (36      /FIRST DISK FULL?
JMP      CLOP
SAD      (74      /SECOND DISK FULL?
JMP      CLOP
SAD      (13z     /ALL DISKS FULL?
JMP      CLOQ

S        .ENTER 5,FILE
LEFT     JMS ADCSET
        JMP .+3
        .DSA ONE      /ONE SAMPLE
        .DSA RETURN
        .IDLE

SAMP     0
ONE      1
TIMERR   0
N        1750      /1000(10) INPUT BUFFER SIZE
STOP     0
RETURN   RETURN+700001
        0          /ENTRY (LEVEL 7)
LAC      BUFFI
AND      (740000  /IGNORE DATA
SZA
JMP      IN
LAW      -240
SZA! IAC
JMP      .-1
JMS      ADCSET  /TRY AGAIN
JMP      .+3
.DSA     ONE
.DSA     RETURN
JMP      OFF
IN       LAC      (ACFIz
        TCA
        TAD      CM      /GET RELATIVE DISPLACEMENT
        DAC      OUTXR#  /TO OUTPUT ARRAY
        LAC      LOIM
        DAC      IMPT#   /RESET INTERMEDIATE ARRAY
        LAW      -740
        DAC      M740#   /480 SAMPLES PER MIN
        LAW      -4
        DAC      MINT#   /4 MIN PER OUTBUFF
        DAC      STOP    /CONTINUE DATA COLLECTION
        LAW      -z40
        SPA! IAC      /WASTE 250US
        JMP      .-1
        JMS      ADCSET  /RESTART ADC DATA TAKING
        JMP      .+3
        .DSA N
        .DSA PRADD     /ADDRESS OF COHERENT INTEGRATION ROUTINE
/ ZERO INTERMEDIATE ARRAY
LAW      -740
PAX

```

FSCAT program (cont.)

```

      CLR
      DZM      IMARR+740.X
      AXS      I
      JMP      .-2
/ PLAY IT SAFE-ZERO SETUP ACPI 2 & MEANS
      LAC      (JMS      STORE
      DAC      PCLR
      DAC      RCLR
      DAC      ICLR
      LAC      (JMS      MNSTR
      DAC      MXCLR
      DAC      MYCLR
OFF  .RLXIT   RETURN+1
CLOP ISZ      S      /INCREMENT DAT SLOT
      ISZ      L
      ISZ      WATE
      ISZ      PAUS+1
      ISZ      GOO
      ISZ      OERR   /ALSO FOR TERMINATION DUE TO ERROR
      ISZ      BOUT   /WRITE ON NEXT DISK
      JMP      S
CLOO .CLOSE   7      /ALL DISKS FULL. QUIT
      .EXIT
PRADD COHINT+500000
ADERR 0      /ADC FAILURE (CLOCK EXPIRED)
      LAW      5774   /ISSUE TERMINAL ERROR
      DAC      ERCODE
      LAC      ADERR
      DAC      ERARG
      LAC*     (202
      ISA      /PROTECT THE MONITOR
      JMS      ERROR
      DBK
      .RLXIT   ADERR
      .DEFIN   .INT M
      LAC      BUFF1,X+M
      LLS      10
      LRSS     10
      TAD      PD1,X
      DAC      PD1,X
      .ENDM
COHINT 0      /ENTRY
      LAC      TIMERR
      SNA
      JMP      TTT    /NO ERROR
      LAC      COHINT
      DAC      ERARG
      LAW      5773
      DAC      ERCODE
      LAC*     (202
      ISA

```

FSCAT program (cont.)

```

      JMS      ERROR
      DBK
      JMP      QUIT
TTT   LAC      BPFLG
      TCA
      PAX
      AAC      50
      PAL
BEGINT DZM      PDI ,X
      .INT     0
      .INT     50
      .INT     170
      .INT     170
      .INT     240
      .INT     310
      .INT     360
      .INT     430
      .INT     500
      .INT     550
      .INT     620
      .INT     670
      .INT     740
      .INT     1010
      .INT     1060
      .INT     1130
      .INT     1200
      .INT     1250
      .INT     1320
      .INT     1370
      .INT     1440
      .INT     1510
      .INT     1560
      .INT     1630
      .INT     1700
      SPA
      TAD      (-1      /CONVERT TO 1/2 S COMP
      DAC      PDI ,X
      AXS      1
      JMP      BEGINT
/ NOW FORM ACFS
      JMS      ACFLZ    /31.6 MSEC
/ TEST IF MINUTE COMPLETE
      ISZ      M740
      JMP      QUIT
/ NEW MIN STARTS WITH NEXT POINT
      LAW      -740
      DAC      740      /RESET MINUTE COUNTER
      LAC      (JMS     STORE
      DAC      PCLR     /SET UP TO CLEAR
      DAC      RCLR     /NEXT ACF IN
      DAC      ICLR     /OUTPUT BUFFER

```

FSCAT program (cont.)

```

JMS      MNSUB  /SUBTRACT DC AND CLEAR
LAC      OUTXR  /POINT TO NEXT ACF
TAD      N
DAC      OUTXR
LAC      (JMS   MNSTR
DAC      MXCLR
DAC      MYCLR
ISZ      MINT
JMP      QUIT
/OUTPUT BUFFER FULL
DZM      STOP  /NO MORE DATA PLEASE
DZM      SUBR  /IGNORE NEXT BUFFER
ISZ      SEQ
LAC      SEQ
DAC*     SEQAD
LAS
DAC*     WDAD
BOUT     .REALW 5.4,CM,400z,SYNC,6
JMP      QUIT
/WANT TO INTERRUPT PROCESSING. FIRST STOP CLOCK.
CLOF
WATE     .REALW 5.4,CM,400z,PAUS,0
QUIT     LAW    -1  /FREE BUFFER TO A1)
DAC      COMFLG
.RLXIT   COHINT
FILE     .SIXBT '23MAR'
EXT      .SIXBT '78A'
/ ACF12 INTEGRATES PRESENT DATA WITH INTERMEDIATE ARRAY
/ AND FORMS DC ESTIMATE. FINALLY PRESENT DATA ARE INCLUDED
/ IN THE IMARR
ACF12    0  /ENTRY
LAC      BPFLG
TCA
TAD      (PDI-1
DAC*     (16  /USE AUTO INC REG 16 FOR X'S
AAC      24  /17 FOR Y'S
DAC*     (17
LAC      IMPT
DAC*     (14  /USE 14 & 15 FOR IMARR
DAC*     (15
TCA
TAD      HGIM
TCA      /NEG # POINTS ABOVE IMARR DISCONTINUITY
DAC      CONTR#
LAW      -24  /DO 20 HEIGHTS
DAC      CNTHT#
LAC      OUTXR
PAX
/ACF12,X REFERENCES OUTPUT ARRAY
LCONPH  AAC      62  /25 DOUBLES PER HEIGHT
PAL
LAC*     16  /GET X(T)

```

'SGAT' program (cont.)

```

GSM                                /ABS VAL(I'S COMP):SIGN TO LINK
DAC      XYTØ
DAC      XXTØ
DAC      PX
LAC      (CLL
SZL!CLL                                /TEST SIGN
AAC      2                                /STL=CLL+2
DAC      XXTØSN
XOR      (2                                /OPPOSITE SIGN FOR I(K)
DAC      XYTØSN                            /I(K)=YX+(-X)Y
LAC      PX
MULS                                /CLEAR EAE SIGN;GET X**2
PX      Ø
PCLR    JMS      STORE                    /OR JMS DADD TO SUM
LAC*    17
GSM                                /GET Y(T)
DAC      YXTØ
DAC      YYTØ
DAC      PY
LAC      (CLL
SZL!CLL                                /TEST SIGN
AAC      2                                /STL=CLL+2
DAC      YYTØSN
DAC      YXTØSN
LAC      PY
MULS                                /GET Y**2
PY      Ø
JMS      DADD                            /SUM TO POWER
AXR      2                                /POINT TO R(1)
/ DO R(K)
LOOPT=XXTØSN
XXTØSN  XX                                /STL OR CLL;GET SIGN OF X(T)
LAC*    14                                /GET Y(T+K)
MULS
XXTØ    Ø                                /FORM PRODUCT
RCLR    JMS      STORE                    /OR JMS DADD TO SUM
YYTØSN  XX                                /STL OR CLL;GET SIGN OF Y(T)
LAC*    14                                /GET Y(T+K)
MULS                                /PRODUCT(I'S COMP)
YYTØ    Ø
JMS      DADD                            /ADD TO OUTPUT POINT
AXR      2                                /POINT TO I(K)
/DD I(K)
YXTØSN  XX                                /GET SIGN OF Y(T)
LAC*    15                                /GET X(T+K)
MULS                                /I'S COMP PRODUCT
YXTØ    Ø
ICLR    JMS      STORE                    /OR JMS DADD TO SUM
YXTØSN  XX                                /GET MINUS SIGN OF X(T)
LAC*    15                                /GET Y(T+K)
MULS                                /I'S COMP PRODUCT

```

FSCAT program (cont.)

```

XYTØ 0
      JMS      DADD      /SUM TO I(K)
      ISZ      CONTR     /z POINTS PER LAG
      ISZ      CONTR     /TEST FOLDOVER
      JMP      DOWN
      LAW      -740      /FOLD TO BOTTOM OF IMARR
      TAD*     (15       /RESET 15
      DAC*     (15
      DAC*     (14       /RESET 16(ONCE PER AC#12)
DOWN:  AXS      2         /POINT TO NEXT LAG; TEST AC# DONE
      JMP      LOOP
      PXA
      ISZ      CNTHT     /TEST LAST HEIGHT
      JMP      LOOPH     /DO NEXT HEIGHT
/ ACFS DONE; ALWAYS RESET STORE TO DADD
      LAC      (JMS      DADD
      DAC      PCLR
      DAC      RCLR
      DAC      ICLR
/ STORE PRESENT DATA IN IMARR & SUM(STORE) TO MEANS
/ REVISE IMPT. THE IMARR DISCONTINUITY ADDRESS
      LAC      IMPT
      SAD      LOIM      /MIN VALUE?
      LAC      HGIM      /YES, GET MAX VALUE
      AAC      -2        /DECREMENT TO NEW POINT
      DAC      IMPT      /SAVE
      TCA
      TAD      LOIM
      TCA
      PAX
      LAC      (740
      PAL
      LAW      -24
      DAC      CNTHT     /DO 20 HEIGHTS
      LAC*     (16       /16 STILL POINTS TO Y'S
      AAC      -24
      DAC*     (17       /17 POINTS TO X'S
      LAC      (MN-1
      DAC*     (14       /14&15 POINT TO MN ARRAY
      DAC*     (15       /DOUBLE WORDS
LOOP:  LAC*     17       /GET X(T)
      DAC      IMARR,X   /STORE IN IMARR
MXCLR: JMS      MNSTR     /OR MNADD TO SUM TO MN ARRAY
      LAC*     16       /GET Y(T)
      DAC      IMARR,X+1 /STORE IN IMARR
MYCLR: JMS      MNSTR     /STORE(OR ADD) TO MN ARRAY
      AXS      30       /POINT TO NEXT HEIGHT IN IMARR
      JMP      DTT
/ FOLD TO NEXT HEIGHT IN IMARR
      AXR      -360
      AXR      -360     /DECREMENT KR BY 740

```

FSCAT program (cont.)

```

DTI      ISZ      CNHT      /TEST LAST HEIGHT
        JMP      LOOP      /DO NEXT HEIGHT
/DONE WITH PRESENT DATA: RESET MNSTR TO MNADD & RETURN
        LAC      (JMS      MNADD)
        DAC      MXCLR
        DAC      MYCLR
        JMP*     ACFIz      /RETURN
/MNADD CONVERTS AC TO 2'S COMP & ADDS TO MN ARRAY
/IN UPSIDE-DOWN FORMAT (I.E. LSW:MSW )
MNADD    0        /ENTRY
        SPA
        IAC      /CONVERT 2'S COMP
        SHAL     /SIGN(MSW) TO LINK
        TAD*     14      /ADD LSW'S
        DAC*     15      /SAVE
        SNL      /TEST CARRY XOR SIGN
        JMP      NOTH    /DON'T ALTER MSW
        SPA:CLA: IAC      /GET +1 IF POS
        LAW      -1      /GET -1 IF NEG
        TAD*     14      /ADD TO MSW
        DAC*     15
        JMP*     MNADD

NOTH     CLA      /MUST INCREMENT 14&15
        JMP      .-4     /ANYWAY
/MNSTR CONVERTS AC TO 2'S COMP & STORES IN MN ARRAY
/ (IN UPSIDE-DOWN FORMAT). REG 14 IS NOT USED.
MNSTR    0        /ENTRY
        SPA
        IAC      /CONVERT
        DAC*     15      /PUT IN LSW
        SPA:CLA  /MSW=0 IF POS
        LAW      -1      /MSW=-1 IF NEG
        DAC*     15      /PUT IN MSW
        JMP*     MNSTR   /RETURN

/SUBROUTINE TO SUBTRACT DC(MEANS) FROM OUTPUT DATA
MISUB    0        /ENTRY
        LAC      (MN-1   /15&16 POINT TO MN ARRAY
        DAC*     (15
        DAC*     (16
        LAW      -24
        DAC      CNHT    /DO 20 HEIGHTS
        LAC      OUTXR
        PAX
        LOPH     AAC      6z      /XR ADDRESSES OUTPUT ARRAY
        PAL
        JMS      SQR      /GET X*X/480 IN DI REGISTER
        DAC      EMPI#    /SAVE DI REGISTER
        LAC:
        DAC      TEMPz#
        JMS      SOR      /GET Y*Y/480 IN DI REGS

```

ORIGINAL PAGE OF
OF FOUR QUALITY

FSCAT program (cont.)

```

/DOUBLE ADD(POS DEF SO CAN 2'S COMP ADD)&1'S COMP RESULT
TAD      TEMPI
DAC      TEMPI      /ADD MSW'S
LACQ
CLL
TAD      TEMP2      /ADD LSW'S; CARRY TO LINK
LMQ      /RETURN TO MQ
LAC      TEMPI
SZL      /TEST CARRY
IAC
CMQ      /1'S COMP RESULT
CLL!CMA
DAC      TEMPI      /SAVE FOR LOOP
LACQ
DAC      TEMP2
LAC      TEMPI      /MEAN TO DI REG
JMS      DADD      /ADD(SUBTRACT) TO ZERO LAG(POWER)
AXR      2          /POINT TO R'S
LOPT    LAC      TEMP2
LMQ      /RESTORE -DC TO DI REG
LAC      TEMPI
JMS      DADD      /ADD TO R(K)
AXS      4          /POINT TO NEXT R; TEST LAST LAG
JMP      LOPT      /DO NEXT LAG
PXA
ISZ      CNTHT     /TEST LAST HEIGHT
JMP      LOPH      /DO NEXT HEIGHT
JMP*     MNSUB     /RETURN
/SQR TAKES MEAN, SQUARES IT & DIVIDES BY 480
/TO AVOID OFLD, MEAN IS FIRST DIVIDED BY SRT(480)
/TO AVOID TRUNCATION ERROR, MEAN&SRT(480) ARE FIRST
/ADJUSTED TO YEILD AN 18 BIT RESULT THEN SQUARED
/AND ADJUSTED BACK. (RESULT IS TRUNCATED BY <1)
SQR      0          /FENTRY(<0.1 MSEC)
LAC*     15         /GET LSW(UPSIDE-DOWN FORMAT)
LMQ
LAC*     15         /MSW
SPA!CLL  /ABS VAL, CLEAR LINK
JMS      COMP2     /2'S COMP IF NEG
DIV      /DO ROUGH DIVIDE
25       /SRT(480)
SZL      /TEST OVFLD
JMP      DCOFLD
CLA
NORM-1   /SHIFT TO GET 18 BIT RESULT
LACS     /GET SC
TAD      (22
AND      (37       /5 BIT SHIFT COUNT
DAC      MSHIFT#   /SAVE
RCL      /TIMES 2
TAD      (LRS     0          /FORM LRS 2*4

```

FSCAT program (cont.)

	DAC	SHFBK	/RE-ADJUST AFTER SQUARE
	LAC	MSHIFT	
	TAD	(LLS	14
	DAC	.+6	/LLS M+12
	LAC*	16	
	LMO		
	LAC*	16	/GET MEAN AGAIN
	SPA!CLL		
	JMS	COMP2	/ABS VAL, CLEAR LINK
	LLS	14	/LEFT SHIFT M+12 BITS
	DIV		/DIVIDE BY
	257213		/SRT(480)*2**12
	LACQ		/GET RESULT
	DAC	.+2	
	MUL		/SQUARE IT
	Ø		
SHFBK	IRS	Ø	/SHIFT BACK BY 2M
	JMP*	SQR	/RETURN
/COMP2	PERFORMS	2'S COMP	OF DI REG
COMP2	Ø		/ENTRY
	DAC	TEMP*	/SAVE MSW
	LACQ		/GET LSW
	CLL!TCA		/COMP LSW
	LMO		
	LAC	TEMP	
	SZL!OMA		/COMP MSW, TEST CARRY
	CLL!IAC		/CARRY IN & CLEAR LINK
	JMP*	COMP2	/RETURN POS DEF DI
/DC OFLO	ISSUES	ERROR IF	DC EXCEEDS 36 BITS
DOUFLU	LAC*	(202	
	ISA		/PROTECT MONITOR
	LAC	CUHINT	
	DAC	FRARG	
	LAW	5772	
	DAC	ERCODE	
	JMS	ERROR	
	DBK		
	JMP	QUIT	/EXIT PGM
/STORE	STORES	THE DI REG	IN THE OUTPUT BUFF
STORE	Ø		/ENTRY
	DAC	ACF12,X	/STORE MSW
	LACQ		
	DAC	ACF12,X+1	/STORE LSW
	JMP*	STORE	/RETURN
/DADD	ADDS	(1'S COMP)	DI REG TO OUTPUT BUFF
DADD	Ø		/ENTRY
	CLL		
	TAD	ACF12,X	/ADD MSW'S: CARRY TO LINK
	DAC	ACF12,X	/STORE
	LACQ		
	SZL!CLL		/TEST CARRY

FSCAT program (cont.)

	IAC		/CRRY AROUND;CARRY OUT TO LINK
	TAD	ACFI 2,X+1	/ADD LSW'S;CARRY OUT TO LINK
	SNL		/TEST CARRY
	JMP	OUT	
	ISZ	ACFI 2,X	/CARRY IN;SKIP ON CARRY AROUND
	SKP		
	IAC		/CARRY AROUND
OUT	DAC	ACFI 2,X+1	/SAVE LSW
	JMP*	DADD	/RETURN
ADCSET	Ø		/ENTRY
	JMS*	.DA	
	JMP	PAST	
WC	.DSA	WC	/ADDRESS OF WORD COUNT
SUBR	.DSA	SUBR	/ADDRESS OF 'SUBR' ARG.
PAST	LAC	(404000	/RAISE TO PRIORITY LEVEL 4
	ISA		
	LAC*	(155	/SETUP ADC ;ONCE ONLY
REAL	DAC	.	
COMFLG	JMS*	.-1	
DIFFC	703701		
BPFLG	ADSVG		
	DBK		
SVAC	LAC*	(151	
ERADD	DAC	REAL	
	LAC	(JMP	INI
	DAC	PAST	
INI	LAW	-1	
	DAC	COMFLG	
	TAD	(BUFF1	
	DAC	BUFI#	
	LAW	-1	
	TAD	(BUFF2	
	DAC	BUF2#	
	TCA		
	TAD	BUFI	
	DAC	DIFFC	
	DAC	BPFLG	
	LAC*	WC	
	TCA		
	DAC	WC	
	LAC*	SUBR	
	DAC	SUBR	
	LAC*	(z02	
	ISA		
	JMS	ADIN	
	DBK		
	JMP*	ADCSET	/RETURN
ADIN	Ø		/ENTRY
	LAC	CLOCK+3	/RESET CLOCK
	DAC*	(7	
	LAC	WC	/SETUP DCH

FSCAT program (cont.)

	DAC*	(26	
	LAC	BPFLG	
	TAD	BUF2	
	DAC*	(27	
	703704		
	703744		/CLEAR FLAGS
	703724		/ENABLE TRANSFERS
	JMP*	ADIN	/RETURN
ADSV	0		/LEVEL 0 ENTRY
	DAC	SVAC	/SAVE AC
	703704		/CLEAR OFLO
	LAC	M740	
	IAC		
	SZA		
	JMP	ADG	
	LAC	MINT	
	IAC		
	SZA		
	SKP		
	DZM	STOP	/DISABLE A/D DURING BUFFEROUT
ADG	703721		/TIMING ERROR??
	JMP	.+3	/NO
	ISZ	TIMERR	/INFORM USER
	703744		/CLEAR FLAG
	ISZ	COMFLG	/SET BUSY FLG ZERO
	JMP	SLOWP	/IT ALREADY WAS--ERROR
	LAC	SUBR	
	SZA		
	JMS*	REAL	/PRIME TO RUN SUBR AFTER EXIT
	LAC	DIFFC	/SWITCH BUFFERS
	XOR	BPFLG	
	DAC	BPFLG	
	LAC	STOP	
	SZA		
	JMS	ADIN	
EXIT	LAC	(404000	/REQUEST MONITOR AFTER EXIT
	ISA		
	LAC	SVAC	
	DBR		
	JMP*	ADSV	
SLOWP	LAC	ADSV	
	DAC	ERARG	
	LAW	5777	
	DAC	ERCODE	
	JMS	ERROR	
	JMP	EXIT	
ERROR	0		/ENTRY TO ERROR PRINTOUT
	LAC*	(166	/MONITOR ERROR SUBROUTINE
ERCODE	DAC	ERADD	
	LAW	5770	
	JMS*	ERADD	

FSCAT program (cont.)

FRARG	777777		/ARGUMENT
	DZM	STOP	
GERR	.CLOSE	5	
	JMP*	ERROR	/RETURN
BUFF1	.BLOCK	1750	
PD1	.BLOCK	50	
BUFF2	.BLOCK	1750	
PD2	.BLOCK	50	
IMARR	.BLOCK	740	
MN	.BLOCK	120	
LOIM	.DSA	IMARR-1	
HGIM	.DSA	IMARR+737	
	.END		

APPENDIX IV POST-PROCESSING PROGRAMS

The programs listed below are for post-processing of the correlation functions which were obtained in real time and stored on disk or DECTape. The source files for the programs POWW, VELL, AREAD, and DINFLT are loaded onto disk 3 of the PDP-15 from the program DECTape. The editor program of the system software is used to modify the file pointer in the AREAD program so as to agree with the file and extension of the first file to be processed. The statements are accessed with the edit command "L ,SIX". After closing the modified AREAD source file the MACRO compiler is used to produce binary files for these two programs. The FORTRAN compiler is used for POWW and VELL. Each time a new data set is processed AREAD must be edited and compiled with the new file name. The source of the data, either disk or DECTape is assigned to .DAT slot 5, the teletype to slot 2, the paper punch to slot 3 and disk 3 to slot -4. The programs POWW, AREAD, and DINFLT are then loaded and executed to produce a paper tape of power data. Similarly VELL, AREAD, and DINFLT are used to produce a velocity paper tape.

AREAD program

```

      .GLOBL SET,GET,..DA,DINFLT
      .IODEV 5
SET  0 /ENTRY DIMEN. ARR(1,1)
      .INIT 5,0,SET
      .SEEK 5,FILE
      ISZ EXT
      JMP* SET
FILE .SIXBT '04APR'
EXT .SIXBT '78A'
GET 0 /ENTRY
      JMS* .DA
      JMP .+2
ARR 0
      LAC* ARR
      DAC R+2
      DAC ARG
R .READ 5,4,ARR,4002
      .WAIT 5
      JMS* DINFLT
      JMP .+2
ARG 0
      JMP* GET
      .END

```

DINFLT program

```

DINFLT .TITLE DINFLT
        .GLOBL .DA,DINFLT
        0      /ENTRY
        JMS*   .DA      /GET ARG
ARG     JMP     .+2
        XX
        IAC    (ARG)   /ARRAY ADDRESS
        TCA
        TAD    ARG     /RELATIVE ADDRESS
        PAX    /USE XR
        TAD    (7640)
LOOP    PAL    /USE LR
        LAC    ARG,X   /GET MSW
        SMA!CLL /CHECK SIGN
        JMP    POS
        LAC    (400000)
        DAC    SIGN    /SET SIGN NEG.
        LAC    ARG,X+1 /GET LSW
        CMA    /ABS VAL; OVFLD TO LINK
        LMQ
        LAC    ARG,X   /GET MSW
        CMA    /ABS VAL; TEST LINK
POS     JMP    PAST
        DZM    SIGN    /SET SIGN POS.
        LAC    ARG,X+1 /GET LSW
        LMQ
PAST    LAC    ARG,X   /GET MSW
        NURM-1 /LEFT SHIFT BOTH
        XOR    SIGN    /ATTACH SIGN
        DAC    ARG,X+1 /PUT IN SECOND WORD
        LAC()
        AND    (777000) /CLEAR EXP BITS
        DSC    /ATTACH EXP
        SNA    /IGNORE ZERO
        JMP    .+3
        XOR    (77
        IAC
        DAC    ARG,X   /PUT IN FIRST WORD
        AXS    Z       /NEXT PAIR
        JMP    LOOP
SIGN    JMP*   DINFLT /RETURN
        0
        .END

```

POWW program

```

DIMENSION IN(4002)
COMMON B(25,20,4),P(20)
EQUIVALENCE (IN(1),B(1,1,1))
PMAX=0.
NR=0
DO 700 IFIL=1,10
CALL SET
DO 700 IREC=1,3
CALL GET(IN)
DO 100 IM=1,4
NR=NR+1
DO 200 IH=1,20
IF(B(1,IH,IM).GT.1.)P(IH)=ALOG10(B(1,IH,IM))
IF(P(IH).GT.PMAX)PMAX=P(IH)
200 CONTINUE
R=FLOAT(NR)
WRITE(3,300)R,(P(IH),IH=1,20)
300 FORMAT(F5.0,20F5.2)
100 CONTINUE
700 CONTINUE
WRITE(2,340) PMAX
340 FORMAT(1H0,6HPMAX =,F10.3)
STOP
END

```

VELL program

```

DIMENSION IN(4002)
COMMON B(25,20,4),AMP(20,13),RE(20,13),AIM(20,13),V(20,4)
COMMON/PATA/VPT(20,128),ALT(20)
EQUIVALENCE (IN(1),B(1,1,1))
VMAX=0.
NR=0
DO 10 I=1,20
ALT(I)=60.+1.5*FLOAT(I)
10 DO 10 J=121,128
VPT(I,J)=0.
DO 700 IFIL=1,10
CALL SET
DO 700 IREC=1,3
CALL GET(IN)
DO 100 IM=1,4
NR=NR+1
DO 200 IH=1,20
L=1
RE(IH,L)=B(1,IH,IM)
DO 50 J=2,25,2

```

VELL program (cont.)

```

L=L+1
RE(IH,L)=B(J,IH,IM)
50 AIM(IH,L)=B(J+1,IH,IM)
200 CONTINUE
DO 202 IH=1,20
DO 202 IL=1,4
202 V(IH,IL)=0.
DO 290 IH=1,20
DO 270 IL=2,4
AMP(IH,IL)=SQRT(RE(IH,IL)**2+AIM(IH,IL)**2)
IF(AMP(IH,IL).LT.(.10*RE(IH,1)))GO TO 262
IF(RE(IH,IL).EQ.0.)GO TO 260
V(IH,IL)=4.67*ATAN2(AIM(IH,IL),RE(IH,IL))/FLOAT(IL-1)
GO TO 270
260 V(IH,IL)=7.335/FLOAT(IL-1)
GO TO 270
262 V(IH,IL)=0.
LMAX=1L-1
GO TO 275
270 CONTINUE
LMAX=L
275 VA1=0.
VA2=0.
DO 280 IL=2,LMAX
VA1=VA1+AMP(IH,IL)*V(IH,IL)
280 VA2=VA2+AMP(IH,IL)
VPT(IH,NR)=VA1/VA2
ABV=ABS(VPT(IH,NR))
IF(ABV.GT.VMAX)VMAX=ABV
IF(ABV.GT.9.99)VPT(IH,NR)=SIGN(9.99,VPT(IH,NR))
290 CONTINUE
100 CONTINUE
700 CONTINUE
DO 300 IH=1,20
WRITE(3,333)ALT(IH)
333 FORMAT(IH,F5.1)
N1=1
N2=16
DO 340 NN=1,8
WRITE(3,344)(VPT(IH,NR),NR=N1,N2)
344 FORMAT(IH,16F5.2)
N1=N1+16
N2=N2+16
340 CONTINUE
300 CONTINUE
WRITE(2,440)VMAX
440 FORMAT(IH0,6HVMAX=,F10.3)
500 STOP
END

```



```

240 PRINT "H2=BASE ALT. E1=START SETTING, INPUT E1"
241 INPUT E1
242 H2=(E1-2)*1.5
251 PRINT "H2=";H2
255 PRINT "VELOCITY"
270 FOR I2=1 TO 20
280 ENTER (1,290,A)H8
290 FORMAT 1X,F5.1,3X
300 FOR I1=1 TO 8
310 ENTER (1,320,A)(FORJ=1TO16,WC I2,(I1-1)*16+J)
320 FORMAT 1X,16F5.2,3X
330 NEXT I1
340 NEXT I2
350 REM INPUT DONE, CONVERT TO INT.
360 FOR I1=1 TO N3
370 FOR I2=1 TO 20
380 WC I2, I1)=WC I2, I1)+100
390 NEXT I2
400 NEXT I1
405 REM STORE
410 PRINT "PLACE DATA TAPE IN TAPE DRIVE"
420 PRINT "FILE NO. WHERE DATA IS TO BE STORED?"
430 INPUT F1
440 PRINT "FILE";F1
450 STORE DATA F1
460 STOP
470 END

```

2. Power data storage program

```

10 DIM DIM(21,128),L$(40),H3,M3,N3,S2,L2,A6,A7,Z4,H2,E1,E2,E3,E4,E5
20 REM POWER STORE 10:42:06:23:78 IN=PAPER TAPE,OUT=CASSETTE
30 DIM DIM(128),WSC(21,128)
40 FOR Y=1 TO 128
50 AC I)=1
60 NEXT I
70 AC I2)=10
80 AC I3)=32
90 AC I4)=32
95 PRINT
100 PRINT "DATE?"
110 INPUT L$
120 PRINT L$
130 L$(LEN(L$)+1)= " POWER (LOG PLOT)"
140 PRINT "START TIME? INPUT HOURS,MINUTES."
150 INPUT H9,M3
170 PRINT "DAYLIGHT SAVINGS TIME?"
180 PRINT "INPUT 6 FOR CST,5 FOR CDT"
190 INPUT Z9
191 H3=H9+Z9-6
193 PRINT "START=";H3*100+M3;"CST"
210 PRINT "NO. OF RECORDS?"
220 INPUT N3
230 PRINT N3
240 PRINT "H2=BASE ALT. E1=START SETTING, INPUT E1"
241 INPUT E1
242 H2=(E1-2)*1.5
251 PRINT "H2=";H2
255 FOR I=1 TO N3
258 ENTER (1,261,A)WC(21,I),(FORJ=1TO20,WC J,I)
261 FORMAT F5.0,20F5.2,4X
264 NEXT I
267 REM INPUT DONE
270 REM MIN,MAX,AVE
273 A5=0
276 S2=15
279 L2=0
282 FOR J=1 TO N3

```

```

285 FOR I=1 TO 20
288 IF WCI,JJ>6.75 THEN 303
291 IF J#1 THEN 300
294 WCI,JJ=7
297 GOTO 303
300 WCI,JJ=WCI,J-1
303 IF WCI,JJ <= L2 THEN 309
306 L2=WCI,JJ
309 IF WCI,JJ >= S2 THEN 315
312 S2=WCI,JJ
315 A5=A5+WCI,JJ
318 NEXT I
321 NEXT J
324 A6=A5/(20*N3)
327 PRINT "POWER"
330 WRITE (15,339)S2,L2,A6
333 PRINT "MAX IS";10*(L2-S2);"DB ABOVE MIN."
336 PRINT "AVE IS";10*(A6-S2);"DB ABOVE MIN."
339 FORMAT "MIN=";F5.2,3X,"MAX=";F6.2,3X,"AVE=";F6.2
350 REM INPUT DONE, CONVERT TO INT.
360 FOR I1=1 TO N3
370 FOR I2=1 TO 20
380 WCI2,I1J=WCI2,I1J*100
390 NEXT I2
400 NEXT I1
410 PRINT "PLACE DATA TAPE IN TAPE DRIVE"
420 PRINT "FILE NO. WHERE DATA IS TO BE STORED?"
430 INPUT F1
440 PRINT "FILE";F1
450 STORE DATA F1
460 STOP
470 END

```

3. Velocity data plot program

```

10 DIM DIM(21,128),L*(40),H3,M3,N3,S2,L2,A6,A7,Z4,H2,E1,E2,E3,E4,E5
20 DIM VEL PLOT VERSION 21:40:10:31:78
30 GO,
40 DIM HIL(128),T*(3)
50 PRINT "PLACE DATA TAPE IN TAPE DRIVE"
60 PRINT "FILE NO. WHERE DATA IS STORED?"
70 INPUT F1
80 PRINT "FILE";F1
90 LOAD DATA F1
100 PRINT L*
120 T#="CST"
150 PRINT "LOCAL START TIME";M3+H3*100;T#
160 PRINT "NO. OF RECORDS=";N3
170 PRINT "H2=EASE ALT.=";H2
190 PRINT "RECOMMENDED PLOT PARAMETERS? 1=YES,0=NO"
200 INPUT R9
210 GOSUB R9+1 OF 1100,1020
220 PRINT "SCALE FOR 1 M/S=";H
230 PRINT "PEN UP LIMIT M/S=";L3
240 H1=H3
241 T6=5*(H3/5-INT(H3/5))
242 T7=15*(H3/15-INT(H3/15))
243 IF T6>0 THEN 245
244 T6=5
245 IF T7>0 THEN 247
246 T7=15
247 REM T6,T7 DONE
350 REM AXIS
260 SCALE -80,700,-15,115
270 XAXIS 0,-1,0,(6-T6)*5

```

```

275 HAXIS 0,25,(6-T6)*5,(6-T6)*5+(INT(N3/5))*25
276 IPLOT 10,0,1
277 LABEL (*,1.2,1.7,0,8/11)T#
280 HAXIS 0,5,0,105
290 HAXIS 105,-1,0,(6-T6)*5
295 HAXIS 105,25,(6-T6)*5,(6-T6)*5+(INT(N3/5))*25
300 REM HEIGHT LABELS
310 PLOT 0,0,1
320 FOR I=1 TO 20 STEP 2
330 IPLOT 0,10,1
340 LABEL (*,1.5,1.7,0,8/11)
350 CPLOT -Y,-0.3
360 H1=H1+3
370 LABEL (380,1.5,1.7,0,8/11)H1
380 FORMAT F6.1
390 NEXT I
400 REM TITLE
410 IPLOT 100,-112,1
420 LABEL (*,1.5,1.7,0,8/11)L#
430 REM HAXIS LABEL
440 FOR I5=16-T7 TO N3 STEP 15
450 M4=M3+I5-1
470 PLOT 5*I5,1,1
500 T6=100*M3+M4+40*INT(M4/60)
510 LABEL (*,1.5,1.7,0)
520 CPLOT -0.3,-0.5
530 LABEL (540,1.2,1.7,270,8/11)T6
540 FORMAT F5.0
550 NEXT I5
560 REM AXIS DONE
570 FOR I1=1 TO 20
580 OFFSET 0.5*I1
590 XAXIS 0,1,650-(120-N3)*5,0
600 REM C2=-1 FOR LAST ZERO
610 REM C2=1 FOR LAST NOT ZERO
620 C2=-1
630 FOR I2=1 TO N3
640 X=I2*5
650 Y=D(I1,I2)*H/100
660 IF Y=0 OR ABS(Y) >= L3*H THEN 710
670 REM NOT ZERO
680 C1=2
690 GOTO 720
700 REM ZERO
710 C1=1
720 C3=C1*C2
730 C2=(-1)^C1
740 PLOT X,Y,C3
750 NEXT I2
760 REM
770 NEXT I1
780 REM SCALE
790 OFFSET 655,55
800 FOR I=1 TO 100
810 B4=I*H
820 IF B4 >= 5 THEN 840
830 NEXT I
840 YAXIS 0,B4,-1*B4,B4
850 LABEL (*,1.2,1.7,0,8/11)
860 FOR I=1 TO 3
870 U1=B4*(I-2)
880 PLOT 15,U1,1
890 CPLOT 0.3,-0.3
900 LABEL (910,1.2,1.7,0,8/11)U1/H
910 FORMAT F3.0
920 NEXT I
930 CPLOT -3,2
940 LABEL (4,1.2,1.7,0,8/11)"SCALE"
950 PRINT "NEW PLOT WITH THIS DATA? PREPARE PLOTTER"
960 PRINT "1=YES"
970 INPUT R
980 IF R=1 THEN 190

```

```

990 PRINT
1000 STOP
1010 REM PLOT PARA. ROUTINES
1020 IF H2>36 THEN 1060
1030 H=5
1040 L3=1
1050 GOTO 1080
1060 H=1
1070 L3=7.5
1080 RETURN
1090 STOP
1091 REM VERT. TICKS=5 PLOTTER UNITS. H=NO. OF PLOTTER UNITS FOR 1 M/S
1100 PRINT "SCALE FOR 1 M/S?"
1110 INPUT H
1111 REM ABS. VALUE OF VEL. < L3 TO BE PLOTTED.
1120 PRINT "PEN UP LIMIT M/S?"
1130 INPUT L3
1140 RETURN
1150 STOP
1160 END

```

4. Power versus time at a fixed altitude plot program

```

10 DIM D1(2),L(40),H3,M3,N3,S2,L2,A6,A7,Z4,H2,E1,E2,E3,E4,E5
20 REM POWER PLOT HORIZ. 14:00:07:15:78
30 DE
40 DIM T(120),T*(3)
50 PRINT "PLACE DATA TAPE IN TAPE DRIVE"
60 PRINT "FILE NO. WHERE DATA IS STORED?"
70 INPUT F1
80 PRINT "FILE";F1
90 LOAD DATA F1
100 PRINT L#
120 T#="CST"
150 PRINT "LOCAL START TIME";M3+H3*100;T#
160 PRINT "NO. OF RECORDS=";N3
181 WRITE (15,164)S2,L2,A6
162 PRINT "MAX IS";10*(L2-S2);"DB ABOVE MIN."
163 PRINT "AVE IS";10*(A6-S2);"DB ABOVE MIN."
164 FORMAT "MIN=";F5.2,3X;"MAX=";F6.2,3X;"AVE=";F6.2
168 SCALE -80,700,-15,115
170 PRINT "H2=BASE ALT.=";H2
190 PRINT "RECOMMENDED PLOT PARAMETERS? 1=YES,0=NO"
200 INPUT P9
210 LOCUS P9+1 OF 1720,1830
212 PRINT "BASE="B;"HEIGHT="H;"LIMIT="L3
215 PEN THRESHOLD IS T5
220 T5=L3*10+S2
222 OFFSET 0,0
223 PLOT 5,111,1
224 LABEL (225,1.2,1.7,0,8/11)S2,L2,B,L3
225 FORMAT "MIN=";F5.2,3X;"MAX=";F6.2,3X;"BASE=";F5.2,3X;"LIMIT=";F3.0,X;"DB"
226 PEN
240 H1=H2
241 T6=5*(M3/5-INT(M3/5))
242 T7=15*(M3/15-INT(M3/15))
243 IF T6=0 THEN 245
244 T6=5
245 IF T7=0 THEN 247
246 T7=15
247 FOR T6 TO T7 STEP 5
250 FOR H1 TO H2
270 XAXIS 0,-1,0,(6-T6)*I
275 XAXIS 0,25,(6-T6)*5,(4-T6)*5+(INT(M3/5))*25
276 IPLOT 10,0,1
277 LABEL (*,1.2,1.7,0,8/11)T#
280 YAXIS 0,5,0,105
290 XAXIS 105,-1,0,(6-T6)*5

```

```

295 DIM T(105,25),(6-T6)*5,(6-T6)*5+(INT(N3/5))*25
300 PEN HEIGHT LABELS
310 PLOT 0,0,1
320 FOR I=1 TO 20 STEP 2
330 IPLOT 0,10,1
340 LABEL (*,1.5,1.7,0.8/11)
350 CPLOT -7,-0.3
360 H1=H1+3
370 LABEL (380,1.5,1.7,0.8/11)H1
380 FORMAT F6.1
390 NEXT I
400 PEN TITLE
410 IPLOT 100,-112,1
420 LABEL (*,1.5,1.7,0.8/11)L#
430 PEN AXIS LABEL
440 FOR I5=16-T7 TO N3 STEP 15
450 M1=M1+I5-1
470 PLOT 5*I5,1,1
500 T5=100*N3+M4+40*INT(M4/60)
510 LABEL (*,1.5,1.7,0)
520 CPLOT -0.3,-0.5
530 LABEL (540,1.2,1.7,270,8/11)T6
540 FORMAT F5.0
550 NEXT I5
560 REM AXIS DONE
920 REM GIVEN HEIGHT VS TIME
930 REM INIT. T ARRAY
940 FOR K=1 TO 128
950 T(K)=0
960 NEXT K
1340 FOR H9=1 TO 20
1350 OFFSET 0,5*H9
1355 C3=-1
1360 FOR I1=1 TO N3
1370 H=I1*5
1380 I2=H9-1
1390 GOSUB 1906
1400 Y=(Z0-8)*H
1410 GOSUB 1600
1420 NEXT I1
1430 PEN
1440 NEXT H9
1470 PEN
1510 REM LABEL 10 DB SCALE
1520 OFFSET 0,0
1530 YAXIS 665,H,105-H,105
1540 LABEL (*,1.2,1.7,0.8/11)
1550 CPLOT -2.3,0.3
1560 LABEL (*,1.2,1.7,0.8/11)"10 DB"
1562 PRINT "NEW PLOT WITH THIS DATA? PREPARE PLOTTER"
1564 PRINT "1=YES"
1566 INPUT R
1568 IF R=1 THEN 190
1570 PRINT
1572 STOP
1580 PEN C2=-1 FOR LAST HIDDEN
1590 PEN C2=1 FOR LAST NOT HIDDEN
1600 IF (TC(I1)-5)>>Y THEN 1660
1610 PEN NOT HIDDEN
1620 TC(I1)=Y
1630 C1=0
1640 GOTO 1680
1650 PEN HIDDEN
1660 TC(I1)=TC(I1)-5
1670 C1=1
1680 C3=C1+C2
1690 C2=(C1)*C1
1700 PLOT X,Y,C3
1710 RETURN
1715 PEN HEIGHT FACTOR H DETERMINES THE NO. OF VERTICAL PLOT UNITS
1716 PEN FOR 10 DB. NOTE THAT VERT. TICKS ARE 5 PLOT UNITS.
1720 PRINT "INPUT HEIGHT FACTOR"
1730 INPUT H
1740 PEN BASE VALUE B IS SUBTRACTED FROM ALL DATA BEFORE PLOTTING.
1741 PEN B SHOULD BE NEAR THE MIN. AND SLIGHTLY HIGHER.
1750 PRINT "INPUT BASE VALUE"

```

```

1770 INPUT B
1770 REM LIMIT VALUE IS THE LIMIT IN DB ABOVE THE MIN. ABOVE
1771 REM WHICH THE PLOT WILL BE CLIPPED IF A 1 MIN. SPIKE OCCURS.
1780 PRINT "INPUT LIMIT VALUE IN DB"
1790 INPUT L3
1800 L3=INT(L3)
1810 RETURN
1820 STOP
1830 H=10
1840 B=52+0.45
1850 L3=10+(L2-S2)
1860 RETURN
1870 STOP
1880 REM LIMITING
1890 CC=DC12+1,11,100
1910 IF I1=H3 THEN 1940
1920 IF S2 >= T5 OR DC12+1,11+100 >= T5 THEN 1940
1930 T5=T5
1940 RETURN
1950 END

```

5. Power versus height at a fixed time plot program

```

10 DIM D1(21,150),L*(40),H3,M3,N3,S2,L2,A6,A7,Z4,H2,E1,E2,E3,E4,E5
20 REM POWER PLOT VERT. 00:23:11:01:78
30 DEG
40 DIM T$(128),T*(3)
50 PRINT "PLACE DATA TAPE IN TAPE DRIVE"
60 PRINT "FILE NO. WHERE DATA IS STORED?"
70 INPUT F1
80 PRINT "FILE";F1
90 LOAD DATA F1
100 PRINT L*
120 T*="CST"
150 PRINT "LOCAL START TIME";M3+H3*100;T*
160 PRINT "NO. OF RECORDS=";N3
161 WRITE (15,164)S2,L2,A6
162 PRINT "MAX IS";110*(L2-S2);"DB ABOVE MIN."
163 PRINT "AVE IS";110*(A6-S2);"DB ABOVE MIN."
164 FORMAT "MIN=";F5.2,3X,"MAX=";F6.2,3X,"AVE=";F6.2
168 SCALE -80,700,-15,115
170 PRINT "H2=BASE ALT.=";H2
190 PRINT "RECOMMENDED PLOT PARAMETERS? 1=YES,0=NO"
200 INPUT R9
210 GOSUB R9+1 OF 1720,1830
212 PRINT "BASE="B,"HEIGHT="H,"LIMIT="L3
215 REM THRESHOLD IS T5
220 T5=L3*10+S2
222 OFFSET 0,0
223 PLOT 5,111,1
224 LABEL (225,1.2,1.7,0,8/11)S2,L2,B,L3
225 FORMAT "MIN=";F5.2,3X,"MAX=";F6.2,3X,"BASE=";F5.2,3X,"LIMIT=";F3.0,X,"DB"
226 PEN
240 H1=H2
241 T6=5+(M3/5-INT(M3/5))
242 T7=15+(M3/15-INT(M3/15))
243 IF T6=0 THEN 245
244 T6=5
245 IF T7=0 THEN 247
246 T7=15
247 REM T6,T7 IONE
250 REM AXIS
251 HAXIS 0,-1,0,(6-T6)*5
252 HAXIS 0,25,(6-T6)*5,(6-T6)*5+(INT(M3/5))*25
253 IF T7 10,0,1
254 LABEL (4,1.2,1.7,0,8/11)T*
255 HAXIS 0,5,0,105
256 HAXIS 105,-1,0,(6-T6)*5
257 HAXIS 105,25,(6-T6)*5,(6-T6)*5+(INT(M3/5))*25
260 PEN HEIGHT LABELS

```

ORIGINAL PAGE 15
OF PAPER 01178

```

310 PLOT H,0,1
320 FOR I=1 TO 20 STEP 2
330 IPLOT 0,10,1
340 LABEL (*,1.5,1.7,0,8/11)
350 CPLOT -7,-0.3
360 H1=H1+3
370 LABEL (380,1.5,1.7,0,8/11)H1
380 FORMAT F6.1
390 NEXT I
400 PEN TITLE
410 IPLOT 100,-112,1
420 LABEL (*,1.5,1.7,0,8/11)L$
430 REM X AXIS LABEL
440 FOR I5=16-T7 TO N3 STEP 15
450 M4=M3+I5-1
470 PLOT 5*I5,1,1
500 T6=100*M3+M4+40*INT(M4/60)
510 LABEL (*,1.5,1.7,0)
520 CPLOT -0.3,-0.5
530 LABEL (540,1.2,1.7,270,8/11)T6
540 FORMAT F5.0
550 NEXT I5
560 REM AXIS DONE
850 GOSUB 930
860 PRINT "NEW PLOT? PREPARE PLOTTER"
870 PRINT "1=YES"
890 INPUT R
900 IF R#1 THEN 190
910 STOP
920 REM POWER VS HEIGHT
930 REM INIT. T ARRAY
940 FOR K=1 TO 128
950 T(K)=0
960 NEXT K
980 FOR I1=1 TO N3
990 OFFSET 5*I1,0
1000 REM PLOT ONE MINUTE
1010 REM FIRST POINT
1020 C2=-1
1030 I2=0
1040 GOSUB 1900
1050 Z1=Z2
1060 X=(Z1-B)*H
1070 Y=5
1080 GOSUB 1600
1090 REM REMAINING POINTS
1100 FOR I2=1 TO 19
1110 GOSUB 1900
1120 S=(Z2-Z1)/5
1130 REM S=K INC. BETWEEN PLOT POINTS
1140 FOR I3=1 TO 5
1150 Y=I2+5+I3
1160 X=(Z1-B+I3*S)*H
1170 GOSUB 1600
1180 NEXT I3
1190 Z1=Z2
1200 NEXT I2
1210 PEN
1220 NEXT I1
1230 OFFSET 0,0
1340 XAXIS 100,H,500,500+H
1350 PLOT 500+(H,2),100,1
1360 LABEL (*,1.2,1.7,0,8/11)
1370 CPLOT -2.3,1
1380 LABEL (*,1.2,1.7,0,8/11)"10 DB"
1290 RETURN
1572 STOP
1580 REM C2=-1 FOR LAST HIDDEN
1590 REM C2=1 FOR LAST NOT HIDDEN
1600 IF (T(Y)-5)>0 THEN 1660
1610 REM NOT HIDDEN
1620 T(Y)=X
1630 C:=2
1640 GOTO 1680
1650 REM HIDDEN

```

```
1660 T(Y)=T(Y)-5
1670 C1=1
1680 C3=C1+C2
1690 C2=(-1)^C1
1700 PLOT X,Y,C3
1710 RETURN
1715 REM HEIGHT FACTOR H DETERMINES THE NO. OF HORIZONTAL PLOT UNITS
1716 REM FOR 10 DB. NOTE THAT HORIZ. TICKS ARE 25 PLOT UNITS APART.
1720 PRINT "INPUT HEIGHT FACTOR"
1730 INPUT H
1740 REM BASE VALUE B IS SUBTRACTED FROM ALL DATA BEFORE PLOTTING.
1741 REM B SHOULD BE NEAR THE MIN.
1750 PRINT "INPUT BASE VALUE"
1760 INPUT B
1770 REM LIMIT VALUE IS THE LIMIT IN DB ABOVE THE MIN. FOR
1771 REM WHICH THE PLOT WILL BE CLIPPED IF A 1 MIN. SPIKE OCCURS.
1780 PRINT "INPUT LIMIT VALUE IN DB"
1790 INPUT L3
1800 L3=INT(L3)
1810 RETURN
1820 STOP
1830 H=50
1840 B=SQ+0.08
1850 L3=AG+0.3
1860 RETURN
1870 STOP
1880 REM LIMITING
1900 Z2=DC(2+1,11)/100
1910 IF I1=N3 THEN 1940
1920 IF Z2 <= T5 OR DC(2+1,11+1)/100 >= T5 THEN 1940
1930 Z2=T5
1940 RETURN
1950 END
```

REFERENCES

- Allman, M. E. and S. A. Bowhill [1976], Feed system design for the Urbana incoherent-scatter radar antenna, *Aeron. Rep. No. 71*, Aeron. Lab., Dep. Elec. Eng., Univ. Ill., Urbana-Champaign.
- Appleton, E. V. and M. A. F. Barnett [1925], Local reflection of wireless waves from the upper atmosphere, *Nature, Lond.*, *115*, 333.
- Armistead, W. G., J. V. Evans and W. A. Reid [1972], Measurements of D- and E-region electron densities by the incoherent scatter technique at Millstone Hill, *Radio Sci.* *7*, 153-162.
- Aso, T., S. Kato and R. M. Harper [1977], Arecibo middle atmosphere experiment, *Geophys. Res. Lett.*, *4*, 10-12.
- Bailey, D. K., R. Bateman, L. V. Berkner, H. G. Booker, G. F. Montgomery, E. M. Purcell, W. W. Salisbury and J. B. Wiesner [1952], A new kind of radio propagation at very high frequencies observable over long distances, *Phys. Rev., 2nd series* *86*, 141-145.
- Bailey, D. K., R. Bateman and R. C. Kirby [1955], Radio transmission at VHF by scattering and other processes in the lower ionosphere, *Proc. IRE*, *43*, 1181-1231.
- Balsley, B. B. [1978a], Design considerations for coherent radar systems for probing the troposphere, stratosphere, and mesosphere, Preprints, *18th Radar Meteor. Conf.*, 387-390, published by Amer. Meteor. Soc.
- Balsley, B. B. [1978b], The use of sensitive coherent radars to examine atmospheric parameters in the height range 1-100 km, Preprints, *18th Radar Meteor. Conf.*, 190-193, published by Amer. Meteor. Soc.
- Balsley, B. B., W. L. Ecklund, D. A. Carter and P. E. Johnston [1979], The Poker Flat MST radar: first results, *Geophys. Res. Lett.*, *6*, 921-924.
- Balsley, B. B. and D. T. Farley [1976], Auroral zone winds detected near the tropopause with the Chatnika UHF doppler radar, *Geophys. Res. Lett.*, *3*, 525-528.
- Bauer, P., P. Waldteufel and C. Vialle [1974], The French quadrastatic incoherent scatter facility, *Radio Sci.*, *9*, 77-83.
- Blair, J. C., R. M. Davis, Jr. and R. C. Kirby [1961], Frequency dependence of D-region scattering at VHF, *J. Res. NBS*, *65D*, 417-425.
- Booker, H. G. and W. E. Gordon [1950], A theory of radio scattering in the troposphere, *Proc. IRE* *38*, 401-412.

- Bowles, K. L. [1958], Observation of vertical incidence scatter from the ionosphere at 41 Mc/sec, *Phys. Rev. Lett.*, 1, 454-455.
- Bowles, K. L. [1961], Incoherent scattering by free electrons as a technique for studying the ionosphere and exosphere: some observations and theoretical considerations, *J. Res. NBS*, 65D, 1-14.
- Bowles, K. L. [1964], *Radio Wave Scattering in the Ionosphere, Advances in Electronics and Electron Physics*, 17, (ed.) L. Marton, Academic Press, New York, 55-176.
- Czechowsky, P., J. Klostermeyer, J. Röttger, R. Rüster, G. Schmidt and R. P. Woodman [1976], The SOUSY-VHF-radar for tropo-, strato- and mesospheric sounding, Preprints, *17th Radar Meteor. Conf.*, 343-347, published by Amer. Meteor. Soc.
- Dougherty, J. P. and D. T. Farley [1960], A theory of incoherent scattering of radio waves by a plasma, *Proc. Royal Soc. A*, 269, 79-99.
- Eckersley, T. L. [1932], Studies in radio transmission, *J. Inst. Elec. Engrs. (London)* 71, 405-454.
- Ecklund, W. L., D. A. Carter and B. B. Balsley [1979], Continuous measurement of upper atmospheric winds and turbulence using a VHF doppler radar: preliminary results, *J. Atmos. Terr. Phys.*, in press.
- Ecklund, W. L., D. A. Carter and K. S. Gage [1977], Sounding of the lower atmosphere with a portable 50-MHz coherent radar, *J. Geophys. Res.*, 82, 4969-4971.
- Edwards, B. [1974] (Ed.), Research in Aeronomy, April 1 - September 30, 1974, *Prog. Rep. 74-2*, Aeron. Lab., Dep. Elec. Eng., Univ. Ill., Urbana-Champaign.
- Evans, J. V. [1967] (Ed.), Thomson Scatter Studies of the ionosphere - an informal conference record, *Aeron. Rep. No. 19*, Aeron. Lab., Dep. Elec. Eng., Univ. Ill., Urbana-Champaign.
- Evans, J. V. [1969], Theory and practice of ionosphere study by Thomson scatter radar, *Proc. IEEE* 57, 496-530.
- Evans, J. V. and M. Loewenthal [1964], Ionospheric backscatter observations, *Planet. Space Sci.*, 12, 915-944.
- Flock, W. L. and B. B. Balsley [1967], VHF radar returns from the D region of the equatorial ionosphere, *J. Geophys. Res.*, 72, 5537-5541.

- Gordon, W. E. [1958], Incoherent scattering of radio waves by free electrons with applications to space exploration by radar, *Proc. IRE*, 46, 1824-1829.
- Gordon, W. E. and L. M. Lalonde [1961], The design and capabilities of an ionospheric radar probe, *Trans. IRE*, AP-9, 17-22.
- Green, J. L., J. M. Warnock, R. H. Winkler and T. E. VanZandt [1975a], Studies of winds in the upper troposphere with a sensitive VHF radar, *Geophys. Res. Lett.*, 2, 19-21.
- Green, J. L., J. M. Warnock, R. H. Winkler and T. E. VanZandt [1975b], A sensitive VHF radar for the study of winds, waves and turbulence in the troposphere, stratosphere and mesosphere, Preprints, 16th Radar Meteor. Conf., 313-315, published by Amer. Meteor. Soc.
- Greenhow, J. S., H. K. Sutcliffe and G. D. Watkins [1963], The electron scattering cross-section in incoherent backscatter, *J. Atmos. Terr. Phys.*, 25, 197-207.
- Gregory, J. B. [1961], Radio wave reflections from the mesosphere. I. Heights of occurrence, *J. Geophys. Res.*, 66, 429-445.
- Harper, R. M. and R. F. Woodman [1977], Preliminary multiheight radar observations of waves and winds in the mesosphere over Jicamarca, *J. Atmos. Terr. Phys.*, 39, 959-963.
- Hess, G. C. and M. A. Geller [1976], The Urbana meteor-radar system: design, development, and first observations, *Aeron. Rep. No. 24*, Aeron. Lab., Dep. Elec. Eng., Univ. Ill., Urbana-Champaign.
- Ioannidis, G. and D. T. Farley [1974], High resolution D-region measurements at Arecibo, *Radio Sci.*, 9, 151-157.
- Lalonde, L. M. [1966], A short pulse backscatter study of the lower ionosphere, *Electron Density Profiles in Ionosphere and Exosphere*, (Ed.) J. Frihagen, North Holland Publ. Co., Amsterdam and J. Wiley & Sons, New York, 515-521.
- Leadabrand, R. L. [1967], The SRI 1300 MHz radar, in Thomson scatter studies of the ionosphere - an informal conference record, (Ed.), J. V. Evans, *Aeron. Rep. No. 19*, Aeron. Lab., Dep. Elec. Eng., Univ. Ill., Urbana-Champaign, 59-63.
- Leadabrand, R. L., M. J. Baron, J. Petrickes and H. F. Bates [1972], Chatanika, Alaska, aurora-zone incoherent-scatter facility, *Radio Sci.*, 7, 747-756.

- Miller, K. L., S. A. Bowhill, K. P. Gibbs and I. D. Countryman [1978], First measurements of mesospheric vertical velocities by VHF radar at temperate latitudes, *Geophys. Res. Lett.*, *5*, 939-942.
- Norton, K. A. and J. B. Wiesner [1955] (Eds), The scatter propagation issue, *Proc. IRE*, *43*(10).
- Pineo, V. G., L. G. Kraft and H. W. Briscoe [1960], Ionospheric backscatter observation at 440 Mc/s, *J. Geophys. Res.*, *65*, 2629-2633.
- Rastogi, P. K. and S. A. Bowhill [1975], Remote sensing of the mesosphere using the Jicamarca incoherent-scatter radar, *Aeron. Rep. No. 68*, Aeron. Lab., Dep. Elec. Eng., Univ. Ill., Urbana-Champaign.
- Rastogi, P. K. and S. A. Bowhill [1976a], Scattering of radio waves from the mesosphere - I. Theory and observations, *J. Atmos. Terr. Phys.*, *38*, 399-411.
- Rastogi, P. K. and S. A. Bowhill [1976b], Scattering of radio waves from the mesosphere - II. Evidence for intermittent mesospheric turbulence, *J. Atmos. Terr. Phys.*, *38*, 449-462.
- Rastogi, P. K. and R. F. Woodman [1974], Mesospheric studies using the Jicamarca incoherent-scatter radar, *J. Atmos. Terr. Phys.*, *36*, 1217-1231.
- Rüster, R., J. Röttger and R. F. Woodman [1978], Radar measurements of waves in the lower stratosphere, *Geophys. Res. Lett.*, *5*, 119-122 and 555-558.
- Villars, R. and V. F. Weisskopf [1955], On the scattering of radio waves by turbulent fluctuations of the atmosphere, *Proc. IRE* *43*, 1232-1239.
- Warnock, J. M., T. E. VanZandt, J. L. Green and R. H. Winkler [1978], Comparison between wind profiles measured by doppler radar and by rawinsonde balloons, *Geophys. Res. Lett.*, *5*, 109-112.
- Williams, P. J. S. and G. N. Taylor [1974], The UK incoherent scatter radar, *Radio Sci.*, *9*, 85-88.
- Woodman, R. F. and A. Guillen [1974], Radar observations of winds and turbulence in the stratosphere and mesosphere, *J. Atmos. Sci.*, *31*, 493-503.